

REPORT DOCUMENTATION PAGE				Form Approved OMB No. 0704-0188	
<small>Public reporting burden for this collection of information is estimated to average 1 hour per response, including the time for reviewing instructions, searching data sources, gathering and maintaining the data needed, and completing and reviewing the collection of information. Send comments regarding this burden estimate or any other aspect of this collection of information, including suggestions for reducing this burden to Washington Headquarters Service, Directorate for Information Operations and Reports, 1215 Jefferson Davis Highway, Suite 1204, Arlington, VA 22202-4302, and to the Office of Management and Budget, Paperwork Reduction Project (0704-0188) Washington, DC 20503.</small>					
PLEASE DO NOT RETURN YOUR FORM TO THE ABOVE ADDRESS.					
1. REPORT DATE (DD-MM-YYYY) 11-30-2009		2. REPORT TYPE Final Report		3. DATES COVERED (From - To) July 22, 2008 -- July 30, 2009	
4. TITLE AND SUBTITLE Advanced Propulsion for Gun Launched Projectiles and Missiles: Phase I-Low Cost Flight Test Platform Development				5a. CONTRACT NUMBER N00014-08-C-0676	
				5b. GRANT NUMBER 	
				5c. PROGRAM ELEMENT NUMBER 	
6. AUTHOR(S) Karl V. Hoose, Principal Investigator				5d. PROJECT NUMBER 08PR07435-00 1048192	
				5e. TASK NUMBER 	
				5f. WORK UNIT NUMBER 	
7. PERFORMING ORGANIZATION NAME(S) AND ADDRESS(ES) Applied Thermal Sciences, Inc. P.O. Box C Sanford, ME 04073				8. PERFORMING ORGANIZATION REPORT NUMBER 	
9. SPONSORING/MONITORING AGENCY NAME(S) AND ADDRESS Office of Naval Research 875 North Randolph Street, Suite 1425 Arlington, VA 222013-1995				10. SPONSOR/MONITOR'S ACRONYM(S) ONR	
				11. SPONSORING/MONITORING AGENCY REPORT NUMBER 	
12. DISTRIBUTION AVAILABILITY STATEMENT Approved for public release; Distribution is unlimited.					
13. SUPPLEMENTARY NOTES Demonstration of low cost, flight test platform to obtain vital flight data on ramjet/scramjet engine operation.					
14. ABSTRACT Applied Thermal Sciences' (ATS's) goal of this effort was to demonstrate a low cost, short duration flight test platform to obtain vital flight data on ramjet/scramjet engine operation. Previous work conducted by ATS, under an IR&D program, resulted in flight tests of an ATS designed vehicle boosted to supersonic speeds. Under this program, the rocket motors used for boost were the largest readily available commercially. Adding a ramjet test article to the vehicle design required larger rocket motors to reach speeds of Mach 1.5-2.0. Applied Thermal Sciences expertise in solid propellant rocket motor development was employed during this program to develop a booster to meet flight Mach numbers needed for demonstration. Therefore, ATS developed the rocket motor, flight vehicle, and ramjet test article for this work. Applied Thermal Sciences successfully achieved the major goal of demonstrating ramjet separation during flight at supersonic speeds. In addition, the ramjet test article included some unique features allowing closed inlet during boost, and open inlet at separation. Stability of flight after separation was also accomplished and documented.					
15. SUBJECT TERMS Low cost flight vehicle; Ramjet test article development; Flight testing					
16. SECURITY CLASSIFICATION OF:			17. LIMITATION OF ABSTRACT SAR	18. NUMBER OF PAGES 	19a. NAME OF RESPONSIBLE PERSON Karl V. Hoose
a. REPORT U	b. ABSTRACT U	c. THIS PAGE U			19b. TELEPHONE NUMBER (Include area code) 207-459-7777

INSTRUCTIONS FOR COMPLETING SF 298

1. REPORT DATE. Full publication date, including day, month, if available. Must cite at least the year and be Year 2000 compliant, e.g., 30-06-1998; xx-08-1998; xx-xx-1998.

2. REPORT TYPE. State the type of report, such as final, technical, interim, memorandum, master's thesis, progress, quarterly, research, special, group study, etc.

3. DATES COVERED. Indicate the time during which the work was performed and the report was written, e.g., Jun 1997 - Jun 1998; 1-10 Jun 1996; May - Nov 1998; Nov 1998.

4. TITLE. Enter title and subtitle with volume number and part number, if applicable. On classified documents, enter the title classification in parentheses.

5a. CONTRACT NUMBER. Enter all contract numbers as they appear in the report, e.g. F33615-86-C-5169.

5b. GRANT NUMBER. Enter all grant numbers as they appear in the report, e.g. 1F665702D1257.

5c. PROGRAM ELEMENT NUMBER. Enter all program element numbers as they appear in the report, e.g. AFOSR-82-1234.

5d. PROJECT NUMBER. Enter all project numbers as they appear in the report, e.g. 1F665702D1257; ILIR.

5e. TASK NUMBER. Enter all task numbers as they appear in the report, e.g. 05; RF0330201; T4112.

5f. WORK UNIT NUMBER. Enter all work unit numbers as they appear in the report, e.g. 001; AFAPL30480105.

6. AUTHOR(S). Enter name(s) of person(s) responsible for writing the report, performing the research, or credited with the content of the report. The form of entry is the last name, first name, middle initial, and additional qualifiers separated by commas, e.g. Smith, Richard, Jr.

7. PERFORMING ORGANIZATION NAME(S) AND ADDRESS(ES). Self-explanatory.

8. PERFORMING ORGANIZATION REPORT NUMBER. Enter all unique alphanumeric report numbers assigned by the performing organization, e.g. BRL-1234; AFWL-TR-85-4017-Vol-21-PT-2.

9. SPONSORING/MONITORS AGENCY NAME(S) AND ADDRESS(ES). Enter the name and address of the organization(s) financially responsible for and monitoring the work.

10. SPONSOR/MONITOR'S ACRONYM(S). Enter, if available, e.g. BRL, ARDEC, NADC.

11. SPONSOR/MONITOR'S REPORT NUMBER(S). Enter report number as assigned by the sponsoring/ monitoring agency, if available, e.g. BRL-TR-829; -215.

12. DISTRIBUTION/AVAILABILITY STATEMENT. Use agency-mandated availability statements to indicate the public availability or distribution limitations of the report. If additional limitations/restrictions or special markings are indicated, follow agency authorization procedures, e.g. RD/FRD, PROPIN, ITAR, etc. Include copyright information.

13. SUPPLEMENTARY NOTES. Enter information not included elsewhere such as: prepared in cooperation with; translation of; report supersedes; old edition number, etc.

14. ABSTRACT. A brief (approximately 200 words) factual summary of the most significant information.

15. SUBJECT TERMS. Key words or phrases identifying major concepts in the report.

16. SECURITY CLASSIFICATION. Enter security classification in accordance with security classification regulations, e.g. U, C, S, etc. If this form contains classified information, stamp classification level on the top and bottom of this page.

17. LIMITATION OF ABSTRACT. This block must be completed to assign a distribution limitation to the abstract. Enter UU (Unclassified Unlimited) or SAR (Same as Report). An entry in this block is necessary if the abstract is to be limited.



Applied Thermal Sciences, Inc.

Engineering Research & Development

Advanced Propulsion for Gun Launched Projectiles and Missiles: Phase I – Low Cost Flight Test Platform Development

Final Report

July 2008 thru November 2009

Prepared For:

Gil Y. Graff
Office of Naval Research

Original Contract Number: N00014-08-C-0676

Prepared By:

Karl V. Hoose, Principal Investigator
Ryan Gauthier, Project Lead

Applied Thermal Sciences, Inc.
1861 Main Street
Sanford, ME 04073

Submitted: November 30, 2009



Table of Contents

Table of Contents	2
List of Figures	4
List of Tables	8
Introduction	9
Project Overview.....	9
Project Milestones	10
Task 1 - Boost Vehicle Design & Development	10
Task 1.1 – Vehicle Design.....	11
Supersonic Vehicle with Ramjet Description.....	82
FWD Ramjet Section	82
Ramjet Coupler & MID Payload Bay & Booster Section	84
Task 1.2 - Booster Motor Design	14
Solid Propellant Motor Test.....	15
Booster Motor Testing, September 2008	Error! Bookmark not defined.
Booster Motor Redesign	17
Adhesive Selection	20
Surface Prep	21
Post Cure Oven	22
Booster Motor Hydrostatic Test	22
Booster Motor Testing, October 24, 2008.....	24
Task 1.3 – Flight Vehicle and Motor Fabrication	25
Electronics Testing	30
Task 2 – Ramjet Test Article Development.....	45
Task 2.1 – Preliminary Ramjet Design Analysis.....	64
RAMJET Payload CFD	64
Ramjet Development	64
Task 2.2 – CFD Analysis	66
Initial RAMJET CFD Work	66
ATS Inward Turning RAMJET Design	71
Final Ramjet Design and CFD	76
3D CFD Results of Ramjet Design.....	78
Task 2.3 – Structural Design.....	79
Inward Turning Ramjet Design.....	Error! Bookmark not defined.
Axi-symmetric Ramjet Design	80
Final Ramjet Design.....	80
Task 3 – Flight Testing.....	64
Launch and Recovery Zone	86
Task 3.1 – Boost Vehicle	87
Supersonic Flight Test on April 15 th , 2009	31



April 2009 Flight - 1 st Launch Summary	33
April 2009 Flight - 2 nd Launch Summary	38
April 2009 Flight - Data to Predicted Flight.....	42
Task 3.2 – Boost Vehicle with Dummy Ramjet Test Article	46
June 2009 Flight - FWD “Dummy Ramjet” Section	47
June 2009 Flight - MID Payload Bay Section	48
June 2009 Flight - AFT Motor Section	48
June 2009 Flight - Solid Propellant Motor	49
June 2009 Flight - Electronics	49
June 2009 Flight - Launch on June 5 th 2009.....	50
June 2009 Flight - 1 st Launch.....	53
June 2009 Flight - 2 nd Launch.....	57
June 2009 Flight - Data to Predicted Flight.....	61
Task 3.3 – Boost Vehicle with Separation of Ramjet Test Article	87
November 2009 Flight - FWD Ramjet Section	88
November 2009 Flight - Ramjet Coupler & MID Payload Bay & Booster Section	89
November 2009 Flight - Solid Propellant Motors	91
November 2009 Flight - Electronics.....	93
November 2009 Flight – 1 st Launch	95
November 2009 Flight – 2 nd Launch	96



List of Figures

Figure 1 – Typical Rocket Design	11
Figure 2 – Picture of Ramjet Flight Vehicles	82
Figure 3 – Assembled Ramjet	83
Figure 4 – Ramjet with all components shown	83
Figure 5 – Ramjet Shroud.....	84
Figure 6 –MID Payload Bay Section	85
Figure 7 – Ramjet Coupler Section.....	85
Figure 8 –Booster Section	86
Figure 9 - AN Motor Charges (for reference calipers were set to 2in)	15
Figure 10 – Motor on Thrust Stand.....	16
Figure 11 – Test Data from the Motor Test	16
Figure 12 – Snap Shot from Video during Motor Test.....	17
Figure 13 – Shear Failure of End Cap	17
Figure 14 – 4.000in ID Rocket Motor Design	18
Figure 15 – Mesh and Axial Stress Results for the Plugged End with 2200psi	18
Figure 16 – Mesh and Axial Stress Results for the Nozzle End with 2200psi	18
Figure 17 – 3.625 in ID Rocket Motor Design	19
Figure 18 – 3.625 in FEA Results	19
Figure 19 – Typical Heat Flux Values Through a Nozzle.....	20
Figure 20 – Temperature Distribution after 3.5sec	20
Figure 21 - Post cure oven	22
Figure 22 – Leak in the motor casing at 750 psi.	23
Figure 23 – Photo of the Aluminum and Carbon Fiber/Epoxy Bond Line.....	24
Figure 24 – Pressure & Thrust Data for October 24, 2008 Test	25
Figure 25 - Unassembled Rocket Parts	25
Figure 26 - AFT and MID sections of carbon fiber airframe have been attached together with internal coupling tubes	26
Figure 27 - Payload Bay.....	26
Figure 28 - Forward Electronics Mounts (1 per rocket).....	26
Figure 29 – A centering ring was adhered the outside of the centering tube and another to the inside of the airframe tube.....	27
Figure 30 – The centering tube is permanently attached to the inside of the airframe tube using centering rings and urethane adhesive.....	27
Figure 31 - Fins were adhered to airframe tube and centering tube.	28
Figure 32 – The fin fixture was used to position the fins while adhesive cured.	28
Figure 33 – Rear centering ring.....	28
Figure 34 – The joint and small voids on the outside surface of the airframe tube were filled with epoxy and sanded flush and smooth.....	29



Figure 35 – Electronics (left) will attach to a fiberglass ring inside bottom of nose cone (right).	29
Figure 36 – An aluminum tip on the nose cone will allow a pressure transducer to be located to take measurement of the stagnation pressure during flight.	14
Figure 37 - Aluminum Tip.....	14
Figure 38 - Outer Surface Clear Coated, Buffed and Waxed	29
Figure 39 – Motor Mount Tube and Retainer Clips	46
Figure 40 – FWD Payload Bay with Recovery Section Added	46
Figure 41 – Internal Lines of the Axisymmetric Ramjet Design	65
Figure 42 – SRGUL uses a 1-D approximation through the combustor.	65
Figure 43 - Mach Number contours for the inlet.....	66
Figure 44 - Mach Number and pressure plots. (Length scales are in meters).....	67
Figure 45 - Contours of Mach Number (Left) and streamlines on pressure contours (Right) of the AFT end of cowl.	67
Figure 46 - Inlet showing shock on lip.	68
Figure 47 - Streamlines through the inlet.....	68
Figure 48 - Forward cowl lip.	69
Figure 49 - Small recirculation region	69
Figure 50 - Intricate shock pattern through the inlet to the throat.	70
Figure 51 - Throat.....	70
Figure 52 - Length scales in inches. Mach Number, pressure, and temperature contours	71
Figure 53 - Total pressure	71
Figure 54 - New inward turning RAMJET design. Inlet, side view, nozzle.	72
Figure 55 - Nearly complete meshed computational domain.....	72
Figure 56 - Pressure contour results for a $z = 0$ plane of the 6" diameter no trough case.	73
Figure 57 - Mach Number contours for the no trough design.	73
Figure 58 - Mach Number contours for the design with troughs.....	74
Figure 59 - Pressure contours for the no trough design.....	74
Figure 60 - Pressure contours for the design with troughs.	75
Figure 61 - With troughs case. The mouth of the inlet is the high pressure red circle.	75
Figure 62 – Stream mark.....	76
Figure 63 - Results from the Axisymmetric CFD Simulation	77
Figure 64 - Streamlines at Different Points in the Ramjet.....	77
Figure 65 - Solid Model without Webs for the 3D CFD Analysis.....	78
Figure 66 - Inward Turning Ramjet with Payload	Error! Bookmark not defined.
Figure 67 - Axi-symmetric Ramjet with Payload	80
Figure 68 – Current Ramjet Design	81
Figure 69 – FWD Section of Ramjet	81
Figure 70 – AFT Section of Ramjet	82
Figure 71 – Arial Map of Launch and Recovery Area (Cherryfield, ME)	87
Figure 72 – Launch Vehicle	31



Figure 73 – Vehicle in Launch Rail and Final Preparations	31
Figure 74 – Vehicle Lift Off and Flight.....	32
Figure 75 – Vehicle Recovery	32
Figure 76 – Typical Flight Electronics.....	33
Figure 77 – Aerial View of Launch Site & Vehicle Locations.....	35
Figure 78 – 1 st Vehicle Altitude and Acceleration Data	36
Figure 79 – 1 st Vehicle Velocity and Nosecone Tip Pressure Data	36
Figure 80 - 1 st Vehicle Altitude from On Board Barometer and Calculated from Acceleration Data Comparison	37
Figure 81 – 3D GPS Plot of the 1 st Vehicle Flight Path	38
Figure 82 - 2 nd Vehicle Altitude and Acceleration Data	40
Figure 83 – 2 nd Vehicle Velocity and Nosecone Tip Pressure Data.....	40
Figure 84 – 2 nd Vehicle Altitude from On Board Barometer and Calculated from Acceleration Data Comparison	41
Figure 85 - 3D Plot of the 2 nd Vehicle Flight Path	42
Figure 86 - Comparison of Predicted Accelerations to Recorded Data	43
Figure 87 - Comparison of Predicted Velocities to Recorded Data	43
Figure 88 - Comparison of Predicted Altitude to Recorded Data	44
Figure 89 – Comparison of the Altitude Pressure Data from the Nosecone Tip Pressure Sensor.....	44
Figure 90 – Picture of Flight Vehicle	47
Figure 91 – Assembled “Dummy Ramjet” Closed.....	48
Figure 92 – “Dummy Ramjet” with all components shown	48
Figure 93 – Rocket Attachment Methods.....	49
Figure 94 – R-DAS Flight Computer	50
Figure 95 – Accu-Fire (Right) & Co-Pilot (Left) Electronics	50
Figure 96 – Vehicle Lift Off and Flight.....	51
Figure 97 – Launch Vehicle	51
Figure 98 – Typical Flight Electronics.....	52
Figure 99 – Aerial View of Launch Site & Vehicle Locations.....	54
Figure 100 – 1 st Vehicle Altitude and Acceleration Data	55
Figure 101 - 1 st Vehicle Altitude and Velocity Data	55
Figure 102 – 1 st Vehicle Velocity and Nosecone Tip Pressure Data	56
Figure 103 – 1 st Vehicle Separation Event	56
Figure 104 – 3D Plot of the 1 st Vehicles Flight	57
Figure 105 - 2 nd Vehicle Altitude and Acceleration Data	58
Figure 106 - 2 nd Vehicle Altitude and Velocity Data	59
Figure 107 – 2 nd Vehicle Velocity and Nosecone Tip Pressure Data.....	59
Figure 108 – 2 nd Vehicle Separation Event	60
Figure 109 - 3D Plot of the 2 nd Vehicles Flight	61
Figure 110 – Predicted Data to Flight Data, Comparing Measured Accelerations.....	62



Figure 111 - Predicted Data to Flight Data, Comparing Calculated Velocities	62
Figure 112 - Predicted Data to Flight Data, Comparing Measured Altitude	63
Figure 113 - Predicted Data to Flight Data, Comparing Calculated Altitude	63
Figure 114 – Picture of Flight Vehicle	87
Figure 115 – Assembled Ramjet	88
Figure 116 – Ramjet with all components shown	88
Figure 117 – Ramjet Shroud	89
Figure 118 – MID Payload Bay Section	90
Figure 119 – Ramjet Coupler Section.....	90
Figure 120 – Booster Section	91
Figure 121 – First Stage Motor Thrust Curve.....	92
Figure 122 – Carbon Fiber/Epoxy Motor Casing.....	92
Figure 123 – Second Stage Ramjet Thrust Curve.....	93
Figure 124 – Ramjet Pressure Transducer Locations.....	94
Figure 125 – R-DAS Flight Computer	94
Figure 126 – Accu-Fire (Left) & Co-Pilots (Right) Electronics.....	95
Figure 127 – November 2009 Launch	96
Figure 128 - 3D Plot of the 2 nd Vehicles Flight	97
Figure 129 - 2 nd Vehicle Altitude and Acceleration Data	98
Figure 130 - 2 nd Vehicle Altitude and Velocity Data	98
Figure 131 – 2 nd Vehicle Velocity and Nosecone Tip Pressure Data.....	99
Figure 132 – Frames from Video of Separation Event.....	99



List of Tables

Table 1 – Surface Preparation verses Bond Strength	21
Table 2 – Flight Vehicle #1 Electronics & Serial Numbers	33
Table 3 - Flight Vehicle #2 Electronics & Serial Numbers	33
Table 4 – Summary of 1 st Flight Vehicle Launched	34
Table 5 – Summary of Time and Altitude at +Ma1 for 1 st Flight	34
Table 6 - Summary of 2 nd Flight Vehicle Launched	39
Table 7 - Summary of Time and Altitude at +Ma1 for 2 nd Flight	39
Table 8 – Flight Vehicle #1 Electronics & Serial Numbers	52
Table 9 - Flight Vehicle #2 Electronics & Serial Numbers	52
Table 10 – Summary of 1 st Flight Vehicle Launched	53
Table 11 - Summary of 2 nd Flight Vehicle Launched	58
Table 12 – Pressure Transducers	95
Table 13 - Summary of 2 nd Flight Vehicle Launched	97



Introduction

Flight testing is a crucial step in the development of scramjet engines.¹ The extremely wide operating margin of scramjets necessitates an extensive number of flight tests to accomplish technology transition, and commercialization goals.² Current flight test methods consume enormous amounts of time and money due in large part to technical complexity. Time and funding limitations severely restrict the number of flight tests conducted. This greatly impedes the advancement of technology, and limits the flight experience of the designer. These flight testing constraints result in the increased demand that each flight yields as much data as possible.³ The imperative need for flight data ultimately drives the growth of technical complexity, which increases the risk of failure. Development of a low-cost flight test platform to investigate ramjet and scramjet flow-path performance would serve as a stepping-stone between ground testing and traditional flight testing, and would play a vital role the development of hypersonic air-breathing propulsion systems. By focusing on flow-path performance and characteristics, many flight systems, including guidance and control, can be eliminated from the vehicle. This approach will significantly reduce technical complexity and cost, resulting in many more flight tests that will provide substantial data available for verifying ground testing and computational methods used to design scramjet engines. This “walk before you run” concept will begin with vertical trajectory flight tests in the lower ramjet operating range, followed by future flight tests conducted at hypersonic speeds. This progressive approach will address industry needs through the systematic increase of flight Mach, in conjunction with methodical growth in technical complexity when needed. Establishing this method will provide the designer with an opportunity to investigate flow phenomena, and structural design in a consistent fashion. The flight experience and propulsion knowledge will allow transition to full system flight testing in less time, at a lower cost, and with decreased risk. The ultimate goal is to conduct scramjet engine flight testing for under \$100K per launch.

This report describes the work done under Phase I in development for demonstrating the proposed low cost flight test platform. The major demonstration goal was to separate a ramjet test article from a boost vehicle at supersonic speeds. The following describes the efforts conducted to achieve this goal.

Project Overview

Applied Thermal Sciences’ (ATS’s) goal of this effort was to demonstrate a low cost, short duration flight test platform to obtain vital flight data on ramjet/scramjet engine operation. Previous work conducted by ATS, under an IR&D program, resulted in flight tests of an ATS designed vehicle boosted to supersonic speeds. Under this program, the rocket motors used for boost were the largest readily available commercially. Adding a ramjet test article to the vehicle design required larger rocket motors to reach speeds of Mach 1.5-2.0. Applied Thermal Sciences expertise in solid propellant rocket motor development was employed during this



program to develop a booster to meet flight mach numbers needed for demonstration. Therefore, ATS developed the rocket motor, flight vehicle, and ramjet test article for this work.

Applied Thermal Sciences successfully achieved the major goal of demonstrating ramjet separation during flight at supersonic speeds. In addition, the ramjet test article included some unique features allowing closed inlet during boost, and open inlet at separation. Stability of flight after separation was also accomplished and documented. The following sections describe the work that was completed over the length of the contract.

Project Milestones

Applied Thermal Sciences had an internal program kick-off meeting on August 2, 2008. At that time work started on the program with the design of the booster motor and main flight vehicle. The following is a summary of the major milestones:

- Supersonic Flight Tests
 - ✓ Launch date: **April 15, 2009**
- Subsonic Flight Tests with Separation of the Dummy Ramjet from the Launch Vehicle
 - ✓ Launch date: **June 5, 2009**
- Supersonic Flight Tests with a Dummy Ramjet
 - ✓ Launch Date: **N/A**
- Supersonic Flight Tests with Separation of a Ramjet from the Launch Vehicle
 - ✓ Launch date: **November 18, 2009**

A total of six (6) flight tests were conducted under this program. The Supersonic Flight Test with a Dummy Ramjet milestone was not conducted based on experience gained with the previous four flight tests. There was enough data acquired and experience with flight predictions that ATS moved to the last milestone, and major goal, of the effort; a supersonic flight test with separation of a ramjet test article. The techniques used during the flight test for separation provided an additional milestone benefit. Instead of the ramjet just flying as a drag device, the configuration produced about 4 g's of acceleration.

The following sections cover the design, fabrication, testing, and analysis tasks to reach each of the program milestones.

Task 1 - Supersonic Flight Tests (Flights 1 & 2)

Under this task, ATS designed a boost vehicle to verify supersonic flight predictions/capabilities with an ATS designed and developed rocket motor. Applied Thermal Sciences flight tested two previous vehicles with commercially purchased ammonium perchlorate (AP) solid propellant motors. The commercially purchased motors were large M-size in total impulse, and



purchasing larger motors commercially was very difficult due to availability. However, ATS designs ammonium nitrate (AN) solid propellant motors, where a N-size or larger motor could be developed based on previous experience. Developing the motors at ATS allowed much greater flexibility in design options that ultimately resulted in more coordination over the motor- vehicle integration process. Hence, the decision was made to design, fabricate, and test the motors needed for the flight vehicles.

It was anticipated that much of the boost vehicle design, to accomplish the first task of demonstrating supersonic flight to Mach 1.5, would also be used to carry out the subsequent tasks in the program. Flight vehicles used for accomplishing the first two flight tests were also used to complete flight test #3 and #4; subsonic separation tests of a dummy ramjet test article. New vehicles were developed for the final flight tests, #5 and #6, demonstrating supersonic separation of a ramjet, which required slight modifications to accommodate a coupler section between the ramjet and booster sections. The following sections discuss the development of the boost vehicles.

Task 1.1 – Vehicle Design

Based on previous development work by ATS, it was found that a 6.0 inch diameter boost vehicle could house a large enough motor to propel a 20-25 lb_m ramjet to supersonic speeds; about Mach 1.5-2.0. A typical launch vehicle is shown in Figure 1 depicting flight vehicle components and their location. The flight vehicle design was a 6 inch diameter airframe, constructed of fiberglass and carbon-fiber materials. The vehicle included an onboard commercial-off-the-shelf (COTS) R-DAS flight computer measuring acceleration, altitude, GPS data and on-board pressure measurements. The data was stored on board as well as transmitted to a ground station via the R-DAS onboard telemetry system.

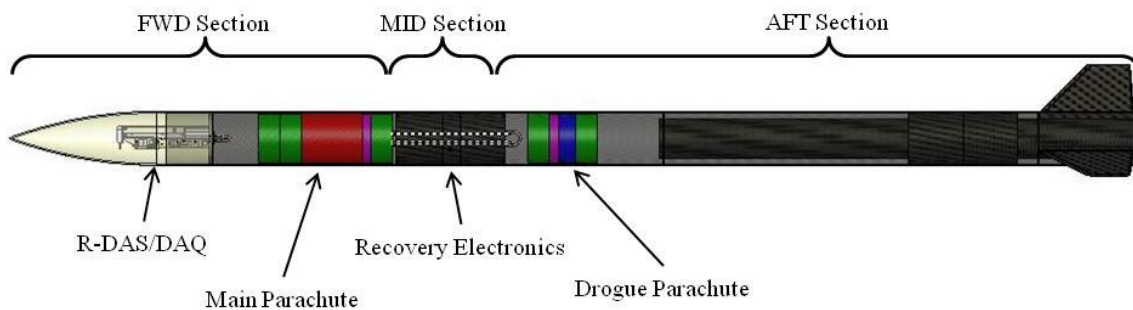


Figure 1 – Typical Rocket Design

Booster & Fin Design



The booster section of the vehicle was designed to withstand a velocity of 3400 ft/sec using short column buckling formulas. The dynamic pressure, at an altitude of 3000 ft, was applied to the frontal area and the thrust was added. The calculation is shown in Figure 2. The estimated dynamic pressure was 93.4 psi (0.94 MPa). This calculation assumes that only the outer airframe is transferring load and the length of the vehicle is from the nosecone tip to the AFT end with no internal stiffening.

$$\begin{aligned}
 \text{RoG} &:= \sqrt{\frac{ID^2 + OD^2}{8}} && \text{Radius of Gyration} && \text{RoG} = 3.031 \cdot \text{in} \\
 \text{SL} &:= \frac{L_{\text{rocket}}}{\text{RoG}} && \text{Slenderness Ration} && \text{SL} = 42.9 \\
 &&&&& \text{SL below 30 - Compression Block} \\
 &&&&& \text{SL 30 to 120 - Short Column} \\
 &&&&& \text{SL above 60 - Long Column} \\
 \hline
 \text{Carbon/Fiber Epoxy} \\
 \sigma_y &:= 32000 \text{ psi} && E := 5.5 \cdot 10^6 \text{ psi} && I_{xx} := \frac{\pi}{64} \cdot (OD^4 - ID^4) && I_{xx} = 5.469 \cdot \text{in}^4 \\
 n &:= 6.0 \text{ psi} && n \text{ value is for Carbon Fiber} && \text{offset} := \frac{OD}{1.5} && \text{Load off set for the centerline of tube} \\
 P_{SC} &:= \frac{\pi}{4} \cdot (OD^2 - ID^2) \cdot (\sigma_y - n \cdot \text{SL}) && P_{SC} = 37785.5 \cdot \text{lbf} && \text{Assumes load is applied at center of tube} \\
 P_{\text{offsetSC}} &:= \frac{P_{SC}}{1 + \frac{8 \cdot \text{offset}}{OD}} && P_{\text{offsetSC}} = 5966.1 \cdot \text{lbf} && \text{Assumes load is offset from center of tube} \\
 FS_{SC} &:= \frac{P_{\text{offsetSC}}}{P_{\text{max}}} && FS_{SC} = 1.59
 \end{aligned}$$

Figure 2 – Basic Airframe Calculations

After the airframe was determined to be adequate; FS_{SC} above 1.0, the fin size was determined. The fin design was based on the fin flutter (fluid induced vibration). This formula shown in Figure 3 uses the fin geometry and vehicle speed to estimate the maximum velocity before fin flutter is initiated. The calculations use the lowest shear strength values of the composite material, resulting in the lowest max velocity for fin flutter.



$$\begin{aligned}
 & \text{Fin}_t := 0.250\text{in} \quad \text{Fin Thickness} \\
 & \text{FinRootChord} := 11.0\text{in} \quad \text{(A) Fin Length Axially Along Airframe (Rule of Thumb: 2 Body Diameters)} \\
 & \text{FinSpan} := 5.5\text{in} \quad \text{(B) Fin Height Radially Out From Airframe (Rule of Thumb: 1 Body Diameter)} \\
 & \text{FinTipChord} := 5.0\text{in} \quad \text{(C) Fin Length Axially at Span Distance} \\
 & \alpha := 5\text{deg} \quad \text{Rocket Angle of Attack} \quad \begin{array}{l} * 0\text{deg Parallel with Flow (Ideal)} \\ * 90\text{deg Perpendicular to Flow} \end{array} \\
 & P_{\text{fin}} := p_{\text{dyn}} \cdot \text{FinRootChord} \cdot (\cos(\alpha) \cdot \text{Fin}_t + \sin(\alpha) \cdot \text{FinSpan}) \quad P_{\text{fin}} = 748.7\text{ lbf} \\
 & \sigma_{\text{epoxy}} := 1500\text{psi} \quad \text{Epoxy shear strength} \\
 & K_t := 3.0 \quad \text{Stress concentration factor (Max) due to geometric change} \\
 & A_{\text{epoxy}} := \text{Fin}_t \cdot \text{FinRootChord} + 2 \cdot \text{FinSpan} \cdot \frac{\text{OD} - \text{ID}}{2} \quad P_{a_{\text{epoxy}}} := \frac{\sigma_{\text{epoxy}}}{K_t} \cdot A_{\text{epoxy}} \quad P_{\text{root}_{\text{epoxy}}} := \frac{\sigma_{\text{epoxy}}}{K_t} \cdot \text{Fin}_t \cdot \text{FinRootChord} \\
 & FS_{\text{fin}} := \frac{P_{a_{\text{epoxy}}}}{P_{\text{fin}}} \quad FS_{\text{fin}} = 2.296 \\
 & G_{\text{Fins}} := 2700 \cdot 10^3 \text{psi} \quad \text{Shear modulus of of the Fins} \\
 & A_{\text{ratio}} := \frac{\text{FinSpan}^2}{\text{FinSpan} \cdot \text{FinTipChord} + 0.5 \cdot \text{FinSpan} \cdot (\text{FinRootChord} - \text{FinTipChord})} \quad \lambda := \frac{\text{FinTipChord}}{\text{FinRootChord}} \\
 & V_{\text{Max}_{\text{flutter}}} := \text{Ma1} \cdot \sqrt{\frac{G_{\text{Fins}}}{\frac{P_{\text{atm}}}{P_{\text{alt}}} \cdot \frac{\lambda + 1}{2} \cdot \frac{39.3\text{psi} \cdot A_{\text{ratio}}^3}{\left(\frac{\text{Fin}_t}{\text{FinRootChord}}\right)^3 \cdot (A_{\text{ratio}} + 2)}}} \quad V_{\text{Max}_{\text{flutter}}} = 3417 \cdot \frac{\text{ft}}{\text{sec}}
 \end{aligned}$$

Figure 3 – Basic Fin Flutter Calculations

For the first two flights, the nose cone on the forward section was constructed of fiberglass with a standard ogive geometry, purchased from a commercial vendor. A modification to the nose cone was required in order to get a stagnation, or total, pressure measurement during flight. The total pressure measurement was added to verify flight speed, and compare against the accelerometer measurements. The nose cone tip includes a pressure port that runs to a pressure transducer embedded into a tapped hole on the backside of the tip, allowing the total pressure to be measured during flight. The tip was bonded into place, as shown in Figure 4.

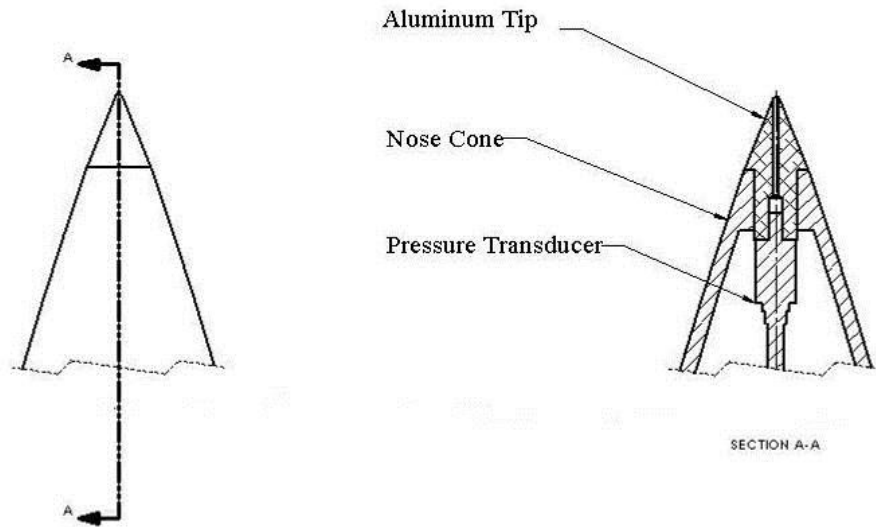


Figure 4 – Aluminum tip on the nose cone for incorporating stagnation pressure measurement during flight.

The aluminum tip (6160-T6) shown in Figure 5 was installed using Lord 7150 A/B urethane adhesive.



Figure 5 - Aluminum Tip

The fiberglass nose cone design was only used on the first two flight to demonstrate Mach 1.5 capability. Subsequent flights required a dummy ramjet and ramjet test articles in place of a standard nose cone. Their design is described in the ramjet development section of this report.

Task 1.2 - Booster Motor Design

Applied Thermal Sciences employed its expertise in solid rocket motor development to design a booster for the flight vehicles. The boosters were sized based on weight of the vehicle, motor, and anticipated ramjet test article needs. The booster motor design for this vehicle is based on ATS composite rocket motor development technology. The design uses commercially available



carbon-fiber epoxy tubing combined with aluminum end depicted in Figure 6. The aluminum ends are used to integrate snap rings into the design to retain the nozzle and end-plug.



Figure 6: ATS Composite Rocket Motor

The following describes the actual designs developed and tested for this effort.

Booster Motor Design and Testing

The ATS rocket booster motors employed an Ammonium Nitrate (AN) solid propellant using a 60% AN, 20% Magnesium, 16.2% R20LM binder and 3.8% Mondur MR curing agent by weight. The initial motor used 9 grains, with geometry of 3.270in OD, 1.500in bore and a length of 6.250in as shown in Figure 7.

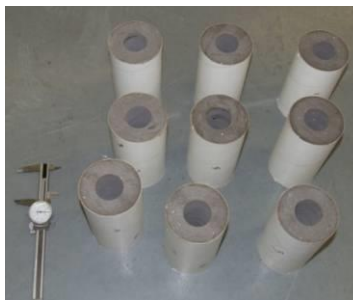


Figure 7 - AN Motor Charges (for reference calipers were set to 2in)

The motor housing was made of carbon-fiber/epoxy with a 4.000in ID and a 4.500in OD capable of withstanding 3000psi internal pressure. The end caps were made of 7075-T6 aluminum. The FWD end-plug was made of 6060-T6 aluminum with 2 O-rings. The AFT nozzle end-plug was made of fine grade extruded graphite; GR008 grade. The nozzle throat diameter was 0.785in with an exit diameter of 1.550 inch, forming an approximate 15 deg expanding nozzle. The



predicted maximum pressure for the motor burn was 1600psi with a maximum thrust of 1260lbf, and a burn time of about 3.5 sec. The motor is shown on the thrust stand in Figure 8. Pressure and thrust data was recorded at 1kHz. The first test took place on Sept. 17, 2008.

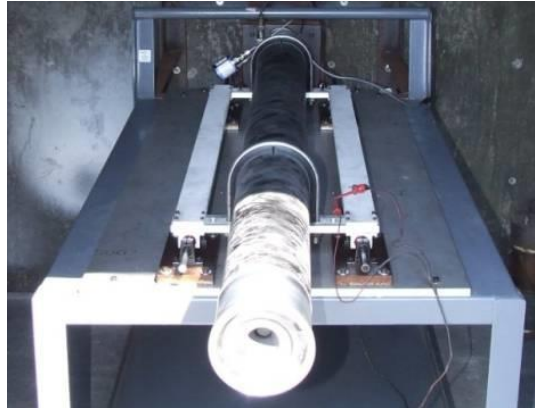


Figure 8 – Motor on Thrust Stand

The test started as predicted with the pressure gradually rising to about 1600psi. At about 1.0 sec the pressure continued to rise to 2165psi and at 1.75sec a CATO (Catastrophic Motor Failure) occurred. The thrust data clipped at 1008 lbf due to a gain setting error, but the load cell had a range of 2000 lbf. This data is shown in Figure 6. A snap shot from the test video, outside the test cell is shown in Figure 7.

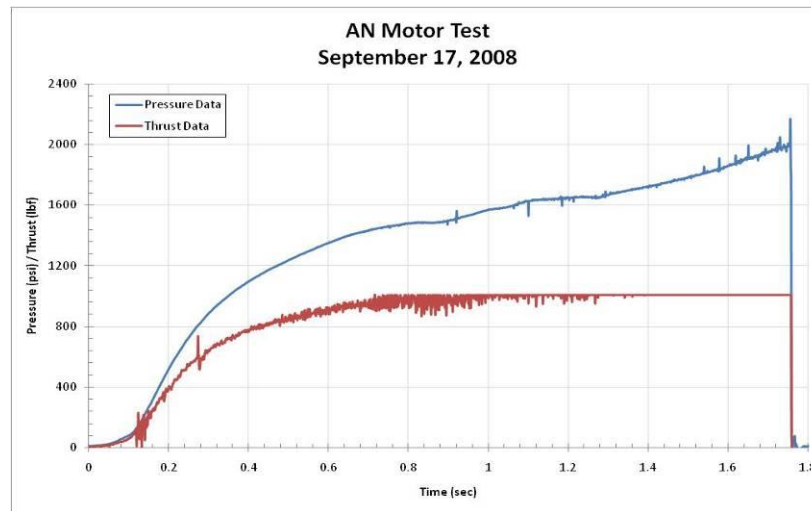


Figure 6 – Test Data from the Motor Test



Figure 7 – Snap Shot from Video during Motor Test

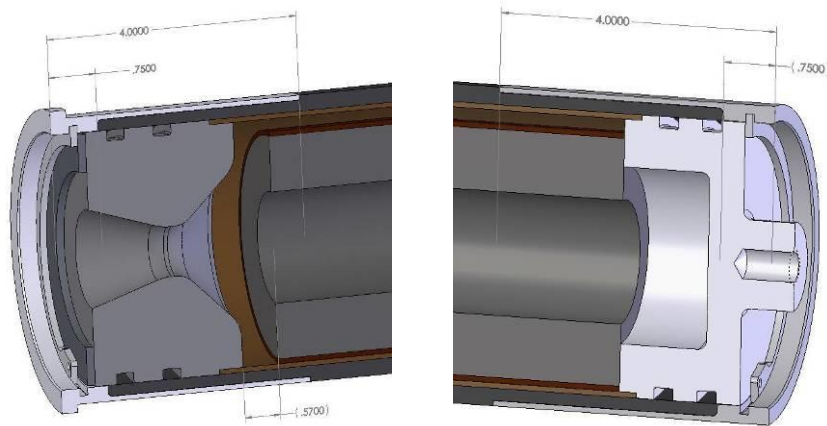
The failure occurred in the aluminum material that holds the snap ring in place. Note the flame below the nozzle exit in Figure 7, which was evidence of a failure at the nozzle-plug or aluminum section at the end of the motor housing. At the end of the test, it was clear that the aluminum section at the nozzle end of the motor housing failed, as shown in Figure 8. Reasons for the failure and potential solutions to the motor failure were then investigated.



Figure 8 – Shear Failure of End Cap

Booster Motor Redesign

The 4.000in ID motor was reanalyzed to understand the test failure, and to eliminate the issue in the next design. The analysis performed was a non-linear FEA using ANSYS software with a 2200psi internal pressure. Both the nozzle end and plugged end were analyzed due to the differences in the geometry as shown in Figure 9.



(a) Nozzle End

(b) Plugged End

Figure 9 – 4.000in ID Rocket Motor Design

This analysis showed that the design was marginal and any material or geometric flaw could have caused the failure. The mesh and axial stress results for the plugged and nozzle end are shown in Figure 10 and Figure 11, respectively.

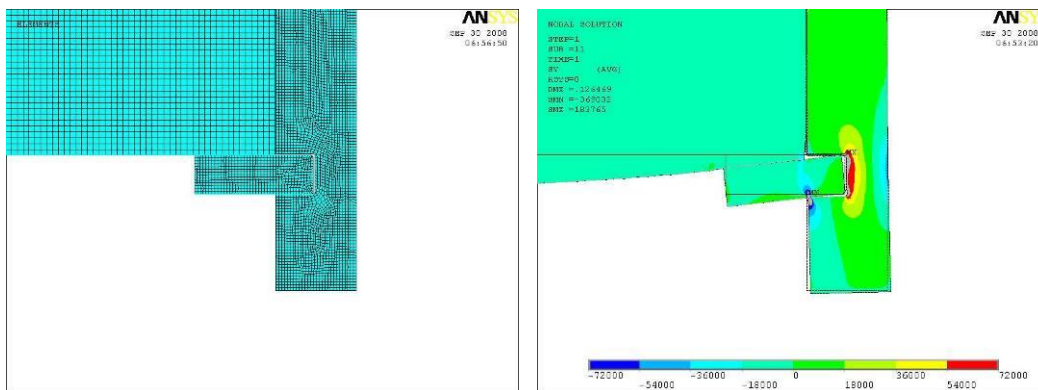


Figure 10 – Mesh and Axial Stress Results for the Plugged End with 2200psi

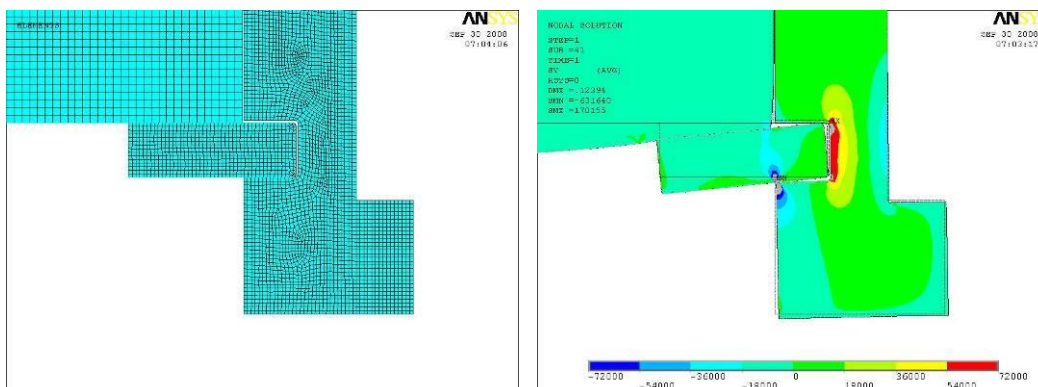
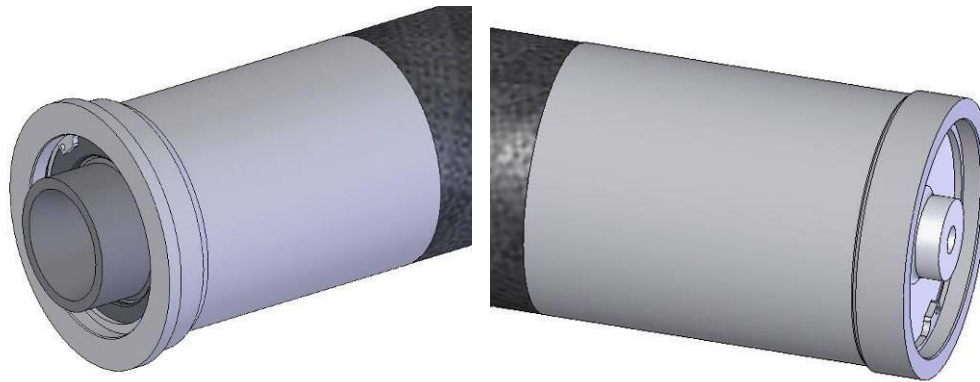


Figure 11 – Mesh and Axial Stress Results for the Nozzle End with 2200psi

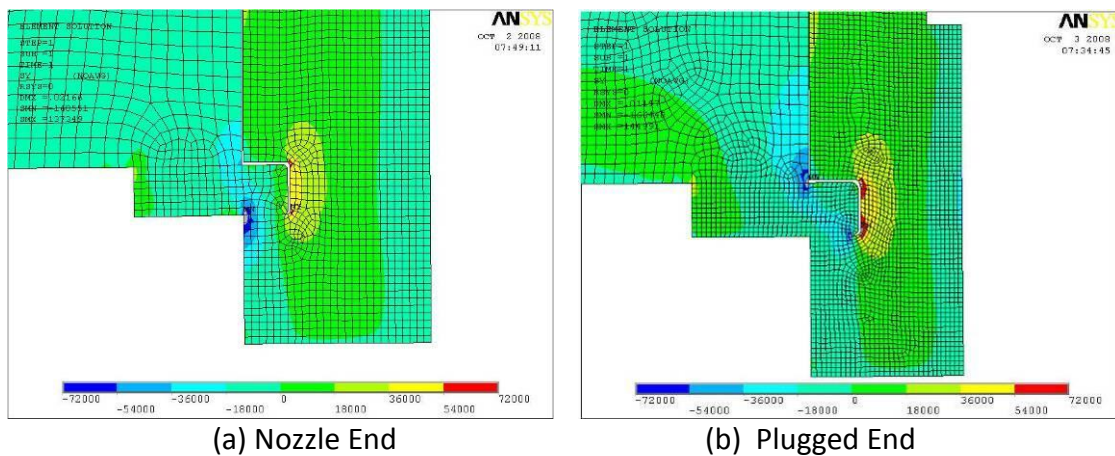


After the motor CATO on September 17, 2008, a plan was developed to design a new motor using a 3.625in ID carbon fiber/epoxy motor casing. Decreasing the diameter of the motor housing allowed for a thicker nozzle end and smaller snap ring. The ends were designed to withstand 3000psi as shown in Figure 12. Thermal and structural FEA models were developed to assist the design effort.



(a) Nozzle End (b) Plugged End
Figure 12 – 3.625 in ID Rocket Motor Design

The linear static FEA models that were developed are axi-symmetric. The structural models had a 3000psi internal pressure applied and the thermal model of the nozzle end was a linear transient model with heat flux and convective heat transfer boundary conditions. The heat flux values used for the nozzle are typical nozzle heat flux values based on Mach number and Area Ratio. The FEA results for the structural analysis are shown in Figure 13. The heat flux values used on the nozzle are shown in Figure 14. The temperature in the nozzle after 3.5sec is shown in Figure 15.



(a) Nozzle End (b) Plugged End
Figure 13 – 3.625 in FEA Results

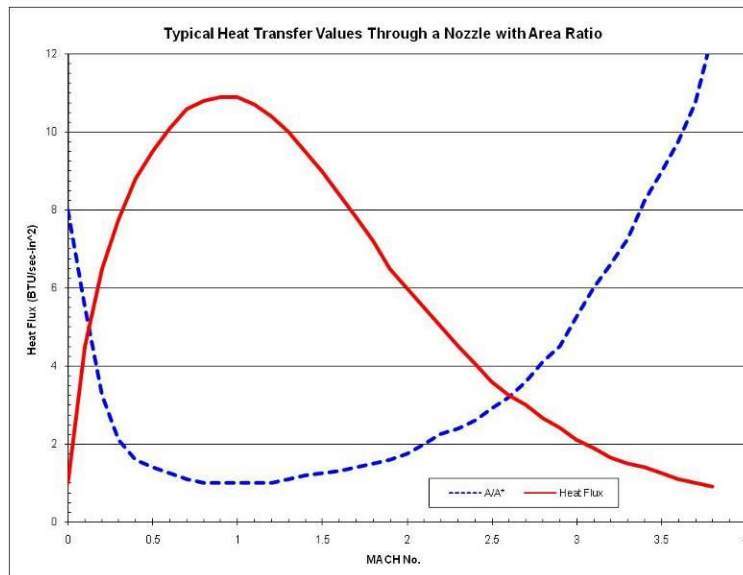


Figure 14 – Typical Heat Flux Values Through a Nozzle

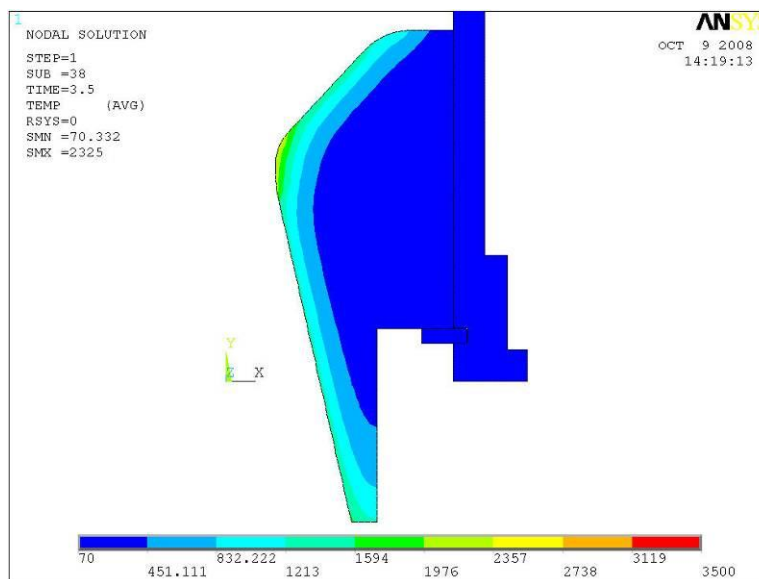


Figure 15 – Temperature Distribution after 3.5sec

Adhesive Selection

The first test with the redesigned motor uncovered a problem with the adhesive used for the aluminum ends of the housing. The motor failed at the adhesive bond line. A review of available adhesive types was conducted to evaluate which type of adhesive would be best suited for bonding the aluminum end caps to the carbon/epoxy casing. Below is a summary of the three families of structural adhesives commonly used today:



- Urethanes
 - ✓ Primarily used for bonding thermoset composites (fiberglass), some thermoplastics and metals with corrosion-resistant coatings/paints¹
 - ✓ Typical operating range, -40 to 180°F¹
 - ✓ Typically more flexible than epoxies, especially at low temp
 - ✓ An etching primer is required for bonding to bare metals²
- Epoxies
 - ✓ Higher strength than urethane, especially at high temps¹
 - ✓ Withstands harsh environments better than urethanes¹
 - ✓ More brittle than urethane, but flexible formulations are available¹
 - ✓ Etching metals is not required, but will increase bond strength³
- Acrylics¹
 - ✓ Cure very quickly
 - ✓ Dissolve most contaminants, little surface cleaning required
 - ✓ Some of the newer formulations offer the same strength as epoxy, but with greater ductility

Further investigation included contacting an applications engineer at 3M and reviewing the application chart on Lord's website. The applications engineer from 3M recommended using a flexible, two-part epoxy adhesive due to the difference in CTE between the carbon/epoxy tube and the aluminum end cap. The Lord application chart also corroborates with 3M's recommendation of using a flexible epoxy for the joint.

After reviewing several acceptable adhesives for our application, the 3M DP190 epoxy was selected as an alternative adhesive to the Lord 7150 urethane adhesive.

Surface Prep

To attain a strong bond to the aluminum casing ends, proper surface prep is required. Below is a summary of various surface treatments and their corresponding bond strength.⁴

Table 1 – Surface Preparation verses Bond Strength

Surface Prep	Bond Strength
Solvent wipe	Low to medium
Abrasion + solvent wipe	Medium to high
Anodize	Medium

¹ Daggett, S., "A Guide to Selection of Methacrylate, Urethane and Epoxy Adhesives", Composite Technology, 4/1/2004

² Minford, J.D., "Handbook of Aluminum Bonding Technology", 1993

³ Ptrie, E.M., "Handbook of Adhesives and Sealants", McGraw Hill, 2006

⁴ Ptrie, E.M., "Handbook of Adhesives and Sealants", McGraw Hill, 2006



Caustic etch	High
Chromic acid etch	Maximum strength

Alternatives to chromic acid etch that involve less toxic chemicals include the phosphoric acid etch, the P-2 etch (sulfuric and ferric acid), and the Sanchem 3000 etching and conversion process.

Post Cure Oven

A post cure oven was fabricated to accelerate the cure time of the 3M DP190 epoxy adhesive which is illustrated in Figure 16. Without a 160°F post cure, the DP190 requires a 7-day cure. The oven was constructed from 6" PVC pipe and utilizes two 100W light bulbs mounted to cleanout plugs at each end to serve as heating elements. The tube was wrapped in fiberglass insulation to decrease the warm up time. A digital temperature controller was used to regulate the oven temperature with a temperature probe at one end of the oven, adjacent to one of the aluminum end caps. Thermocouples were mounted in the center, and at the opposite end from the temperature controller probe to verify symmetric heating of the oven. To facilitate uniform heating of the oven a circulating fan was mounted in one end of the tube. The motor casing was pushed up against the fan which forces air down the inside of the casing with a return loop back between the casing and the PVC pipe during operation.

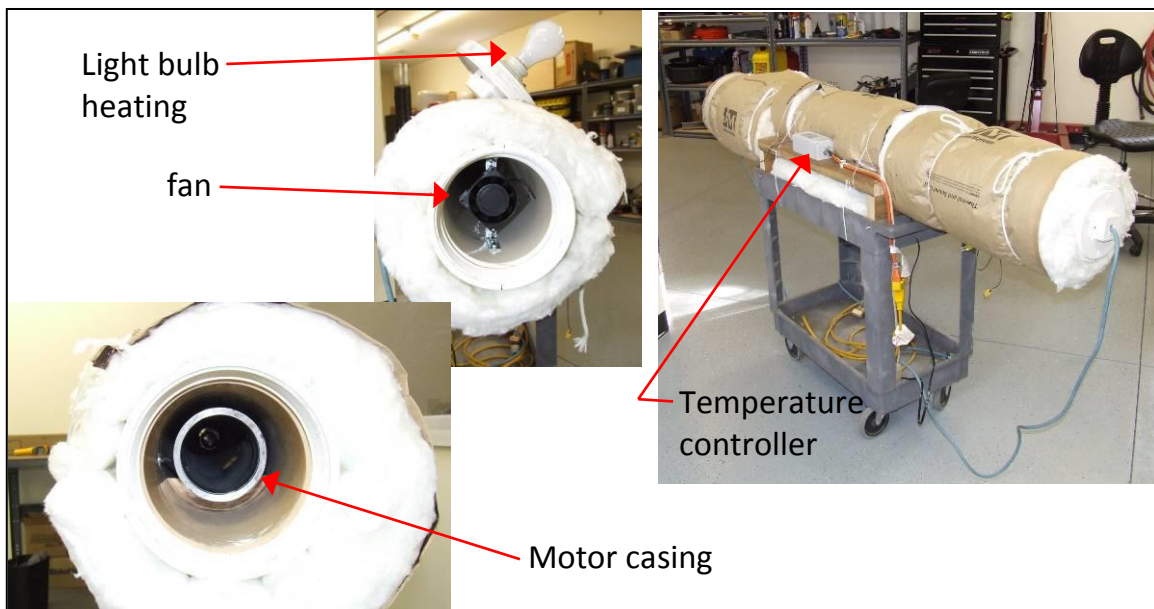


Figure 16 - Post cure oven

Booster Motor Hydrostatic Test



Using the recommended 3M Scotch-Weld DP-190 epoxy adhesive, the motor casting was assembled for hydrostatic testing. The aluminum was grit-blasted and cleaned with a 300 blend cleaner and the carbon fiber/epoxy end was sanded with 60 grit sandpaper and cleaned with a 90% isopropyl alcohol before assembly. After 24 hours of curing, a post cure at 160°F for 2 hours was performed.

After the post cure, the motor casing was hydrostatically tested. During the test, a leak developed at both ends of the motor casing at 750psi (shown in Figure 17). The maximum pressure reached during testing was 1850psi due to leaks.



Figure 17 – Leak detected in the motor casing at 750 psi.

After the test, the ends of the motor casing were cut into sections to examine the bond line. The sample was then photographed under a microscope at a 10x magnification. A typical picture is shown in Figure 18.

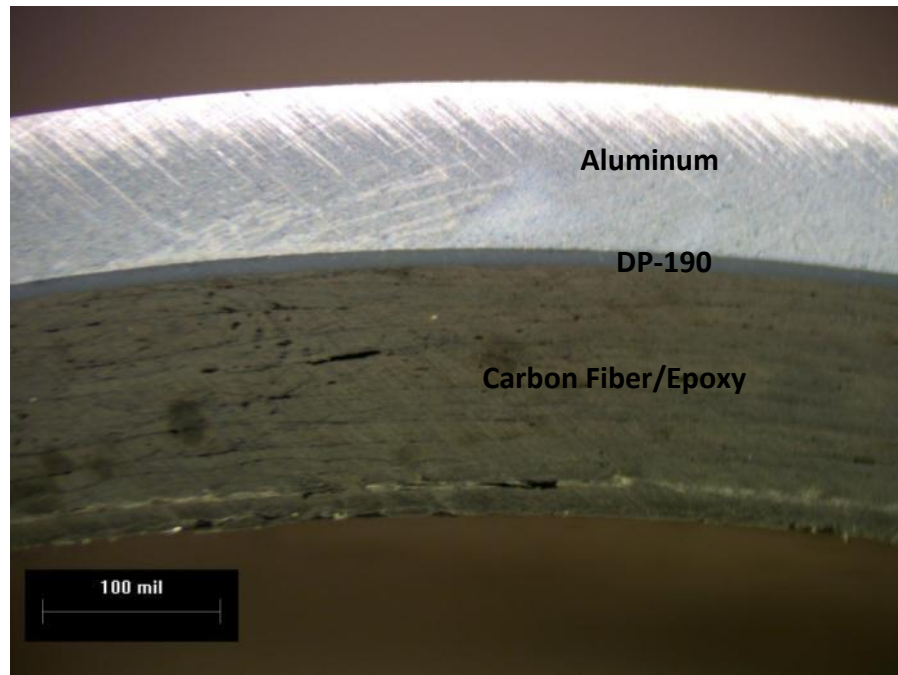


Figure 18 – Photo of the Aluminum and Carbon Fiber/Epoxy Bond Line

The results of the analysis showed a consistent failure at the bond line between the aluminum and adhesive. The failure may have been due to a lack of adhesion, or a weak bond, to the aluminum. Further investigation showed that the 3M was not as strong as the Lord adhesive used initially. In fact, the Lord adhesive turned out to be the easiest to prep, and resulted in the highest pressure capability. Knowing that the Lord adhesive worked to pressures over 2000psia in the first test with the larger motor, a detailed look at the larger and smaller designs showed that a bond line was in the high pressure and high temperature region for the smaller motor. The end-plugs were re-designed to separate all bond lines with at least one O-ring seal, which resulted in the elimination of all leaks.

Booster Motor Testing, October 24, 2008

On October 24, 2008 ATS conducted a second static hot fire test of an AN solid propellant rocket motor. The motor casing employed the new 3.625" ID carbon fiber motor casing. As in the previous test, the propellant geometry used 9 charges with 3.270"OD, 1.500" bore, and 6.250" long having a total propellant weight of 18.393lb. Figure 19 shows the pressure and thrust data of the test compared to the predicted values. The test was a complete success.

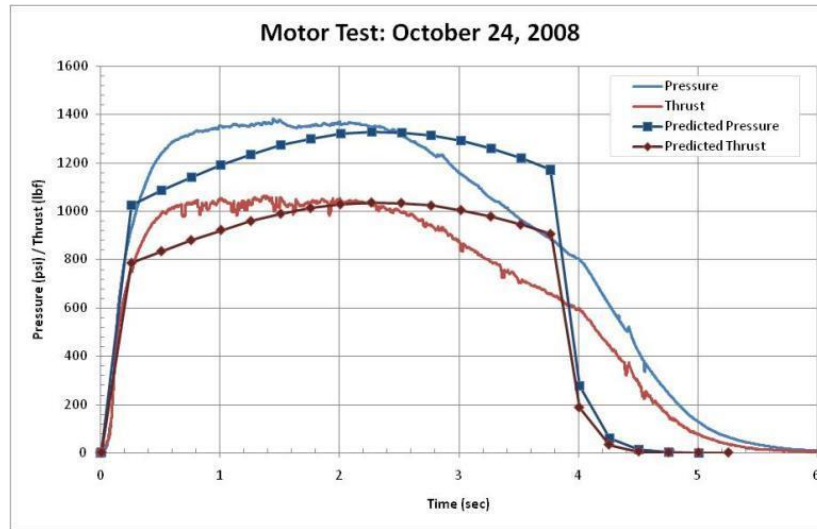


Figure 19 – Pressure & Thrust Data for October 24, 2008 Test

The test produced a maximum thrust of 1065.6 lb, maximum pressure of 1381.4 psi and a total impulse of 17,264 N-s. The performance was determined to be adequate for the first phase flight testing.

Task 1.3 – Flight Vehicle and Motor Fabrication

The following section shows the assembly of the booster(s) sections. Unassembled parts are shown in Figure 20.



Figure 20 - Unassembled Rocket Parts

The AFT and MID sections of carbon fiber airframe tube were bonded together, as shown by Figure 21, using a 12.25 inch long carbon fiber internal coupling tube and Devcon 2 ton epoxy.



Figure 21 - AFT and MID sections of carbon fiber airframe have been attached together with internal coupling tubes

Assembly parts of the forward coupling tube, which doubles as a payload bay, is shown attached in Figure 22.



Figure 22 - Payload Bay

The forward electronics mounting components were assembled and bonded in place using the Devcon 2-ton epoxy, as shown in Figure 23.



Figure 23 - Forward Electronics Mounts (1 per rocket)



A carbon fiber motor centering tube was installed inside the carbon fiber airframe tube. Carbon fiber rings were used as a means of centering and attaching the centering tube. One ring was adhered to the outside of the centering tube and another to the inside of the airframe tube. Figure 24 shows the centering tube was positioned inside the airframe tube and the remaining free surfaces on the centering rings were adhered to their respective adjacent parts. Figure 25 shows the bond line, where the adhesive used was LORD 7150 A/B urethane adhesive.

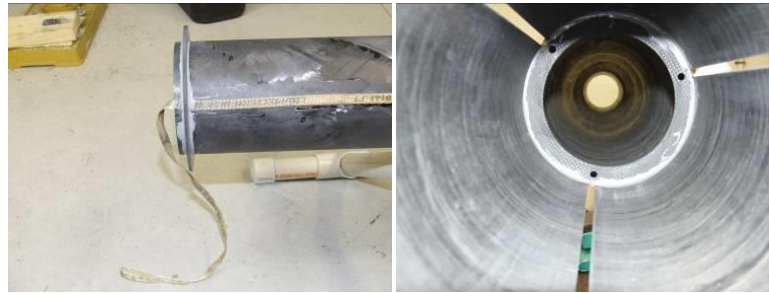


Figure 24 – A centering ring was adhered to the outside of the centering tube and another to the inside of the airframe tube.



Figure 25 – The centering tube is permanently attached to the inside of the airframe tube using centering rings and urethane adhesive.

Carbon fiber fins were attached as shown in Figure 26 using LORD 7150 A/B urethane adhesive. The fin fixture referenced in the monthly reports was used to position the fins. The fixture was designed to locate the fins by inserting a plug into the ID of the centering tube. This aspect of the fixture was not as effective as had been anticipated; however, the fixture was found to be effective if used without the plug and clamped into place as shown in Figure 27.

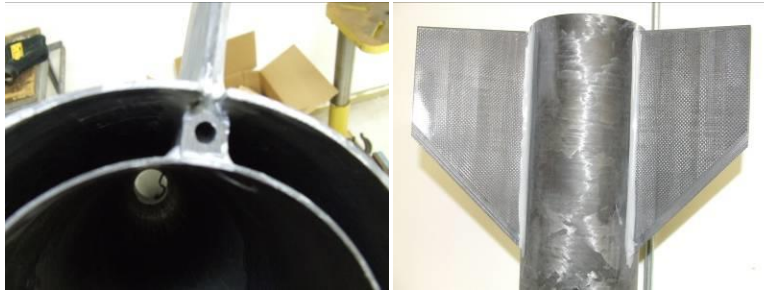


Figure 26 - Fins were adhered to airframe tube and centering tube.

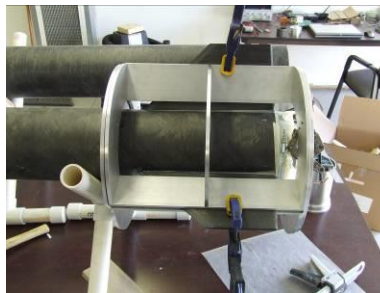


Figure 27 – The fin fixture was used to position the fins while adhesive cured.

The third and final carbon fiber centering ring was bonded into place after fin attachment, at the rear of the vehicle, using LORD 7150 A/B urethane adhesive. Prior to installation, three holes were drilled in the ring, and T-nuts, aligned with the drilled holes, were bonded in place (see Figure 30). This design provides a means of attaching clips to hold the motor in place during the descent portion of flight.



Figure 28 – Rear centering ring.

All outside surfaces of the airframe and fins, as well as the adhesive holding them in place, were sanded smooth and flush. Before sanding, irregularities in the joint on the airframe body were filled with epoxy. The same was done for voids found on the outside surface of the airframe tube. These voids, present due to the tube manufacturer's manufacturing process, were filled with epoxy, as illustrated in Figure 29.



Figure 29 – The joint and small voids on the outside surface of the airframe tube were filled with epoxy and sanded flush and smooth.

A G-10 fiberglass ring, prepared with holes and T-nuts, was bonded into place at the bottom of the nose cone using Devcon 2-ton epoxy. This ring serves as a method of attaching the forward electronics shown in Figure 30.

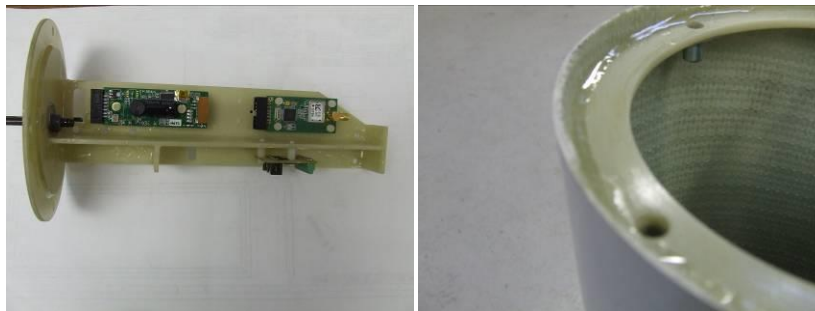


Figure 30 – Electronics (left) are attach to a fiberglass ring inside bottom of nose cone (right).

All outside surfaces of fins, airframe and nosecone were painted with a clear coat by Cabana's Auto Body in Sanford, ME. The surfaces were then buffed and waxed. The finished product is shown in Figure 31.

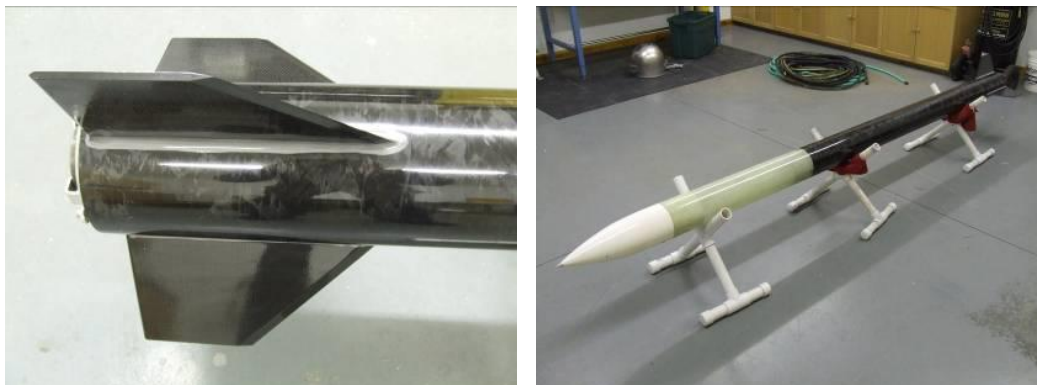


Figure 31 - Outer Surface Clear Coated, Buffed and Waxed



Electronics Range Testing

A test to determine the range of the R-RAS Telemetry Board was conducted. Two of the four Co-Pilots were tested and configured for launch. The R-DAS units were tested aboard an airplane flying about 4500 ft. altitude, and the receiving unit was located at ground level. The maximum distance for receiving telemetry was 6.5 miles for one unit and 8.5 miles for the other. The GPS system locked on satellites in approximately 40 seconds and stayed fixed during testing. Also a complete analog testing of the two electronic assemblies was performed by removing a functional microprocessor from PCB, which was then re-installed for proper operation.

Launch and Recovery Zone

The launch site is located in Cherryfield, ME approximately 1 hour and 30 minutes East, South-East of Bangor, ME. The launch area is on the Jasper Wyman & Son blueberry fields as shown in Figure 113. All FAA and Maine DOT permits were acquired. Richard Willey was the designated LSO (Launch Safety Officer) and David Smith was designated the interface to the FAA and RSO (Range Safety Officer).



Figure 32 – Aerial Map of Launch and Recovery Area (Cherryfield, ME)



Launch #1 - Supersonic Flight Tests on April 15th, 2009

A first launch Flight Plan was assembled and is included in the appendices of this report. Two vehicles were successfully launched and recovered on Wednesday, April 15, 2009. Figure 33 shows one of the two launch vehicles, which was designed to withstand Mach 3.0 flight at low altitudes. The vehicle was designed with a carbon-epoxy booster and fins, and fiberglass for mid-payload and nosecone. Figure 34 shows the vehicle in the launch rail and final ground preparations before launch. Figure 35 and Figure 36 show the launch, flight and recovery of the vehicle.



Figure 33 – Launch Vehicle



Figure 34 – Vehicle in Launch Rail and Final Preparations



Figure 35 – Vehicle Lift Off and Flight



Figure 36 – Vehicle Recovery

The vehicles were equipped with on board DAQ systems, measuring pressure at the nose tip, axial accelerations and barometric pressure inside the payload bay and recovery electronics. The R-DAS system recorded data at a 200Hz sample rate onboard and 5Hz sample rate transmitted to ground station. The electronics are shown in Figure 37 and serial numbers are listed in Table 2 and Table 3. Video of both launches was recorded and are available upon request.

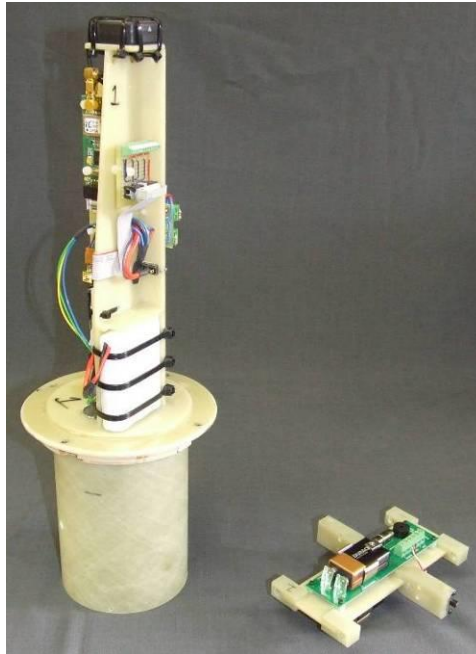


Figure 37 – Typical Flight Electronics

Table 2 – Flight Vehicle #1 Electronics & Serial Numbers

Item Name	Serial Number
R-DAS Main Board	06253
R-DAS GPS Board	97193 00007
R-DAS Telemetry Board	01458
Kulite ELT-76A-190-50A Pressure Transducer	6893-5-118
PML Co-Pilot	1504
PML Co-Pilot	1482

Table 3 - Flight Vehicle #2 Electronics & Serial Numbers

Item Name	Serial Number
R-DAS Main Board	06252
R-DAS GPS Board	97193 00039
R-DAS Telemetry Board	01457
Kulite ELT-76A-190-50A Pressure Transducer	6893-5-137
PML Co-Pilot	1502
PML Co-Pilot	1506

April 2009 Flight - 1st Launch Summary

The 1st vehicle was recovered approximately 2.3 miles South-East of the launch pad as shown in Figure 38. The 24" drogue diameter parachute opened at apogee and the main 78" diameter



parachute opened at 1000 ft. The upper level winds were approximately 35-40 knots. A summary of the data is listed in Table 4. Table 5 lists the time into flight and altitude the vehicle was at or above speed of sound. Figure 39 shows the recorded acceleration and altitude (onboard barometric sensor) and Figure 40 shows the calculated velocity from the acceleration data and nosecone tip pressure. Figure 41 shows the altitude (from the onboard barometric sensor), calculated altitude (from the acceleration data) and the calculated velocity. Note the difference in the altitudes at the start of the launch through max velocity; this is due to the internal pressure of the payload bay lagging the actual external pressure and fluid effects around the vehicle. In addition, this sensor was recording pressure incorrectly based on final altitude from other measurements (i.e. Co-pilot and accelerometers). Figure 42 shows a 3D plot of the vehicle from launch to recovery.

Table 4 – Summary of 1st Flight Vehicle Launched

R-DAS			
GPS Altitude:	19,898	ft	
GPS Launch:	N 44.678649	W 67.890306	
GPS Recovery:	N 44.653935	W 67.859191	
Recorded Altitude:	17,710	ft	
Max Altitude (Calculated):	19,175	ft	
Recorded Acceleration:	18.62	g's	
Velocity:	1668.9	ft/sec	
Ma (c = 1106 fps):	1.51		
Nosecone Tip Pressure:	40.9	psia	
Co-Pilot #1			
Recorded Altitude:	19,495	ft	
Co-Pilot #2			
Recorded Altitude:	n/a	ft	

Note: The calculated stagnations pressure was 42.2 psia at 3,000ft and 1680 fps.

Table 5 – Summary of Time and Altitude at +Ma1 for 1st Flight

	Time <i>sec</i>	Velocity <i>ft/s</i>	Altitude <i>ft</i>
Enter Ma1	2.265	1100	1183.1
Max Velocity	4.375	1668.8	4247.1
Exit Ma1	7.730	1100	8903.1



Figure 38 – Aerial View of Launch Site & Vehicle Locations

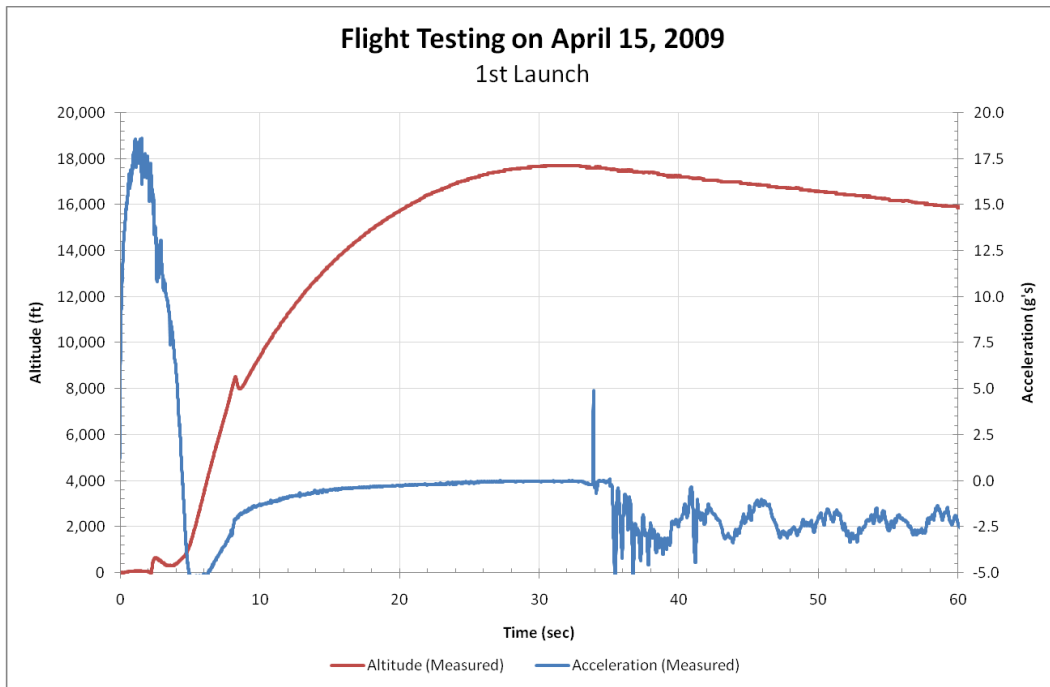


Figure 39 – 1st Vehicle Altitude and Acceleration Data

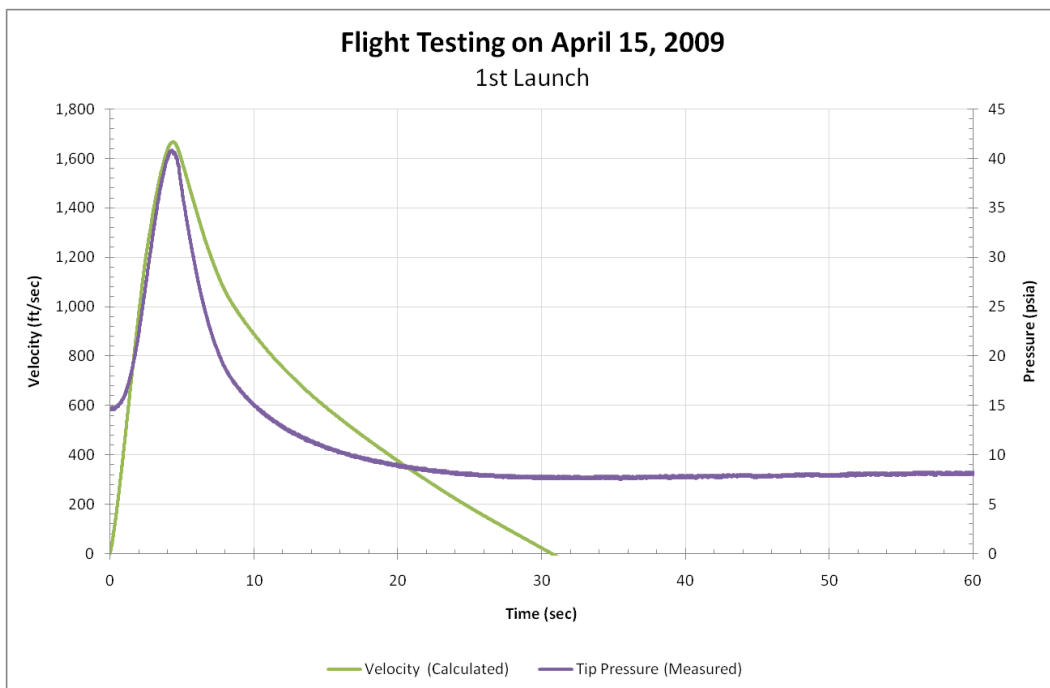


Figure 40 – 1st Vehicle Velocity and Nosecone Tip Pressure Data

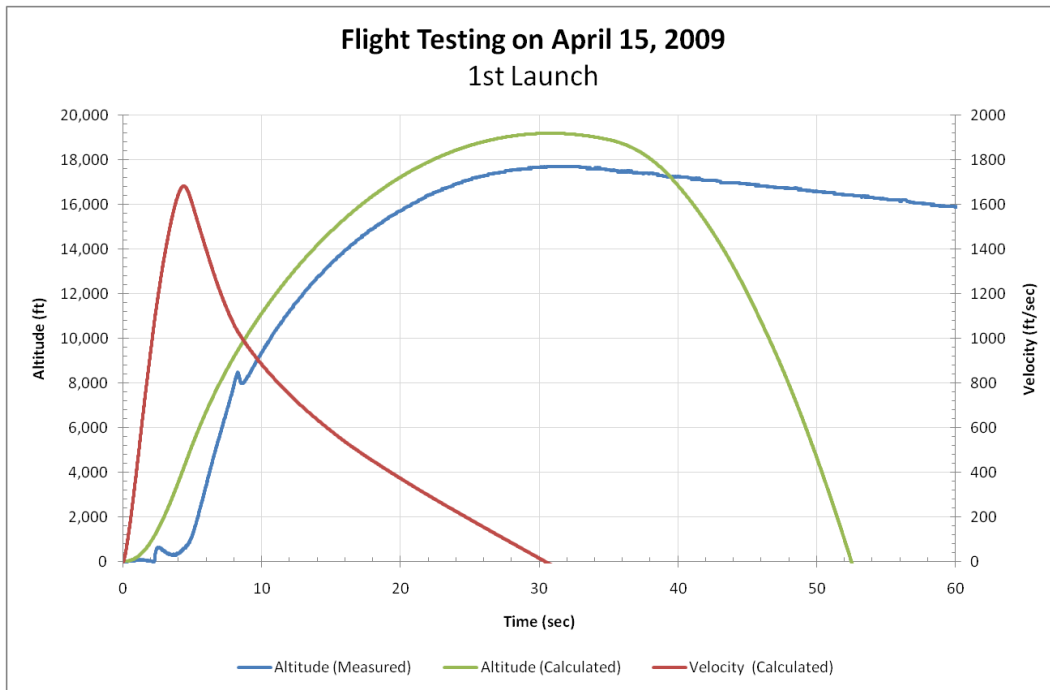


Figure 41 - 1st Vehicle Altitude from On Board Barometer and Calculated from Acceleration Data Comparison

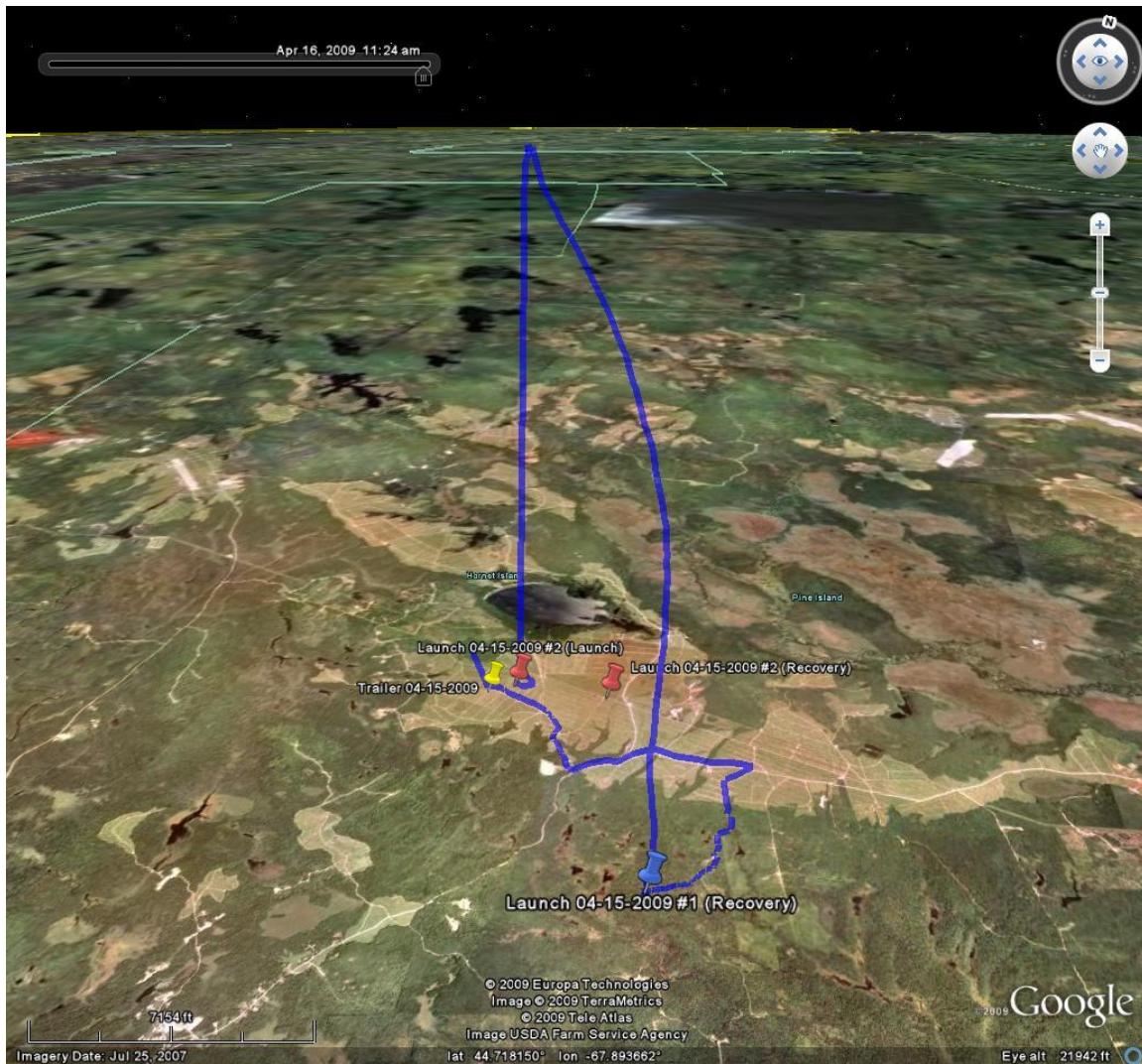


Figure 42 – 3D GPS Plot of the 1st Vehicle Flight Path

April 2009 Flight - 2nd Launch Summary

On the 2nd vehicle the drogue parachute was replaced with a 15ft streamer and the angle of the launch tower was adjusted to a larger angle from vertical and into the wind direction. This vehicle was recovered approximately 0.75mi east of the launch pad as shown in Figure 46. A summary of the data is listed in Table 6. Table 7 lists the time into flight and altitude the vehicle was at or above speed of sound. Figure 43 shows the recorded acceleration and altitude (onboard barometric sensor) and Figure 44 shows the calculated velocity from the acceleration data and nosecone tip pressure. Figure 45 shows the altitude (from the onboard barometric sensor), calculated altitude (from the acceleration data) and the calculated velocity. Again note the difference in the altitudes at the start of the launch through max velocity; this is due to the internal pressure of the payload bay lagging the actual external pressure and fluid



effects around the vehicle. Figure 46 shows a 3D GPS plot of the vehicle from launch to recovery.

Table 6 - Summary of 2nd Flight Vehicle Launched

R-DAS			
GPS Altitude:	19,367	ft	
GPS Launch:	N 44.678686	W 67.890322	
GPS Recovery:	N 44.678880	W 67.876040	
Recorded Altitude:	19,240	ft	
Max Altitude (Calculated):	19,037	ft	
Recorded Acceleration:	19.31	g's	
Velocity:	1683.5	ft/sec	
Ma (c = 1106 fps):	1.52		
Nosecone Tip Pressure:	42.5	psia	
Co-Pilot #1			
Recorded Altitude:	18,847	ft	
Co-Pilot #2			
Recorded Altitude:	n/a	ft	

Note: The calculated stagnations pressure was 37.8psia at 3,000ft and 1680 fps.

Table 7 - Summary of Time and Altitude at +Ma1 for 2nd Flight

	Time <i>sec</i>	Velocity <i>ft/s</i>	Altitude <i>ft</i>
Enter Ma1	2.275	1098	1187.7
Max Velocity	4.345	1683.5	4204.9
Exit Ma1	7.695	1099	8874.5

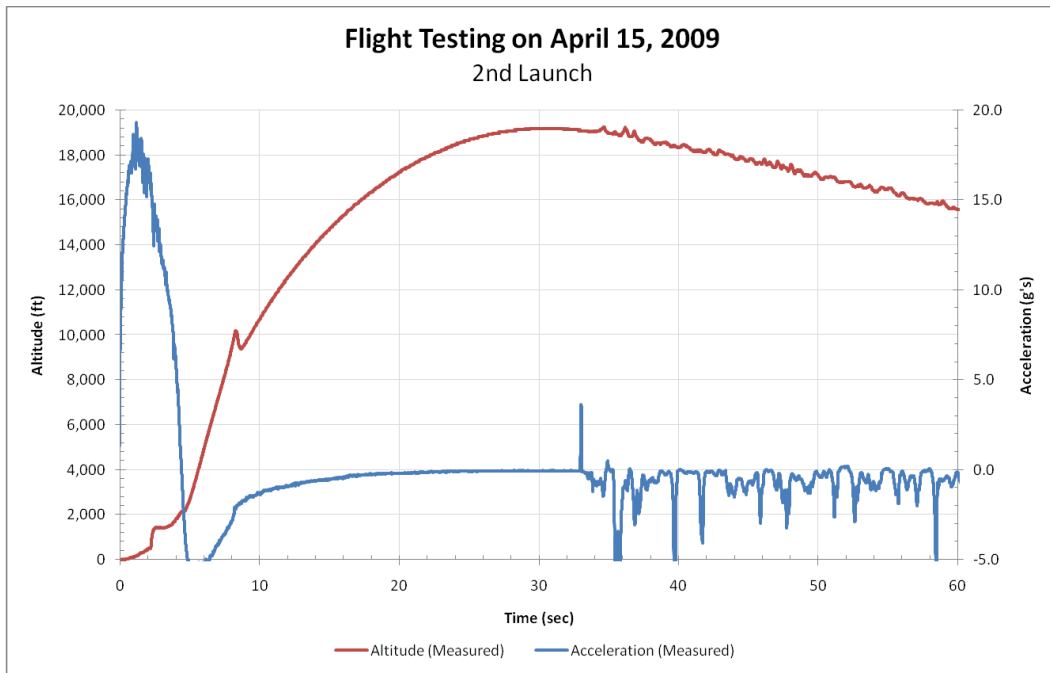


Figure 43 - 2nd Vehicle Altitude and Acceleration Data

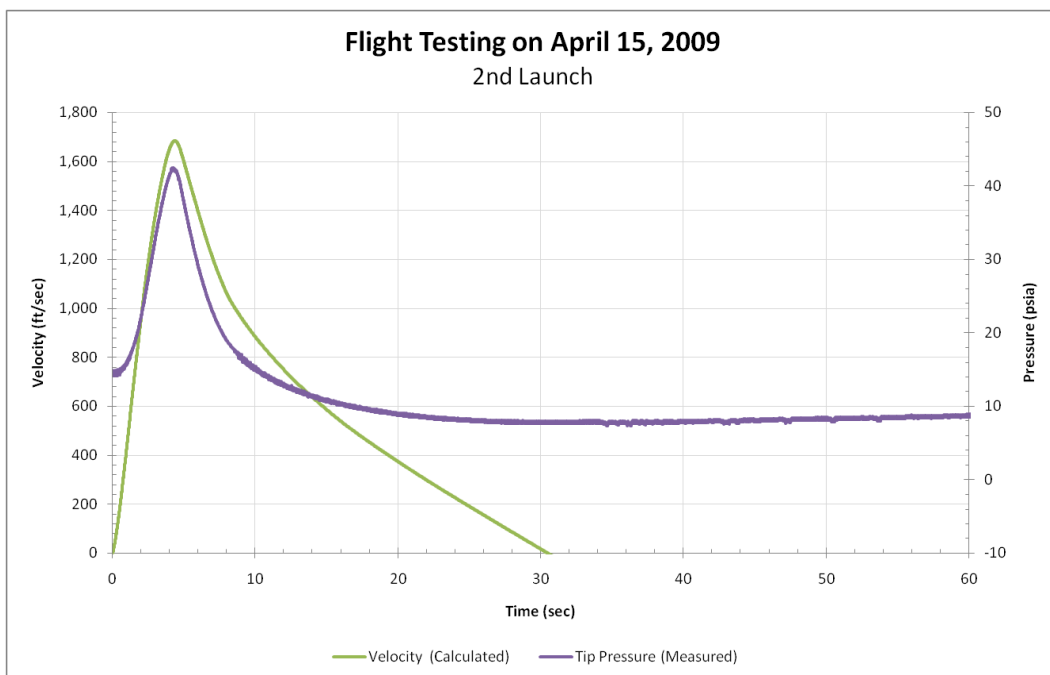


Figure 44 – 2nd Vehicle Velocity and Nosecone Tip Pressure Data

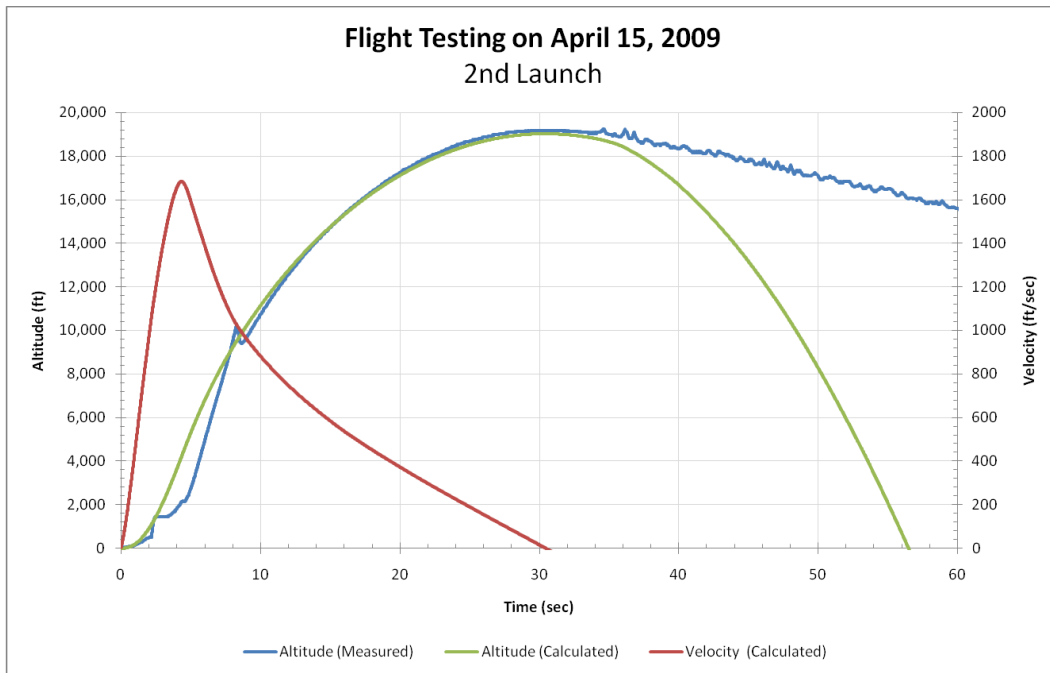


Figure 45 – 2nd Vehicle Altitude from On Board Barometer and Calculated from Acceleration Data Comparison

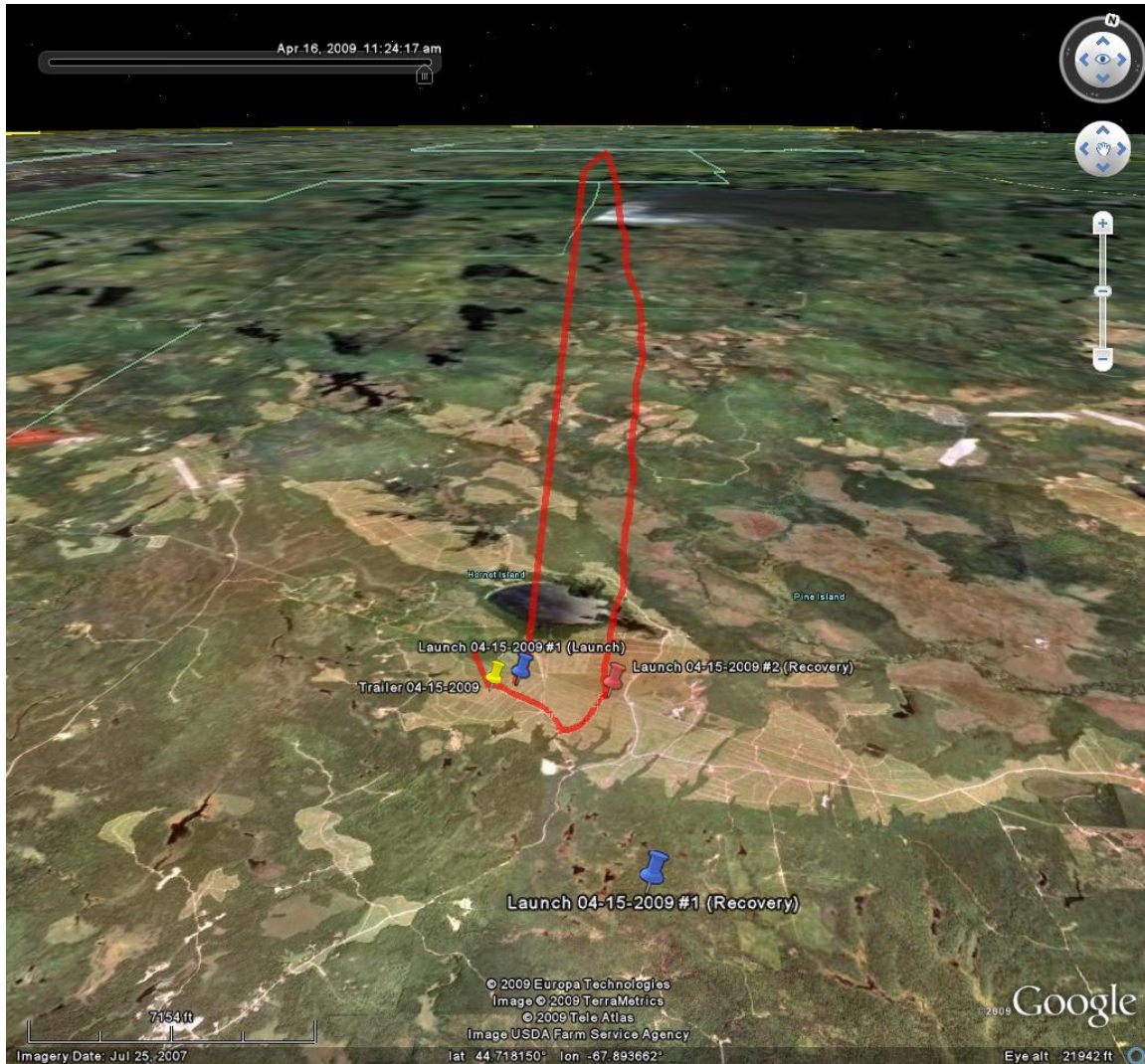


Figure 46 - 3D Plot of the 2nd Vehicle Flight Path

April 2009 Flight - Data to Predicted Flight

Figure 47 show the recorded acceleration on from the onboard accelerometer for both flights compared to the predicted flight from RockSim 8.0 flight software. Figure 48 shows the calculated velocity compared to the predicted velocity from the software. Figure 49 depicts the calculated altitude for both vehicles compared to the predicted altitude. Note that the data from RockSim software uses an absolute value and is only valid to apogee or about 32 seconds. After apogee, the vehicle orientation may vary widely due to many factors, such as tumbling. Overall the data compares extremely well to predicted results.

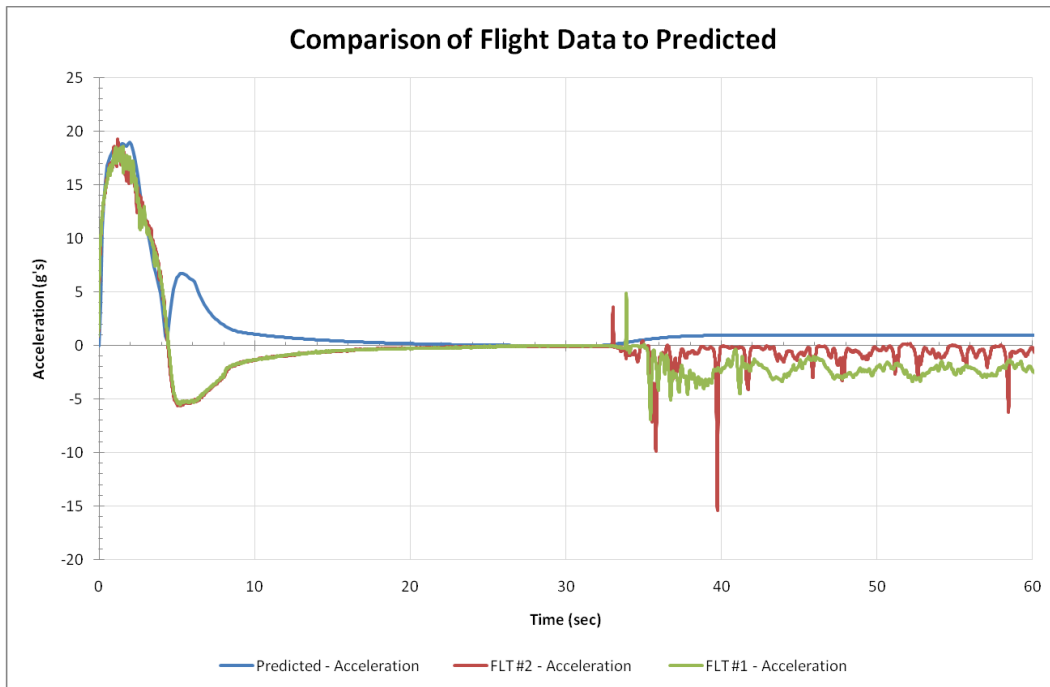


Figure 47 - Comparison of Predicted Accelerations to Recorded Data

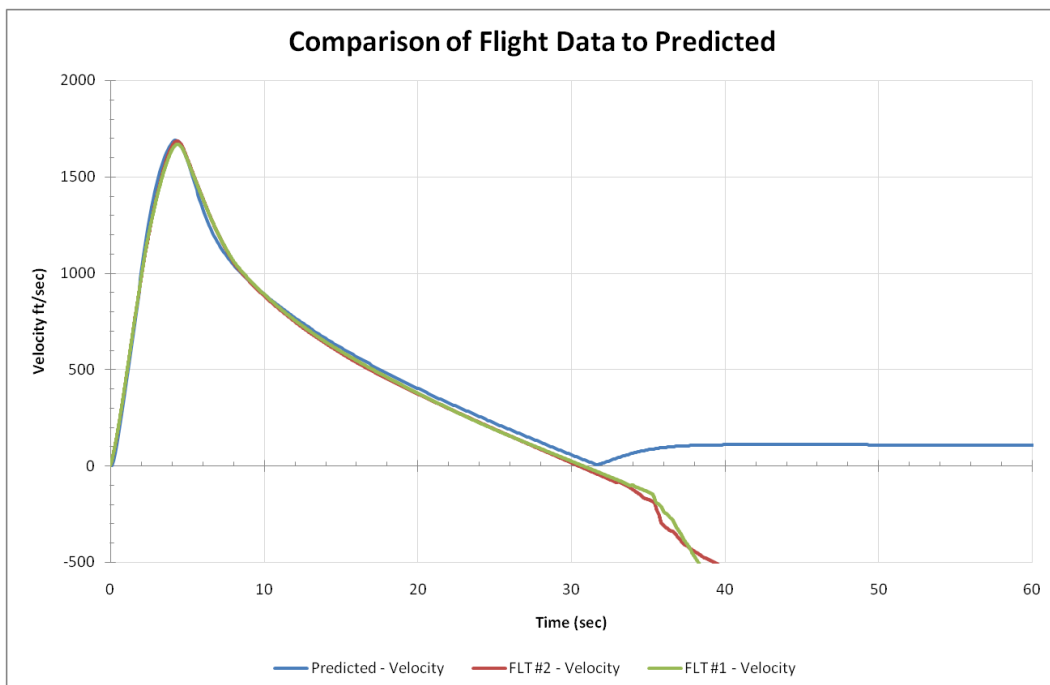


Figure 48 - Comparison of Predicted Velocities to Recorded Data

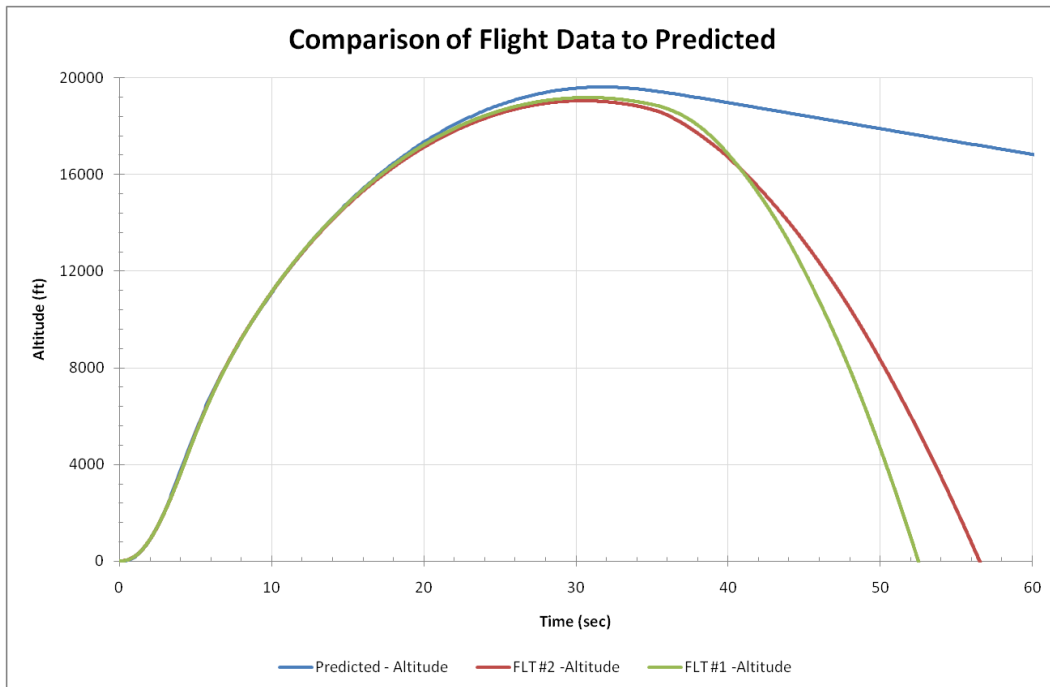


Figure 49 - Comparison of Predicted Altitude to Recorded Data

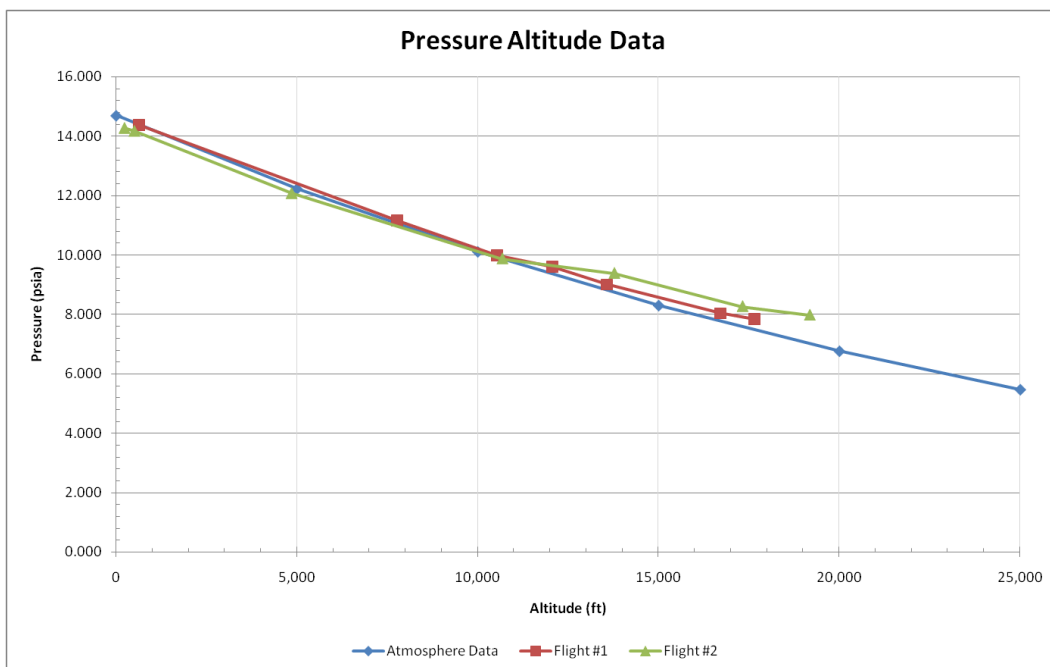


Figure 50 – Comparison of the Altitude Pressure Data from the Nosecone Tip Pressure Sensor

The flight tests at supersonic speed were both very successful. The predicted data match the flight data extremely well. Hence, the RocSim software is satisfactory for predicting flight velocity, acceleration, and altitude for a rocket propelled vehicle. The electronics and



instrumentation used for the flight tests worked well and were quite stable with very low distortion or noise from flight testing. The GPS systems all worked very efficiently, as proven in the first flight test where the vehicle was found, using the telemetry GPS coordinates, in a wooded area 2.3 miles from the launch point. The stored on-board data was easily downloaded to a computer for analysis. With the excellent results from this supersonic flight test, we moved on to the subsonic flight testing with separation.

Launch 2 – Subsonic Flight Tests with Separation of the Dummy Ramjet from the Launch Vehicle (Flights 3 & 4)

The next launch, Launch 2, required the separation of a dummy ramjet at subsonic speeds. The reason these flights were conducted was to gain some experience on the separation process. The technique decided upon was to use black powder to push the dummy ramjet away from the booster section of the vehicle. This appeared to be the simplest method for separation, based on complexity of the system. Computational methods were employed to determine how far to push the two bodies apart to prevent a collision after separation. This information was then transformed into an estimate on black powder required to meet the separation needs. The following sections provide the detail involved with completing the milestone effort.

Booster Motor for Subsonic Flight Tests

The booster motors for the subsonic flight testing were purchased commercially. Since only an M-size motor was required, they are easily acquired through the commercial sector, which eliminated the need to develop a new motor for this specific flight testing.

Two adaptations to the flight vehicles were made that will enable subsonic separation flight tests.

1. A removable motor centering tube, depicted in Figure 51, was built to allow use of the following commercial motor: Animal Motor Works, M2500 Green Gorilla, 75mm motor casing, 7600 N-s casing. Aluminum clips hold the motor casing and centering tube in place during the descent portion of flight.
2. A parachute tube was added to the forward payload as shown in Figure 52. The cap on the tube is held in place by 4 nylon shear pins, which break away when a black powder charge is ignited, deploying a parachute from the uncovered tube.



Figure 51 – Motor Mount Tube and Retainer Clips

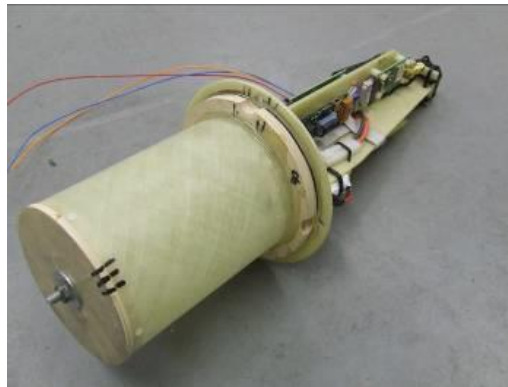


Figure 52 – FWD Payload Bay with Recovery Section Added

Task 3.2 – Boost Vehicle with Dummy Ramjet Test Article

The flight vehicle consists of three main sections: FWD “Dummy Ramjet” section, MID payload bay, and AFT motor section. A picture of one of the vehicles is shown in Figure 53. The overall vehicle lengths are 330.2 cm (130 in) and the airframe outside diameter of 15.77 cm (6.21 in).

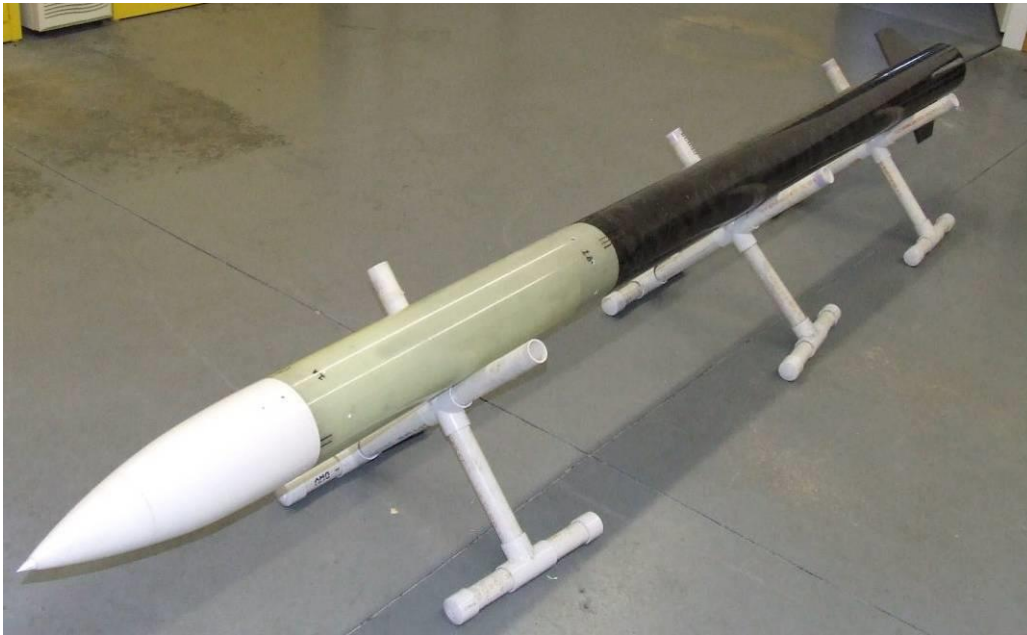


Figure 53 – Picture of Flight Vehicle

June 2009 Flight - FWD “Dummy Ramjet” Section

The FWD “Dummy Ramjet” section houses the flight computer. This flight computer records pressures, accelerations, altitude and GPS data. More information on the flight computer is provided in the “Electronics Section”. The nosecone and FWD airframe section is made of fiberglass/epoxy. The FWD nosecone is a 3:1 ogive 48.26 cm (19 in) long with a 15.67cm (6.170 in) base diameter. The AFT boat tail is a 3:1 ogive tapered to 8.89 cm (3.500 in). The recovery parachute is located in the boat tail section and with 4, #4-40 nylon shear screws shown in Figure 55. The screws are counter sunk into the airframe to minimize drag. A streamer deploys at apogee and a secondary charge fires to deploy the parachute at an altitude of 304.8 m (1000 ft) controlled by the R-DAS electronics.

The “Dummy Ramjet” ejects from the FWD airframe section with a black powder charge controlled by the G-Wiz Accu-Fire. The Accu-Fire system detects motor burn out and fires the charge. This event was designed to occur approximately 3.25 sec after lift-off at maximum velocity. The separation charge produced approximately 2589 N (581 lbf) on the end of the Dummy Ramjet and the booster section. This force separates the two bodies. The estimated maximum drag force on the vehicle was 1150 N (258 lbf) just after motor burnout.



Figure 54 – Assembled “Dummy Ramjet” Closed

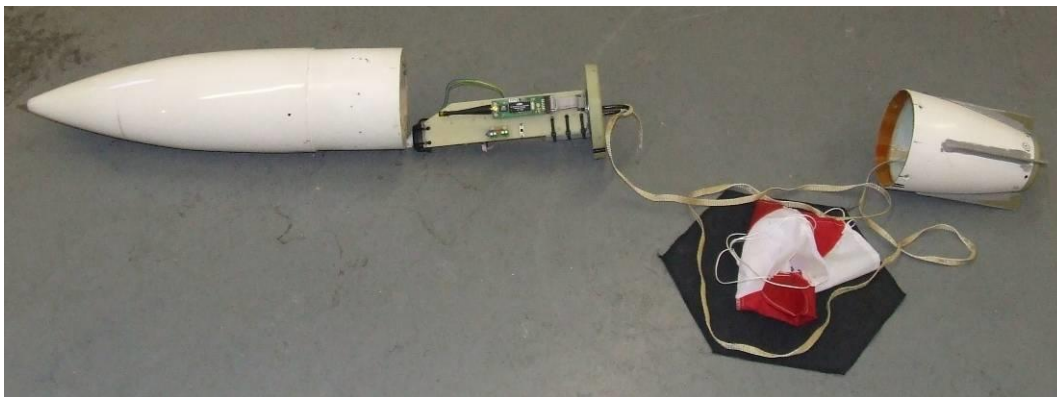


Figure 55 – “Dummy Ramjet” with all components shown

June 2009 Flight - MID Payload Bay Section

The MID payload bay section houses the electronics that will deploy the parachute and the separation of the “Dummy Ramjet”. The MID section is constructed of light weight high strength carbon fiber/epoxy. The FWD airframe section is secured to the MID payload bay by 8, #8 wood screws that are counter sunk in to the airframe as shown in Figure 56.

June 2009 Flight - AFT Motor Section

The AFT motor section was designed for installation of a motor mount adapter for the 75mm 7600ns commercial motor casting. The motor was installed before launch and secured with 3 retainer clip to the AFT motor section. The main parachute was located in the AFT motor section secured to the MID payload bay, the motor and the AFT motor section. The main parachute was deployed at apogee by the electronics in the MID payload pay. The attachment between the MID payload bay and the AFT motor section is a slip fit with no mechanical fasteners.



Figure 56 – Rocket Attachment Methods

June 2009 Flight - Solid Propellant Motor

An Animal Motor Works (AMW) M2500GG was used for the boost phase of the flight. The motor burn time is 3.11 sec with a maximum thrust of 2995.5 N (673.3 lbf) and an average thrust of 2503 N (562.7 lbf). Total impulse of this motor is 7785 n-sec, with a propellant weight of 4248 gm (9.365 lb). A commercial motor was used because it was easily obtainable.

June 2009 Flight - Electronics

R-DAS from AED was used as the main flight data acquisition computer mounted in the vehicle. The R-DAS consists of main board, a GPS expansion board with antenna and a telemetry board. These components along with a battery pack are mounted in the nosecone. The R-DAS samples at a rate of 200 Hz and stored on-board. The system records acceleration, GPS and two (2) pressure readings. One of the pressure transducers is mounted on the R-DAS, and the second is an external miniature Kulite transducer mounted at the tip of the nosecone. Data was sent to a ground station at a rate of 5 Hz and GPS data updates at 2Hz. A picture of the R-DAS flight computers are shown in Figure 57.

PML Co-Pilot controls the deployment of the main parachute in the AFT section. One Co-Pilot is mounted in the MID payload bay. The Co-Pilot was programmed with a Mach Delay (from detection of launch) of 7 sec and deploys the main parachute at apogee and at 304.8 m (1000 ft) above ground level and a back-up. The Co-Pilot system is shown in Figure 58.

A G-Wiz Accu-Fire controlled the separation event. The Accu-Fire was mounted in the MID payload bay. This electronics package was designed to detect motor burn out. Once the motor burnout is detected a signal is sent to fire the black powder charge to separate the “Dummy Ramjet” from the rocket. The Accu-Fire system is shown in Figure 58.

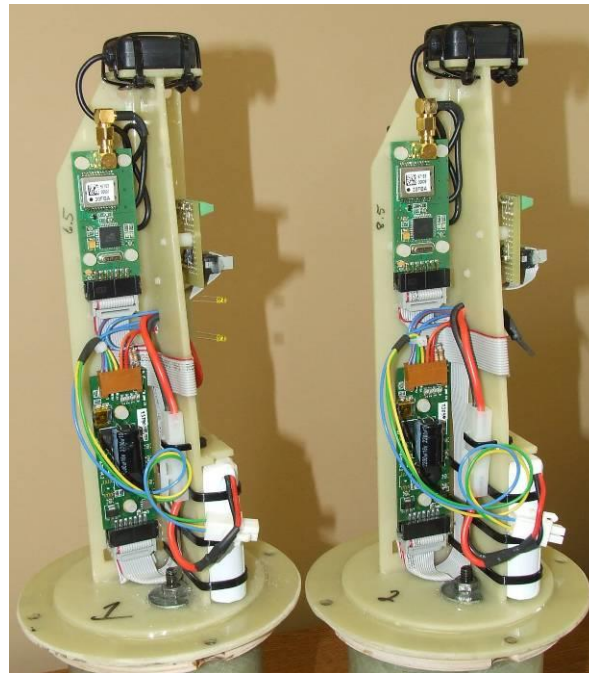


Figure 57 – R-DAS Flight Computer

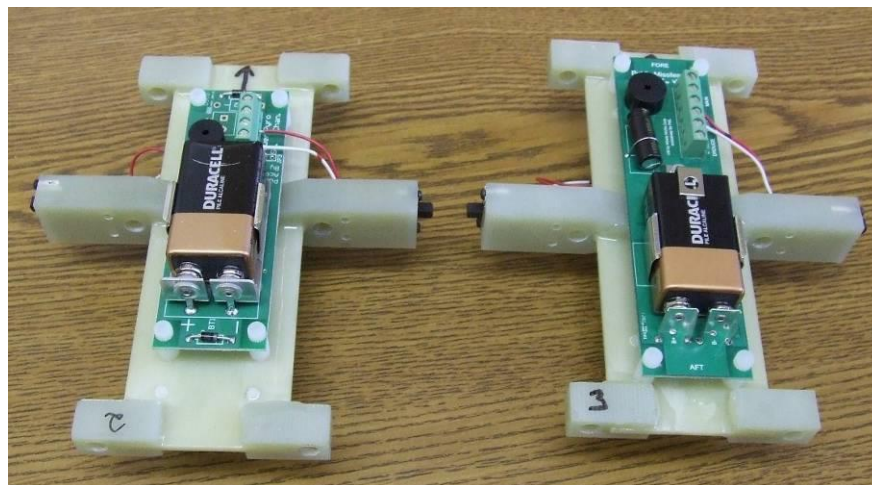


Figure 58 – Accu-Fire (Right) & Co-Pilot (Left) Electronics

June 2009 Flight - Launch on June 5th 2009

Friday, June 5, 2009 Applied Thermal Sciences successfully launched two vehicles to demonstrate subsonic separation of a test article from the forward end of the flight platform. The lift off is shown in Figure 59 and the vehicle platform is shown in Figure 60.



Figure 59 – Vehicle Lift Off and Flight



Figure 60 – Launch Vehicle

The vehicles were equipped with on board DAQ systems, measuring pressure at the nose tip, axial accelerations and barometric pressure inside the payload bay and recovery electronics. The R-DAS system was recording data at a 200Hz sample rate onboard and 5Hz sample rate transmitted to ground station. The electronic are shown in Figure 61 and serial numbers are listed in Table 8 and Table 9. Video was recorded of both launches with the intent of trying to visually document the separation event. Unfortunately, the speed of the event made it difficult to capture, even with a camera mounted on a tripod.

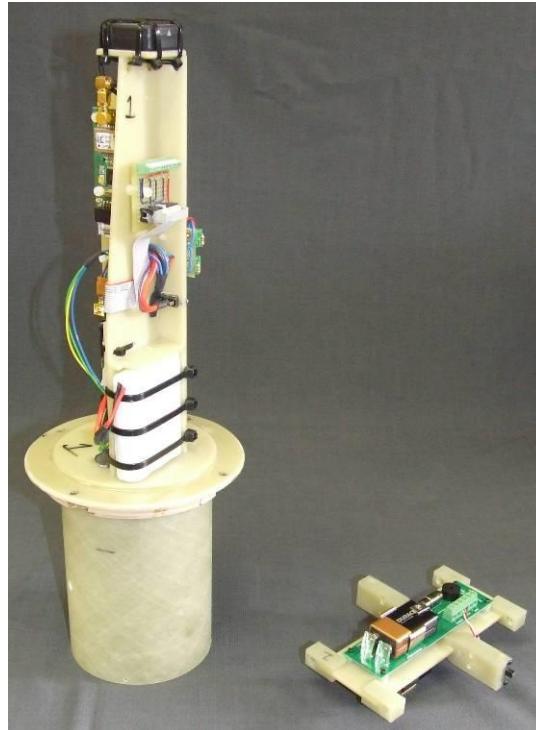


Figure 61 – Typical Flight Electronics

Table 8 – Flight Vehicle #1 Electronics & Serial Numbers

Item Name	Serial Number
R-DAS Main Board	06098
R-DAS GPS Board	97193 00007
R-DAS Telemetry Board	01458
Kulite ELT-76A-190-50A Pressure Transducer	6893-5-118
PML Co-Pilot	1506
Accu-Fire	n/a

Table 9 - Flight Vehicle #2 Electronics & Serial Numbers

Item Name	Serial Number
R-DAS Main Board	06170
R-DAS GPS Board	97193 00039
R-DAS Telemetry Board	01457
Kulite ELT-76A-190-50A Pressure Transducer	6893-5-137
PML Co-Pilot	1502
Accu-Fire	n/a



June 2009 Flight - 1st Launch

The 1st vehicle the “dummy ramjet” and booster separation occurred at approximately 3.50sec after launch at an altitude of 1920 ft. The vehicle velocity before separation was 1036 ft/sec. A visual confirmation of the separations was made with both sections flying straight after separation. The “dummy ramjet” section was recovered approximately 0.12 miles South-East of the launch pad and the booster section was recovered approximately 0.20 miles East of the launch pad as shown in Figure 62. The upper level winds were approximately 10-15 knots. The electronics on the booster and “dummy ramjet” never deployed the recovery systems in flight. A summary of the data is listed in Table 10. Figure 63 shows the recorded acceleration and altitude (onboard barometric sensor) and Figure 64 shows the calculated velocity from the acceleration data and nosecone tip pressure. Figure 65 shows the altitude (from the onboard barometric sensor) and the calculated velocity. Figure 66 shows the first 5 seconds of onboard data focusing of the separation event. Figure 67 shows a 3D plot of the vehicle from launch to recovery.

Table 10 – Summary of 1st Flight Vehicle Launched

R-DAS			
GPS Altitude:	1791.3	ft	
GPS Launch:	W 44.67936	N 67.891497	
GPS Recovery Nosecone:	W 44.67822	N 67.890117	
GPS Recovery Booster:	W 44.67913	N 67.888059	
Recorded Altitude:	4304	ft	
Recorded Acceleration:	31.17	g's	
Velocity:	1036.0	ft/sec	
Nosecone Tip Pressure:	24.9	psia	
Co-Pilot			
Recorded Altitude:	n/a	ft	



Figure 62 – Aerial View of Launch Site & Vehicle Locations

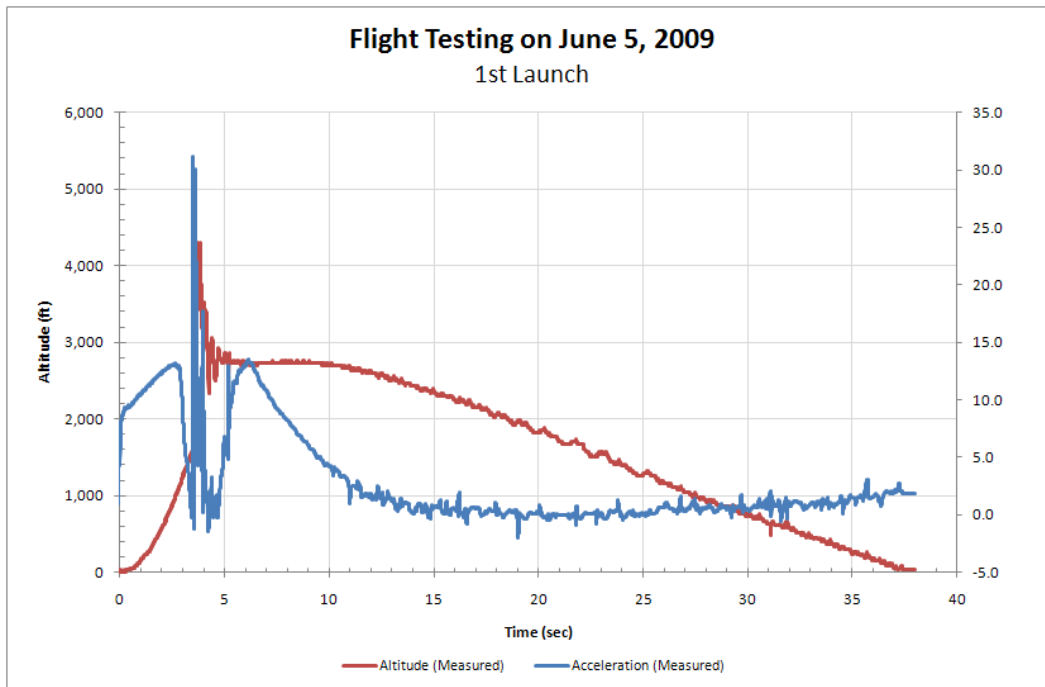


Figure 63 – 1st Vehicle Altitude and Acceleration Data

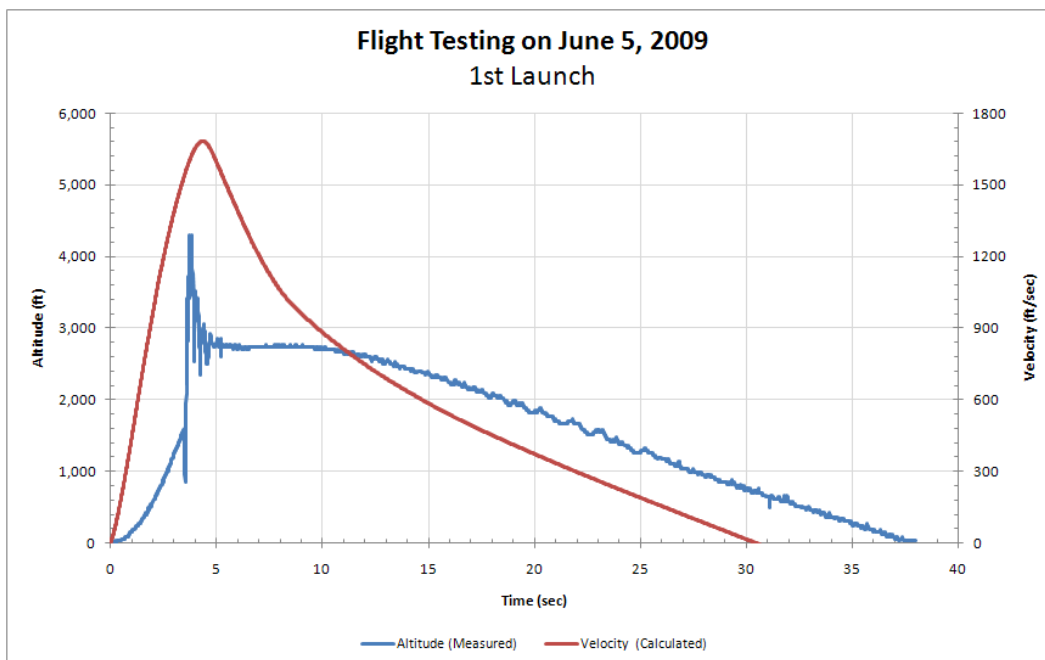


Figure 64 - 1st Vehicle Altitude and Velocity Data

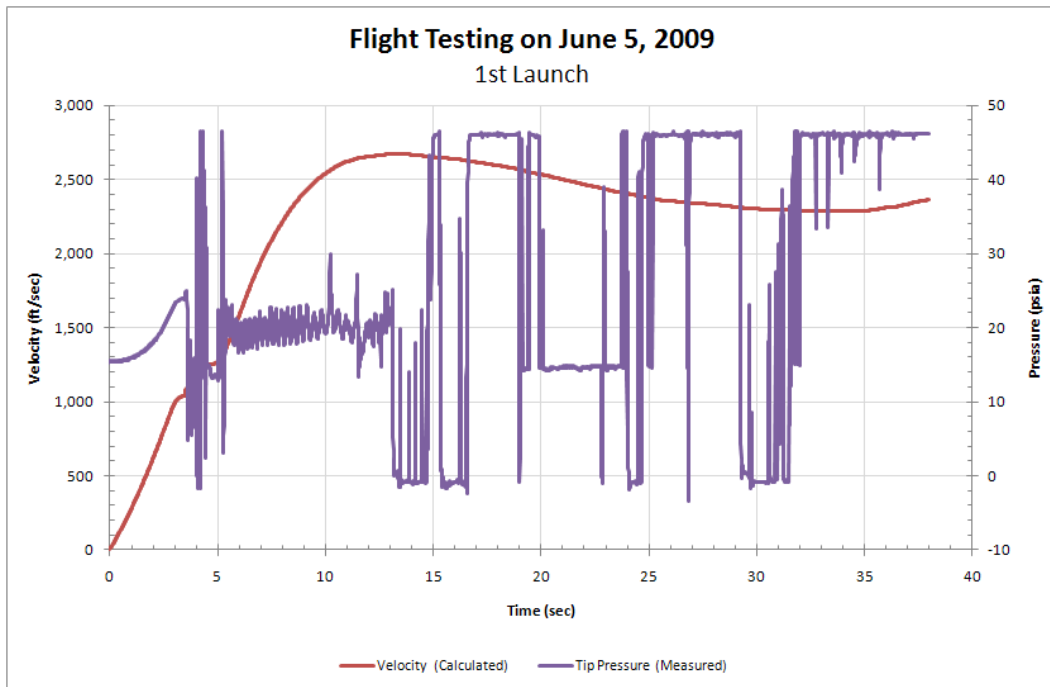


Figure 65 – 1st Vehicle Velocity and Nosecone Tip Pressure Data

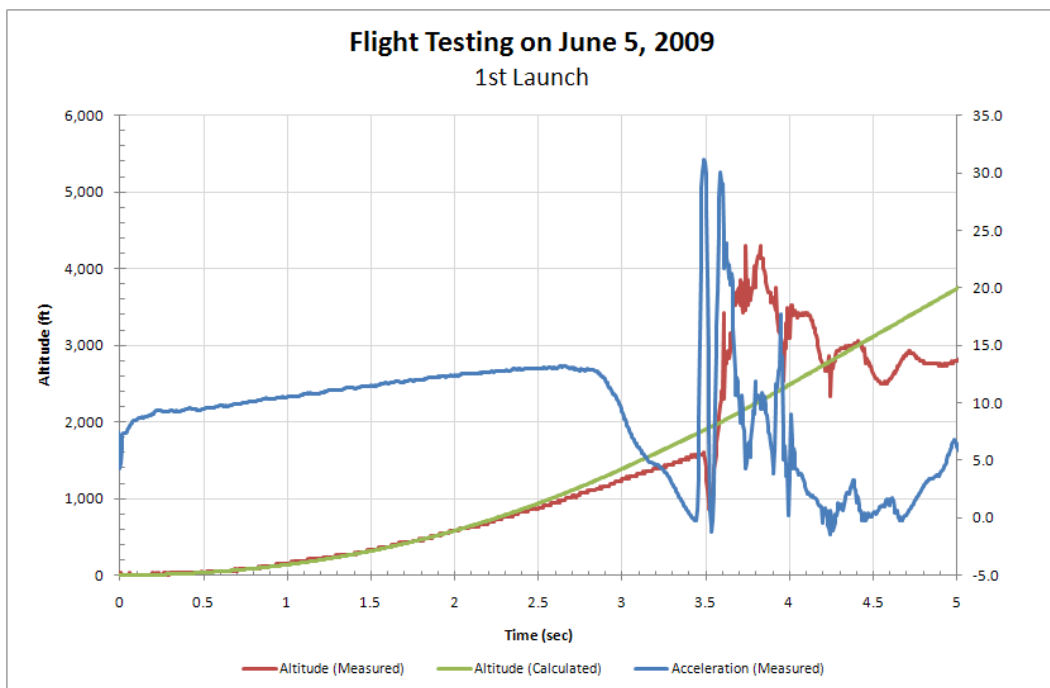


Figure 66 – 1st Vehicle Separation Event

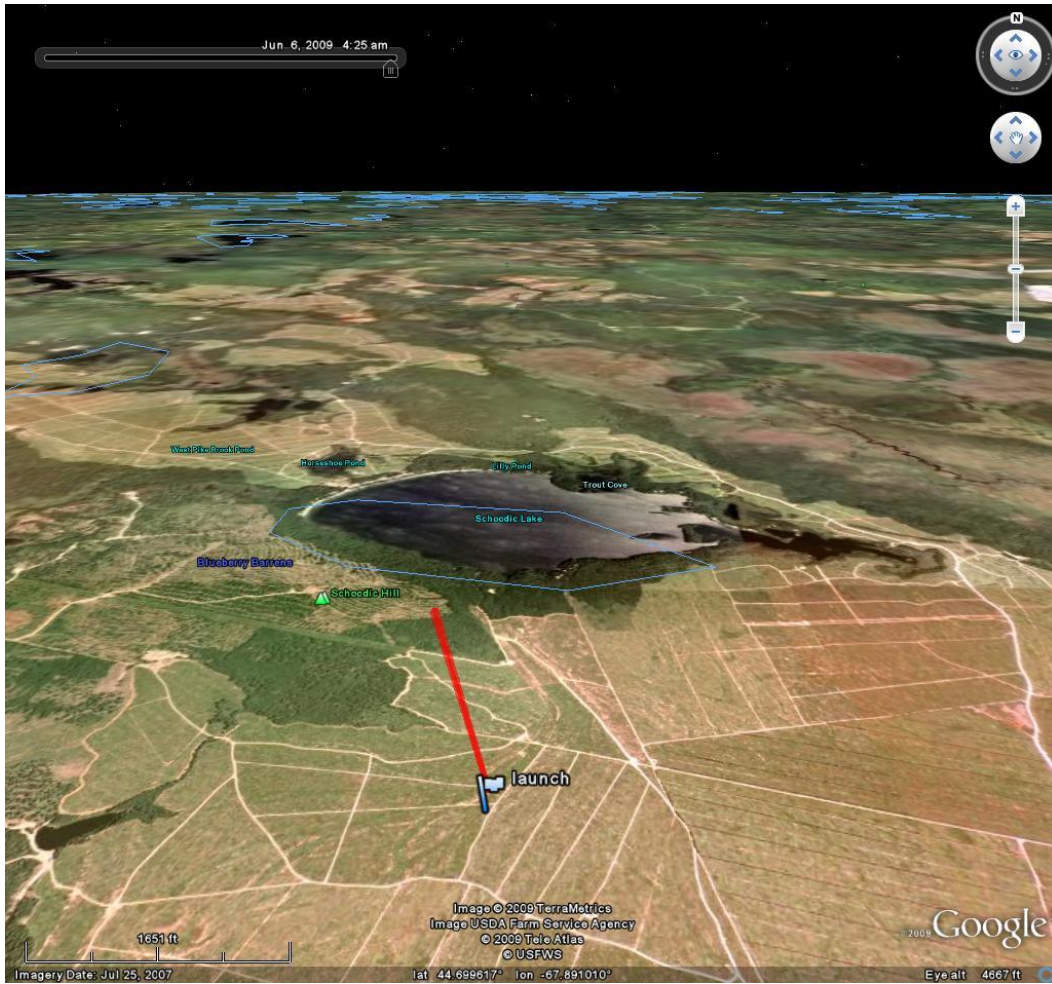


Figure 67 – 3D Plot of the 1st Vehicles Flight

The flight data up to the separation event looked fine, but the acceleration rate at separation was much higher than anticipated. While the separation event looked ok from the ground, the acceleration rate at deployment damaged the on-board electronics.

June 2009 Flight - 2nd Launch

For the 2nd flight, the “dummy ramjet” and booster separation was delayed 2 sec from motor burn-out, which occurred at approximately 4.85sec after launch at an altitude of 3760 ft. The vehicle velocity before separation was 898 ft/sec. A visual confirmation of the separations was made with booster section flying straight and the “dummy ramjet” section flying straight for a short period of time before tumbling. The “dummy ramjet” section was recovered approximately 0.21 miles North of the launch pad and the booster section was recovered approximately 0.54 miles North-East of the launch pad as shown in Figure 62. The upper level winds were approximately 15-20 knots. Then electronics on the booster section deployed the



recovery system at apogee and the recovery system on the “dummy ramjet” never deployed in flight. A summary of the data is listed in Table 11. Figure 68 shows the recorded acceleration and altitude (onboard barometric sensor) and Figure 69 shows the calculated velocity from the acceleration data and nosecone tip pressure. Figure 70 shows the altitude (from the onboard barometric sensor) and the calculated velocity. Figure 66 shows the first 7 seconds of onboard data focusing of the separation event. Figure 72 shows a 3D plot of the vehicle from launch to recovery.

Table 11 - Summary of 2nd Flight Vehicle Launched

R-DAS			
GPS Altitude:	4950.8	ft	
GPS Launch:	W 44.67936	N 67.891497	
GPS Recovery Nosecone:	W 44.68171	N 67.888884	
GPS Recovery Booster:	W 44.68497	N 67.883717	
Recorded Altitude:	5788	ft	
Recorded Acceleration:	29.33	g's	
Velocity:	1124.5	ft/sec	
Nosecone Tip Pressure:	25.65	psia	
Co-Pilot			
Recorded Altitude:	n/a	ft	

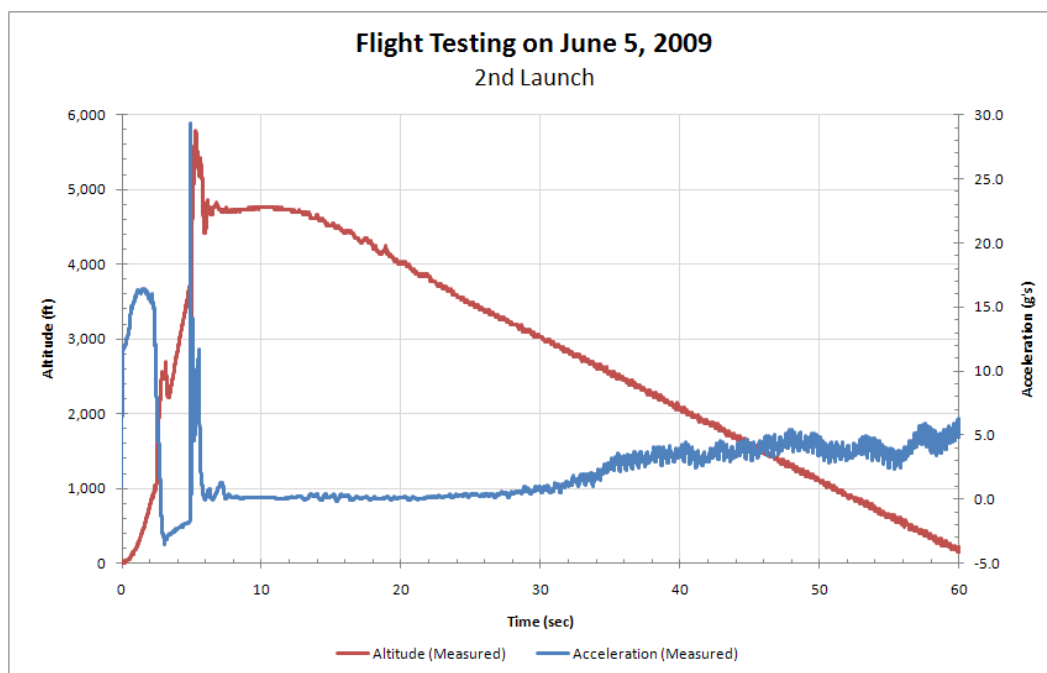


Figure 68 - 2nd Vehicle Altitude and Acceleration Data

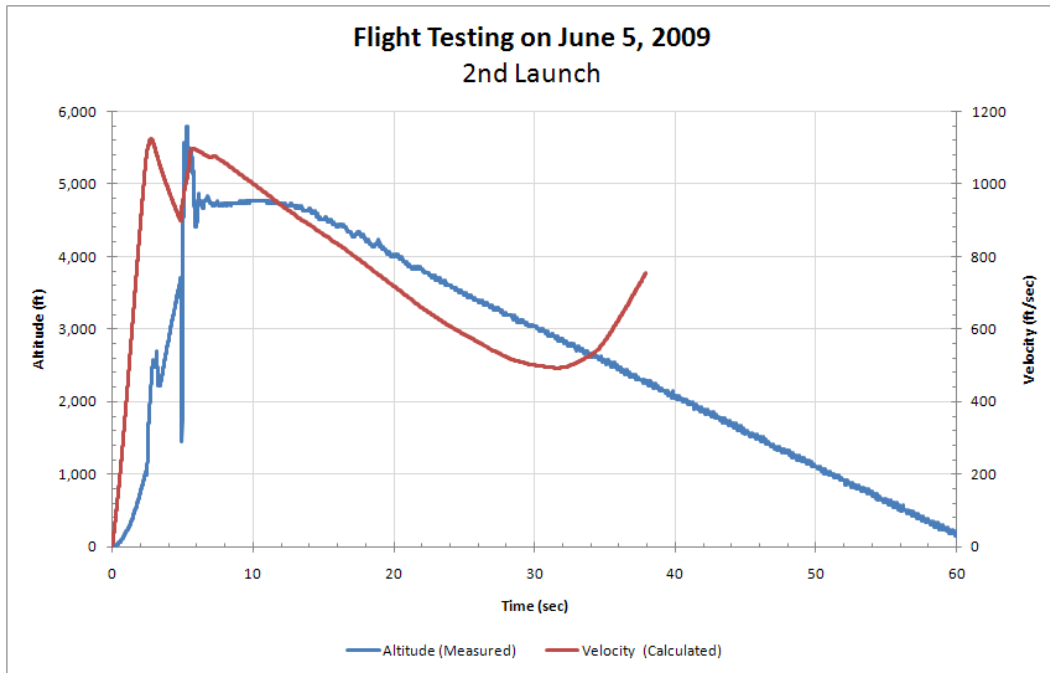


Figure 69 - 2nd Vehicle Altitude and Velocity Data

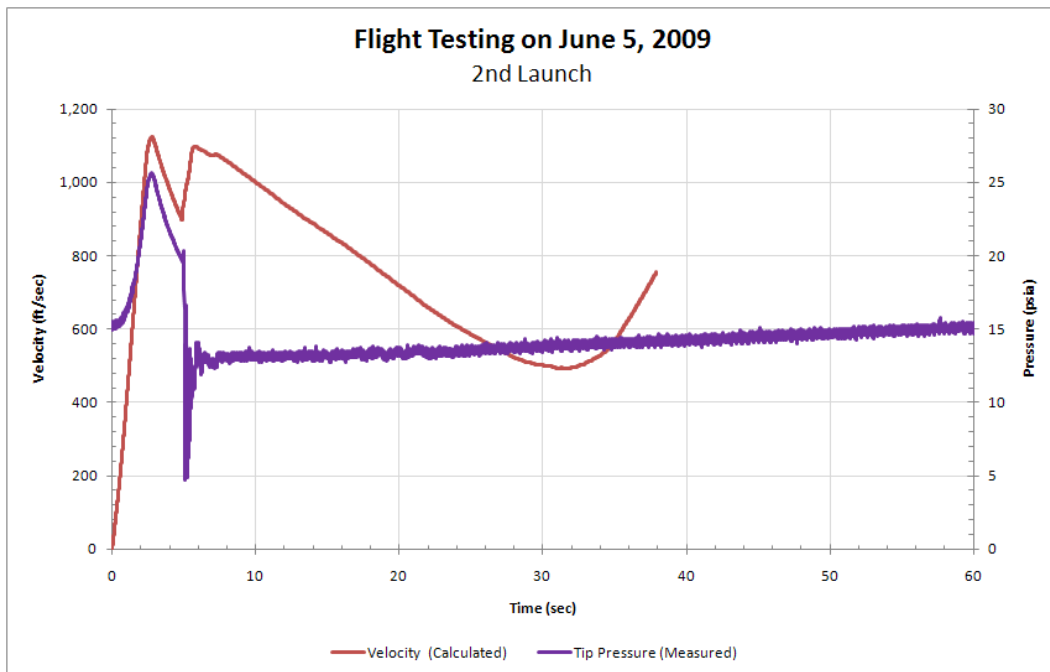


Figure 70 – 2nd Vehicle Velocity and Nosecone Tip Pressure Data

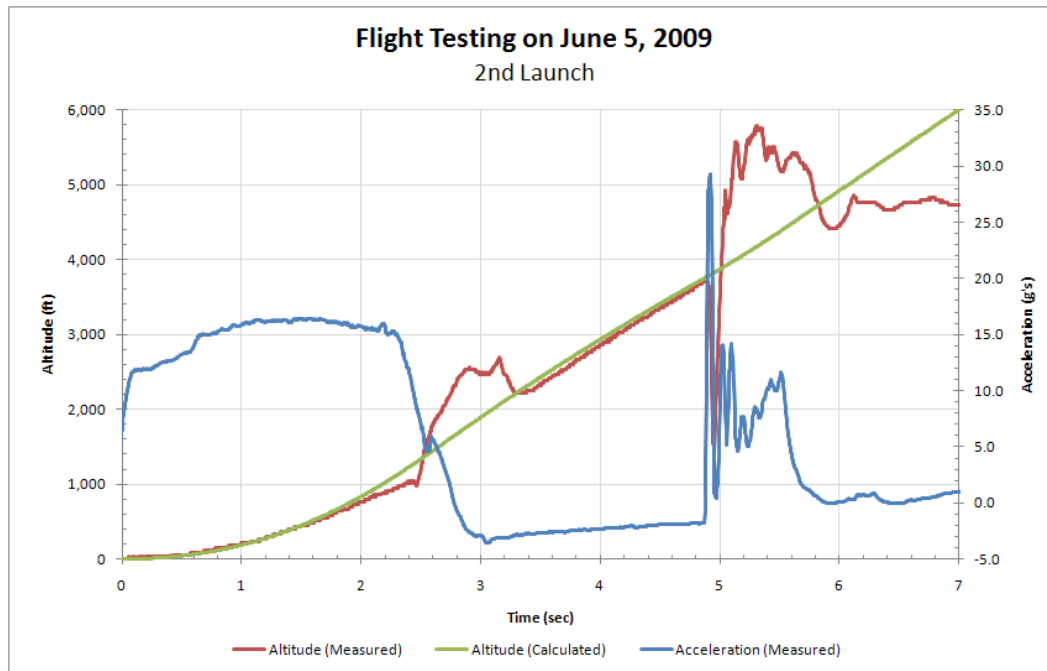


Figure 71 – 2nd Vehicle Separation Event

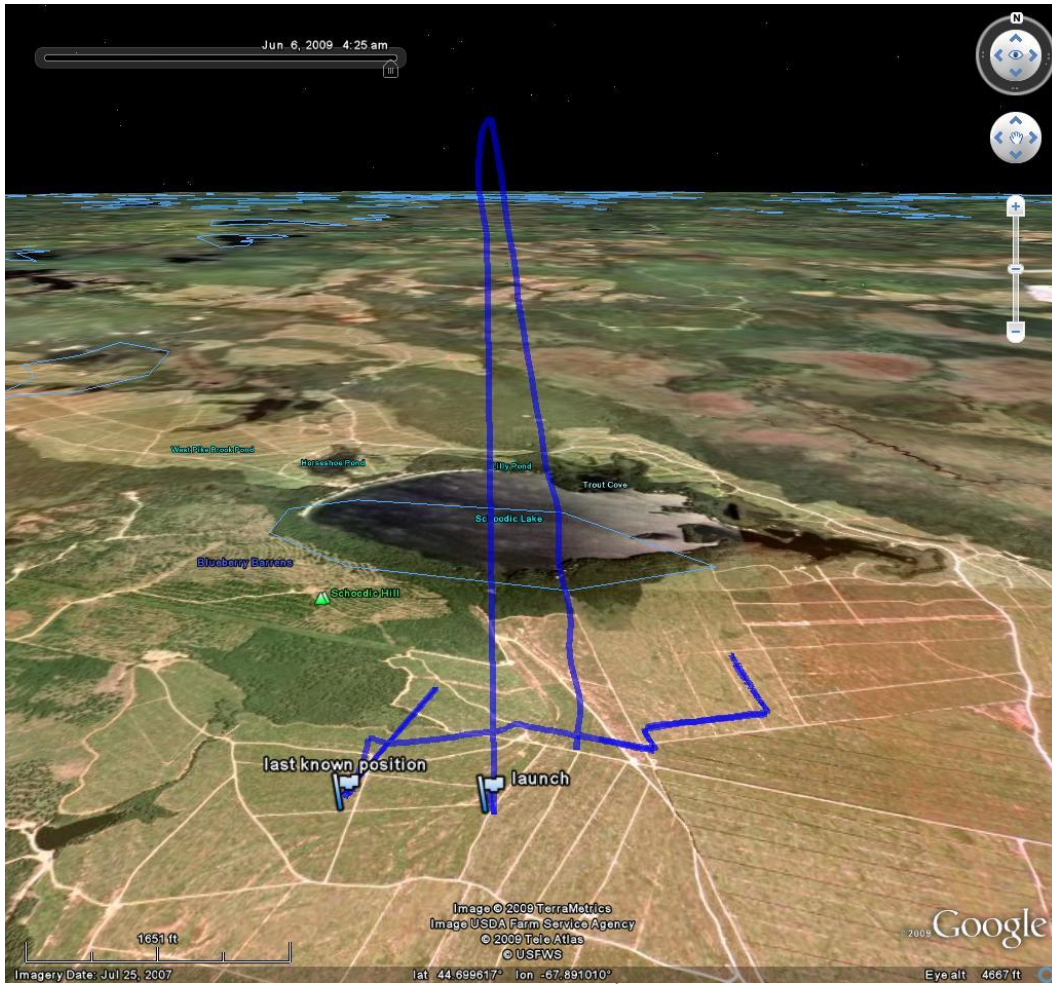


Figure 72 - 3D Plot of the 2nd Vehicle's Flight

June 2009 Flight - Data to Predicted Flight

Figure 73 shows the recorded acceleration on from the onboard accelerometer for both flights compared to the predicted flight from RockSim 8.0 flight software for the first 8 seconds of flight. The same type of commercial motor, Animal Work, M2500GG, APCP ammonium perchlorate solid propellant was used on both vehicles. There was a large variation in peak acceleration and burn time between the two motors as shown in Figure 73. Figure 74 shows the calculated velocity compared to the predicted velocity from the software for the same period of time. Figure 75 shows the measured altitude from the onboard barometric pressure sensors for both vehicles compared to the predicted altitude. Figure 76 shows the calculated altitude from the acceleration data for both vehicles compared to the predicted altitude.

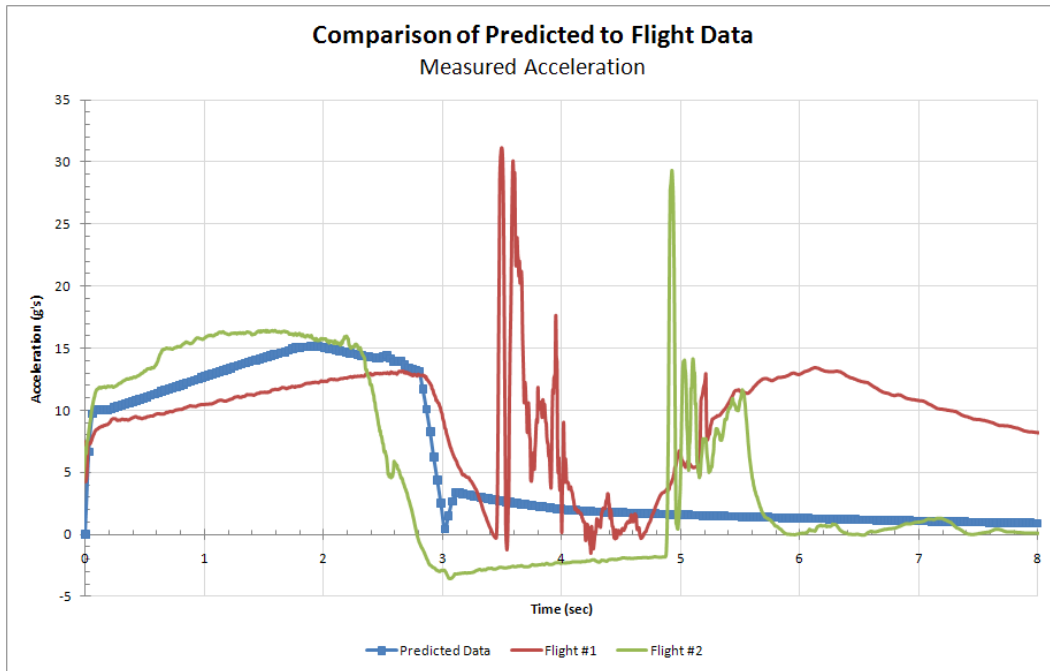


Figure 73 – Predicted Data to Flight Data, Comparing Measured Accelerations

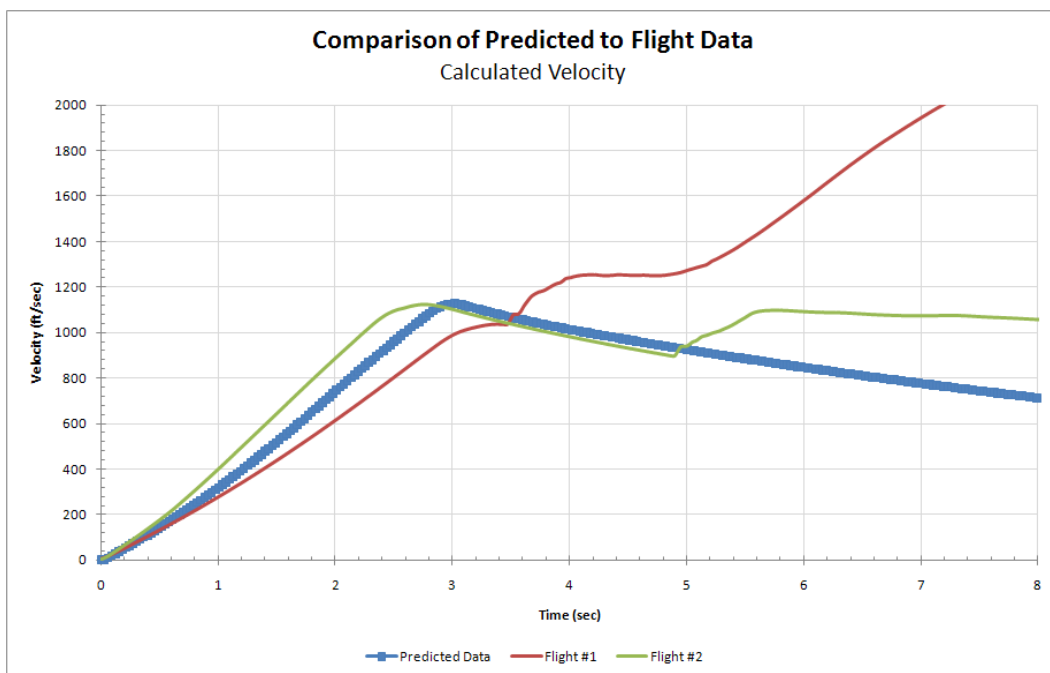


Figure 74 - Predicted Data to Flight Data, Comparing Calculated Velocities

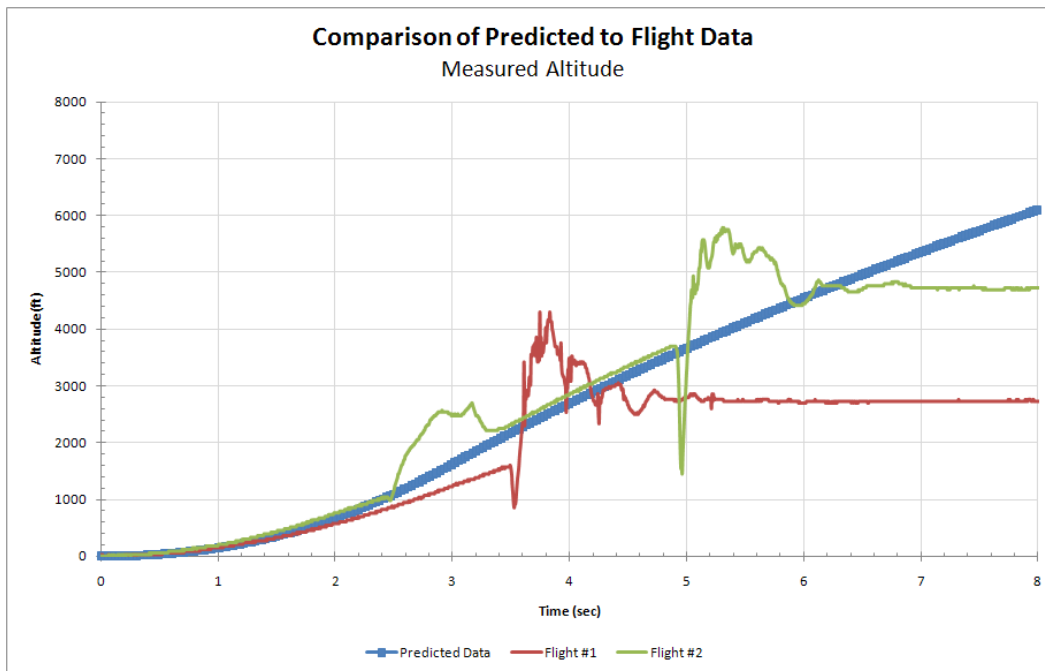


Figure 75 - Predicted Data to Flight Data, Comparing Measured Altitude

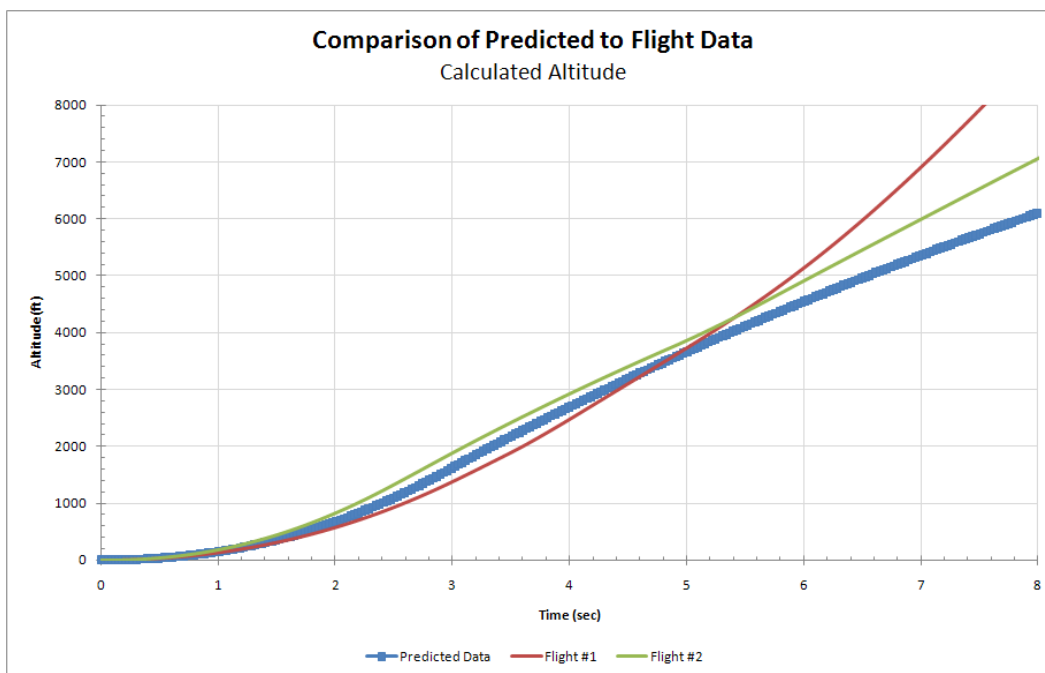


Figure 76 - Predicted Data to Flight Data, Comparing Calculated Altitude

The tumbling of the dummy ramjet after separation was expected because the stability of the vehicle was very low. While both flight tests showed promise for separation of a ramjet test article from the booster, a different method from the black powder charge for separation



would be needed. It was decided to use a small rocket motor for separation because it would provide thrust for a longer time. This would allow time for the booster to slow down to prevent a collision after separation.

Launch 3 – Supersonic Flight Tests with Separation of a Ramjet (Flights 5 & 6)

Ramjet Test Article Development

Task 2.1 – Preliminary Ramjet Design Analysis

Ramjet Payload Investigation

The design specifications for the ramjet included keeping the overall outside diameter to six inches or less to maintain stability of the coupled ramjet/booster configuration, and to facilitate the separation event. Another design goal was to keep the overall length of the ramjet payload to 24 inches or less. The design flight conditions correspond to conditions for the desired separation event of $M = 1.67$ at an altitude of 3000ft. The design starting point comes from a proven ramjet design within the desired geometric scale and Mach Number regime. This design is documented in the paper NACA RM E53K17 “Summary of Free-Flight Performance of a Series of RAMJET Engines at Mach Numbers from 0.80 to 2.20” by Warren J. North, dated February 11, 1954. It was desired to use SRGUL, a computational tool used by NASA to design and optimize ramjet and scramjet engines, to help optimize the flow path lines for the payload ramjet engine. However, the relatively low design Mach Number of 1.67 causes issues with the SRGUL code. Therefore, the CFD code VULCAN was used to produce the presented results.

Ramjet Development

The CFD results of preliminary designs were not showing promising results, a shift to a new a new axi-symmetric ramjet design for Ma 1.5 was initiated. NASA's SRGUL code was first used to develop the initial engine lines. Once a design with promising results was obtained, a full 2D CFD simulation will be performed. Results presented here are for air flow only (no fuel). Figure 77 shows the internal lines of the NASA design using SRGUL. Figure 78 shows Mach number through the combustor, while Figure 79 shows Mach number contours of the inlet from SRGUL.

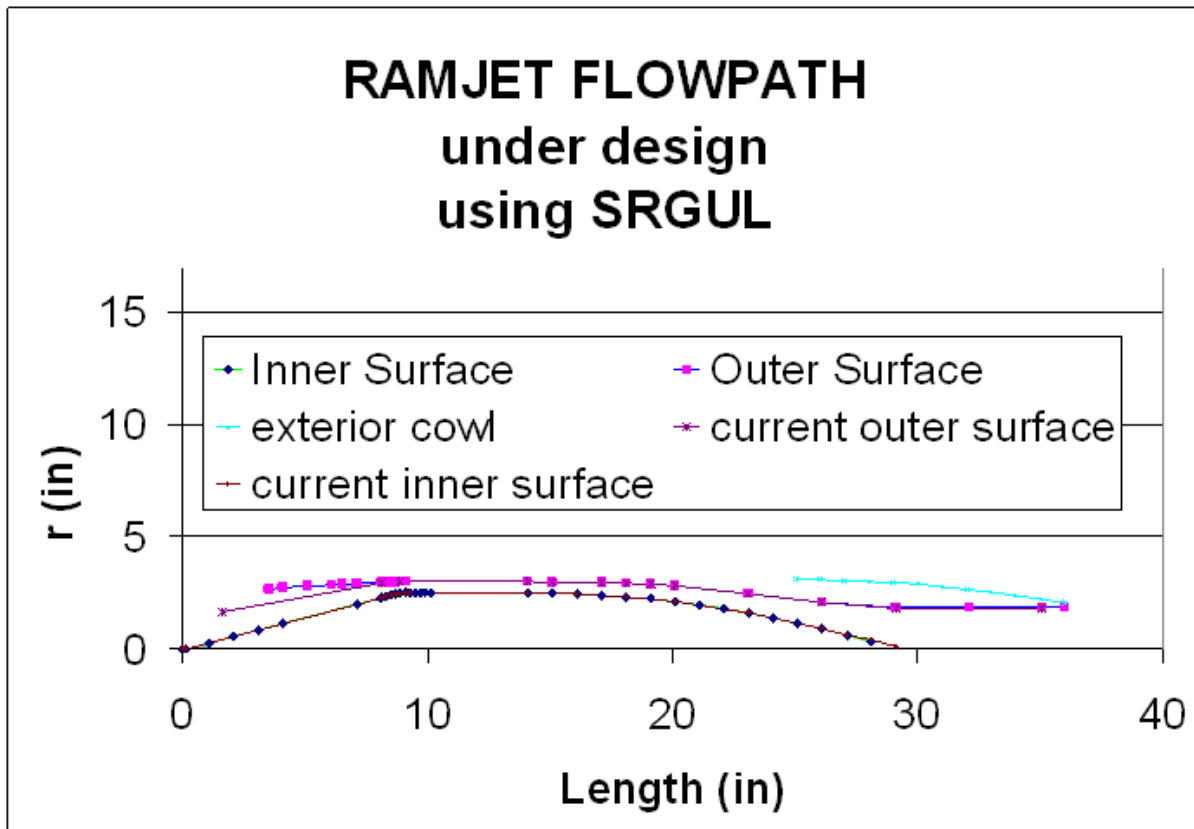


Figure 77 – Internal Lines of the Axisymmetric Ramjet Design

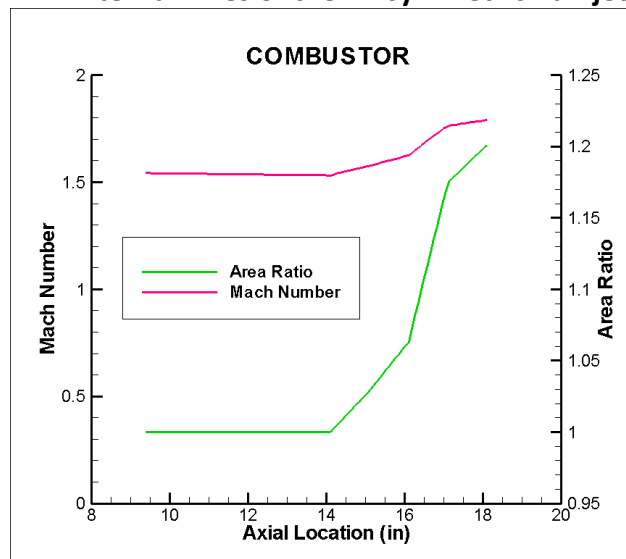


Figure 78 - SRGUL uses a 1-D approximation through the combustor.

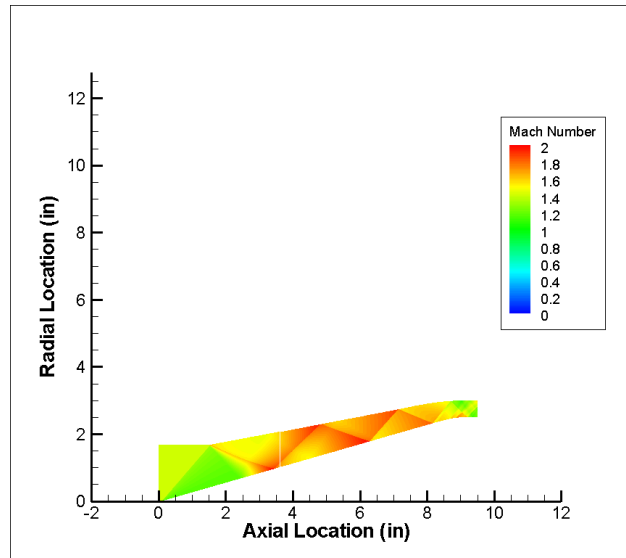


Figure 79 - Mach Number contours for the inlet.

This preliminary analysis with SRGUL help to understand the potential flow conditions prior to using the more time consuming CFD analysis. In addition, when looking at a fueled case, SRGUL will aid efforts to determine area change requirements in the combustor and nozzle sections prior to more detailed CFD analysis. However, the fueled effort was not an objective of this work.

Task 2.2 – CFD Analysis

Initial Ramjet CFD Work

The first Ramjet design revision analyzed with VULCAN was a model that directly scaled down a model developed by NASA to match the desired design criteria of a 6 inch diameter. Length scales were preserved from the geometric scaling even though this resulted in a center body and overall ramjet length that was too long for this application. However, the direct scaling preserves shock angles so it was a prudent place to start. Without considering struts, fins, etc. the flow was axi-symmetric. Thus an axi-symmetric model was used with the axis center at $y = 0$. Initial reference conditions used were a flight Mach Number $M = 1.67$ and an altitude of 3000 ft. The case used thermally perfect air to prepare the model for the introduction of fuel. Results for Revision 1 are shown in Figure 80 to Figure 87. Some information gleaned from the CFD analysis includes a half angle = 26° , a shock angle = 50° , the mass capture is 24.05 lbm/s (relatively high), and the drag for the unfueled case is 430 lbs.

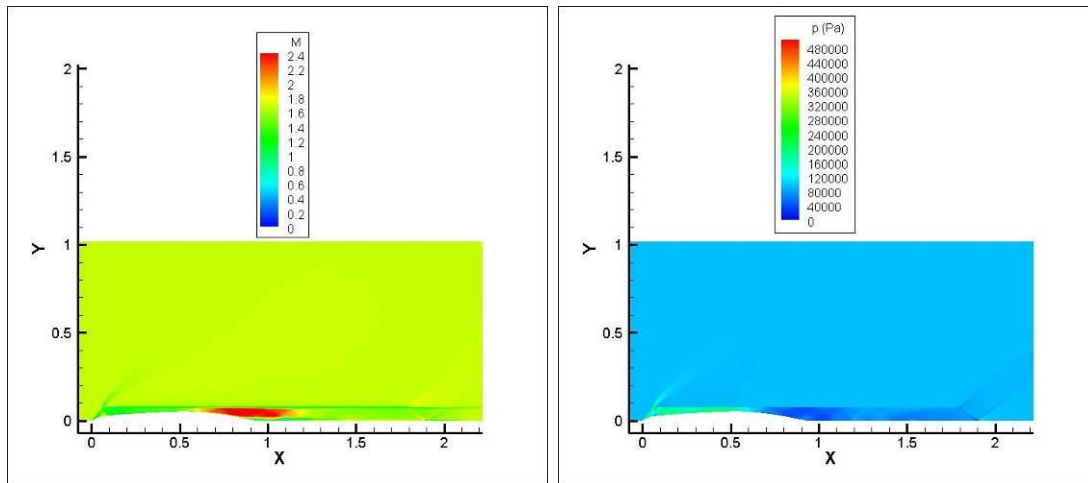


Figure 80 - Mach Number and pressure plots. (Length scales are in meters)

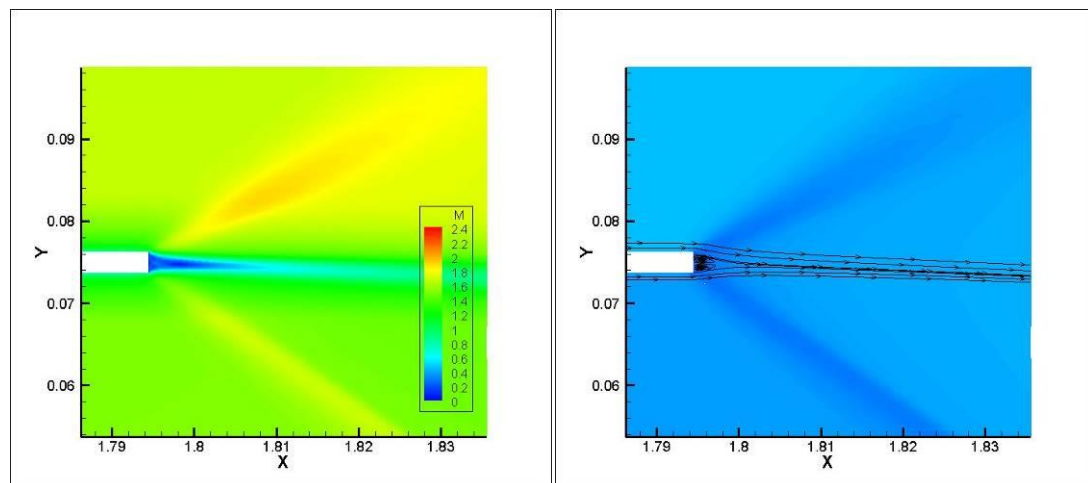


Figure 81 - Contours of Mach Number (Left) and streamlines on pressure contours (Right) of the AFT end of cowl.

Figure 80 shows Mach number and pressure contours for the full length ramjet. Note that the analysis was axi-symmetric so only half of full cross-section was plotted. Figure 82 focuses on the aft end of the cowl to investigate pressure/drag forces. Figure 82 to Figure 85 illustrate the inlet pressure contours on a scale of about 5 atmospheres. A small recirculation region caused by shock interaction at approximately $x = 0.0895$ m was found at these conditions. This area is identified in Figure 83, and a close-up view is shown in Figure 85. Recirculation zones can grow and change with conditions, which adversely affect mass capture and flow stability of the inlet. For these reasons, ATS design objectives were try and prevent and eliminate separation or flow recirculation regions in the inlet.

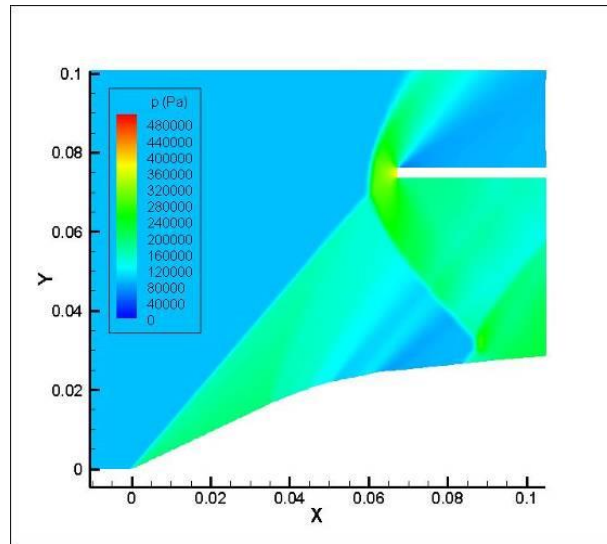


Figure 82 - Inlet showing shock on lip.

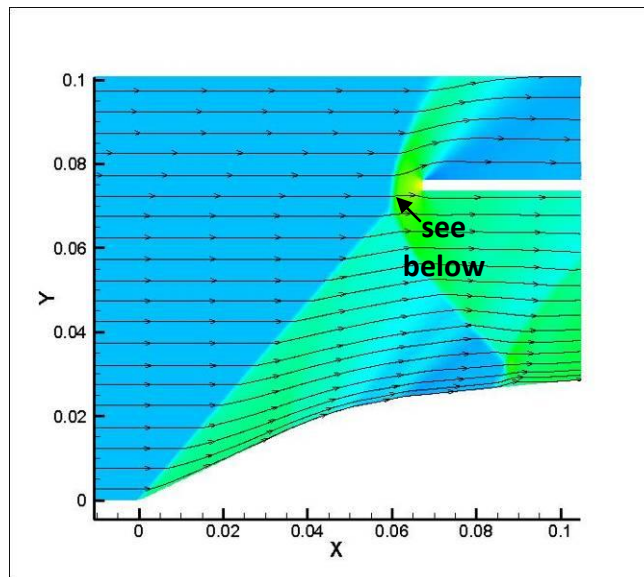


Figure 83 - Streamlines through the inlet.

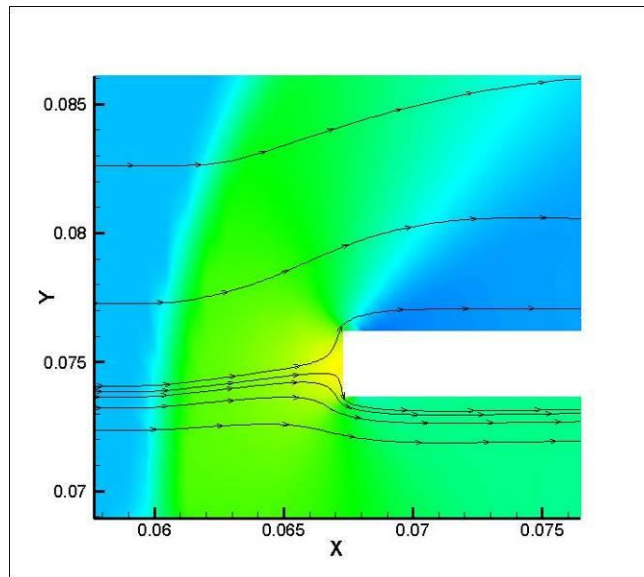


Figure 84 - Forward cowl lip.

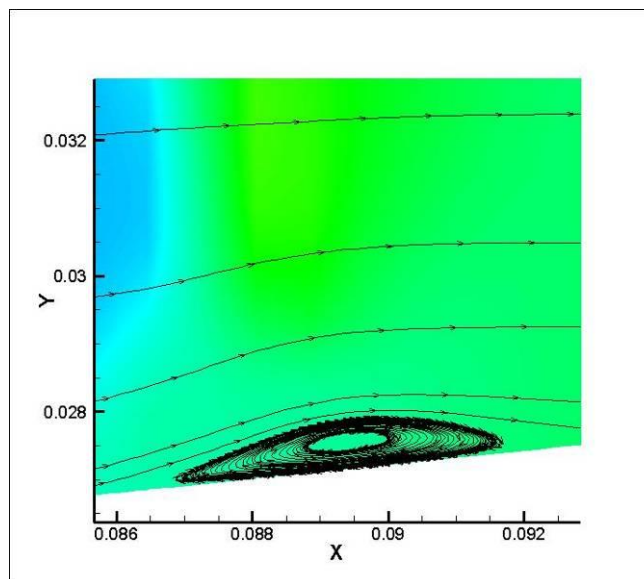


Figure 85 - Small recirculation region

Figure 86 shows the intricate shock pattern through the scaled NASA ramjet engine. Figure 87 shows the throat Mach and pressure profiles in detail. (Note that the scaling for these figures are different than Figure 80 to Figure 86.)

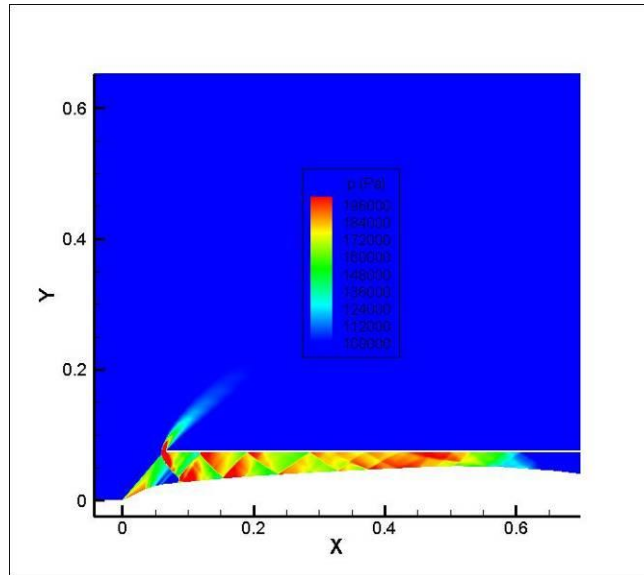


Figure 86 - Intricate shock pattern through the inlet to the throat.

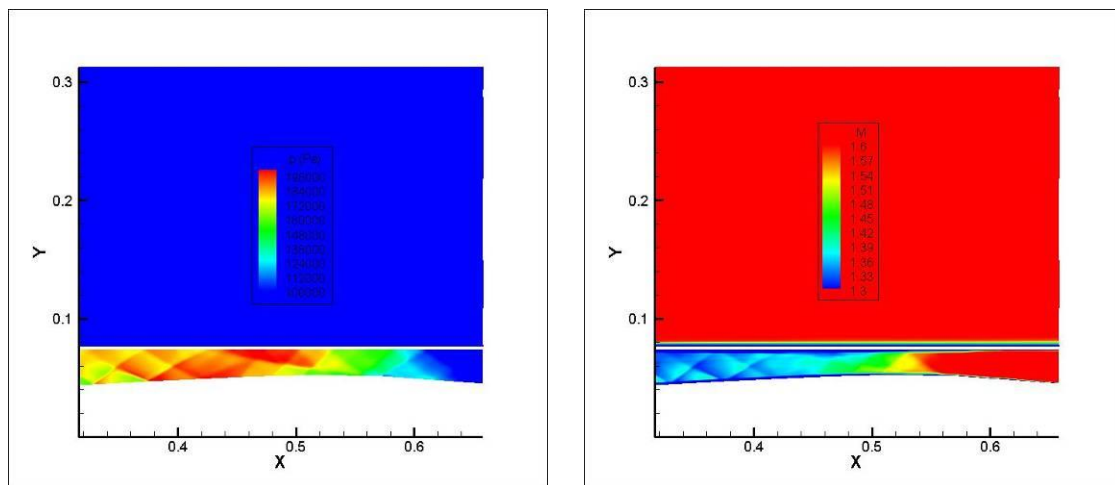


Figure 87 - Throat Mach and Pressure Profiles

Ramjet CFD Revision 2

Based on the results from Revision 1, a new design was formulated as Revision 2. Revision 2 was designed with the following criteria. The overall open length was to be no greater than 24 inches. The tip of the cowl had to be along the existing shock line so that “shock on lip” would be retained. The translation of a possible center-body to close the inlet could not exceed two inches. And the area ratio between that the cowl lip and the throat was maintained the same as in Revision 1. A Revision 2 solid model was developed, a grid was made with ICEM, and the case was analyzed with VULCAN. For this case the air was assumed calorically perfect with $\gamma = 1.4$. Sutherland’s law was used to model viscosity. The reference conditions were again a flight



Mach Number of 1.67 and an altitude of 3000 ft. Results are shown in Figure 88 to Figure 89. The CFD results indicate that inlet was not able to swallow the air flow even without pressure rise due to combustion. The mass airflow was also reduced considerably from the original design. In addition, the low altitude and other flight condition may require modifications to swallow the air flow. Note the large aft recirculation region shown in Figure 89. This is due to the large area change in the cross-section to account for combustion in the original design.

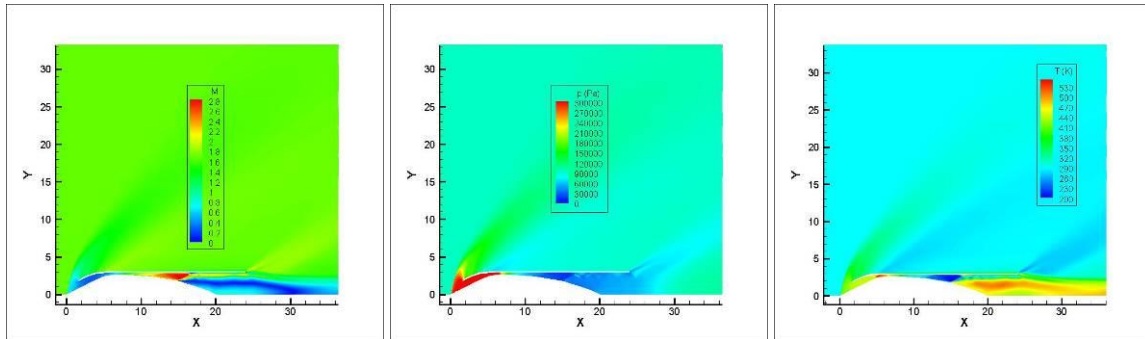


Figure 88 - Length scales in inches. Mach Number, pressure, and temperature contours

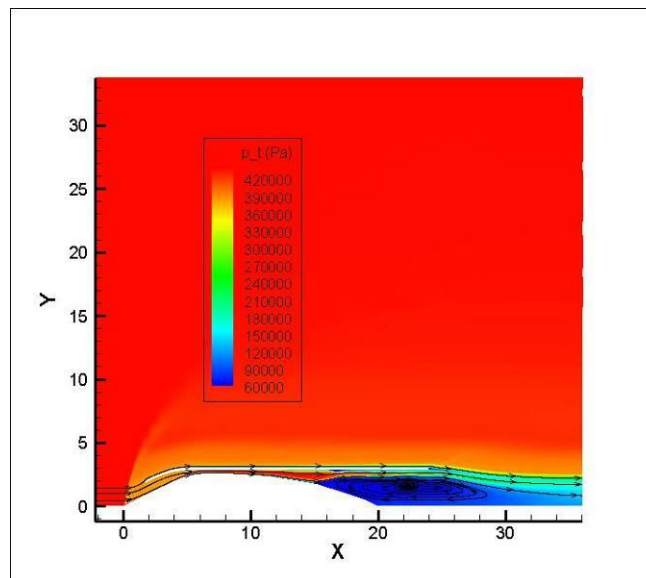


Figure 89 - Total pressure

ATS Inward Turing RAMJET Design

ATS has analyzed many design concepts and also studied the original NACA design in detail. It is clear that an axi-symmetric design could work but may not be as efficient as some other concepts. However, with a constraint of a 6" outer diameter, payload volume can be an issue with some design where there would not be sufficient volume for instrumentation, telemetry, and the fuel system. To keep an adequately sized center-body for on-board electronics, the



inlet contraction ratio would be better matched to a higher flight Mach Number. Therefore, a new ATS design utilizing an inward turning inlet and bleed troughs to provide pressure relief without causing the inlet to un-start was conceived. The new design is shown in Figure 91 and uses the inward turning inlet for compression. The design has the additional attributes of a tubular geometry to couple easily with the booster rocket and the available volume for internal components would exist outside of the engine flow path, which is very desirable for telemetry equipment.

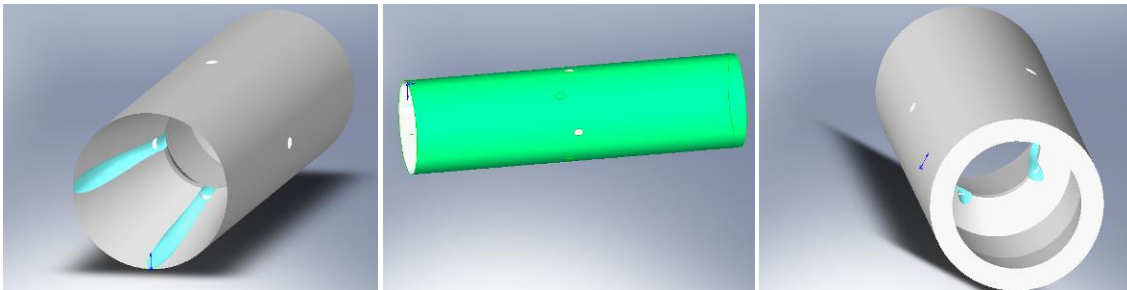


Figure 90 - New inward turning Ramjet design. Inlet, side view, nozzle.

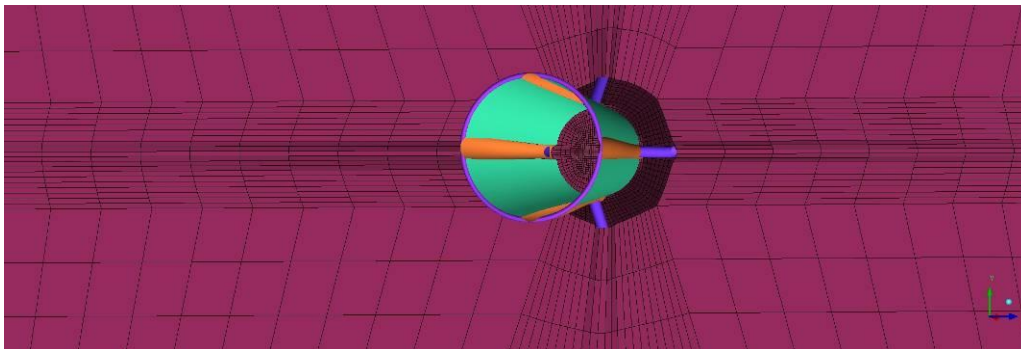


Figure 91 - Preliminary meshed computational domain

In the process of developing the computational domain described above, an intermediated domain that had all the features of the ATS inward turning design except the troughs was produced. CFD analysis was performed to facilitate the simulation of the full design and to provide a case in which to compare with the full design. Such a comparison allows some indication of the effect of the troughs. The with-trough and no-trough cases were compared along with comparing these results with previous axi-symmetric design results.

All CFD results presented were produced using the VULCAN CFD code maintained by NASA Langley. All simulations were conducted at the desired flight conditions of $M = 1.67$ and 3000ft altitude. Figure 94 shows results from a simulation of the 6" diameter no trough design. Mesh lines are shown to illustrate calculation resolution.

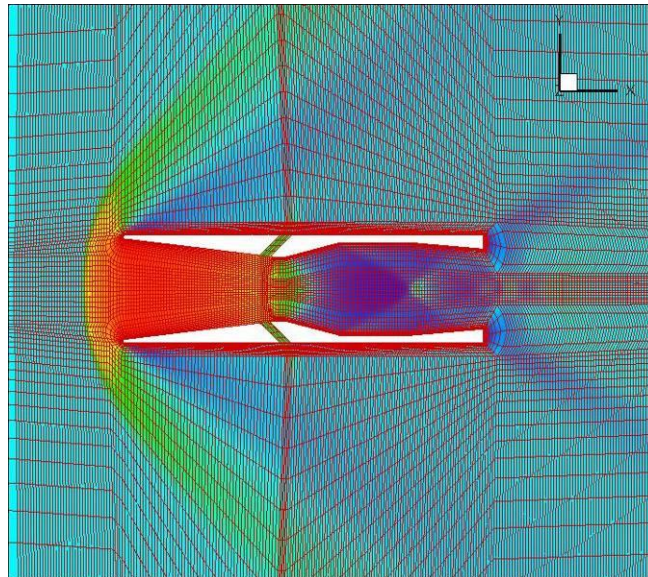


Figure 92 - Pressure contour results for a $z = 0$ plane of the 6" diameter no trough case.

Figure 95 thru Figure 97 and shown to illustrate differences in Mach Number contours and pressure contours for the no-trough and with-troughs cases.

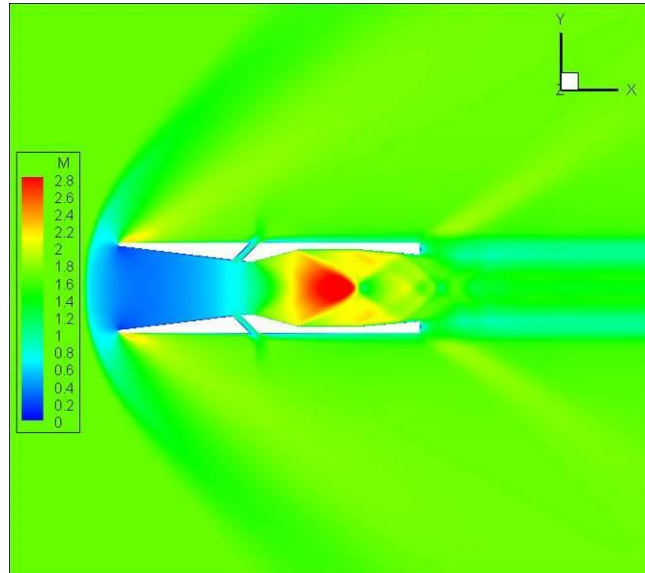


Figure 93 - Mach Number contours for the no trough design.

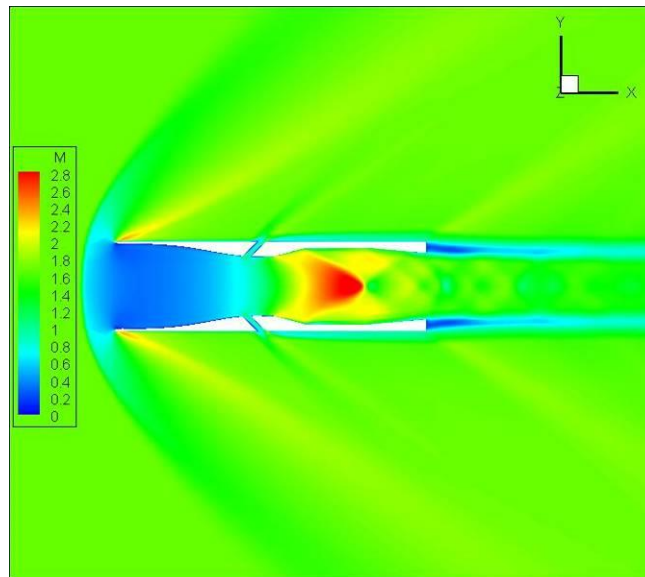


Figure 94 - Mach Number contours for the design with troughs.

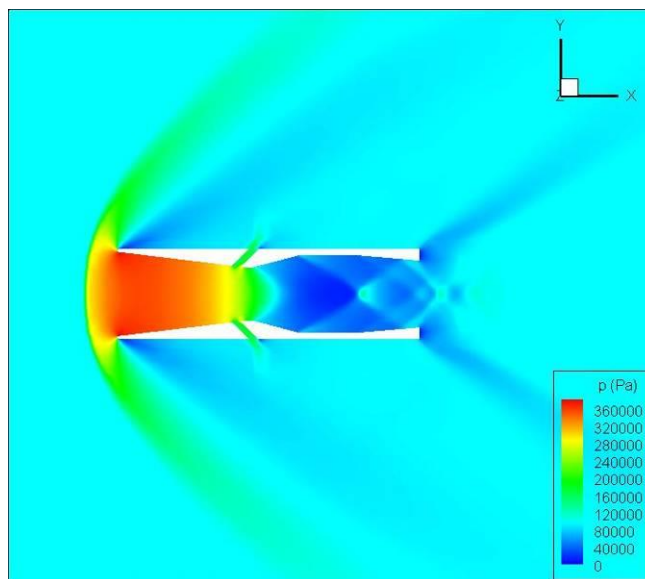


Figure 95 - Pressure contours for the no trough design.

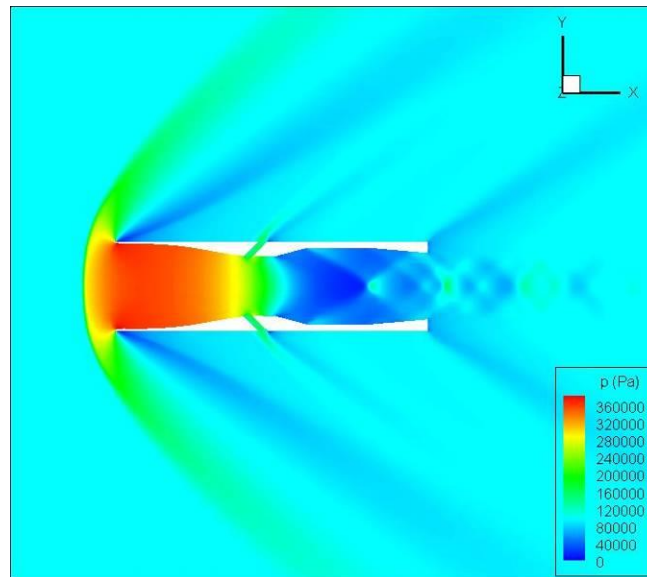


Figure 96 - Pressure contours for the design with troughs.

Note that there is very little difference in Mach number or pressure contours between the no-trough and with-trough cases. Figure 95 to Figure 98 are all for the plane $z = 0$. This plane bisects the engine longitudinally. For the with-trough design, the plane cuts through the upper and lower troughs. Figure 97 and Figure 98 show planes cut for a constant x and colored with contours of pressure with stream-tubes colored with Mach number that basically run from the upper right hand corner of the figure to the lower left hand corner. Figure 97 shows the effect the bow shock standing so far off the body has on the mass capture.

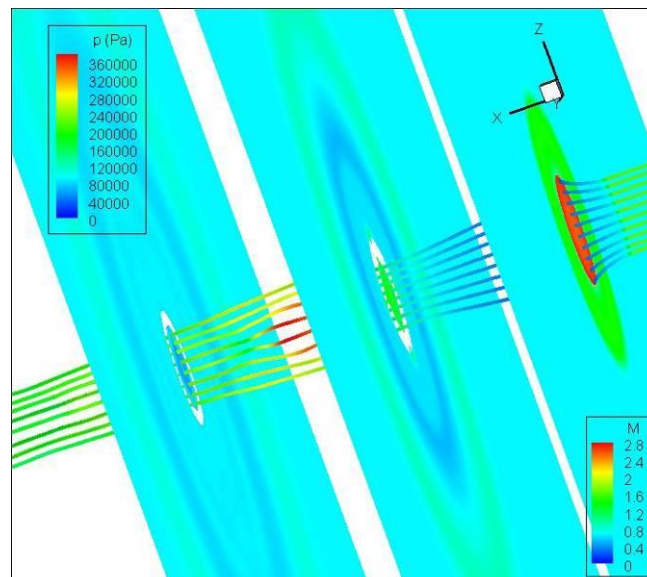


Figure 97 - With troughs case. The mouth of the inlet is the high pressure red circle.

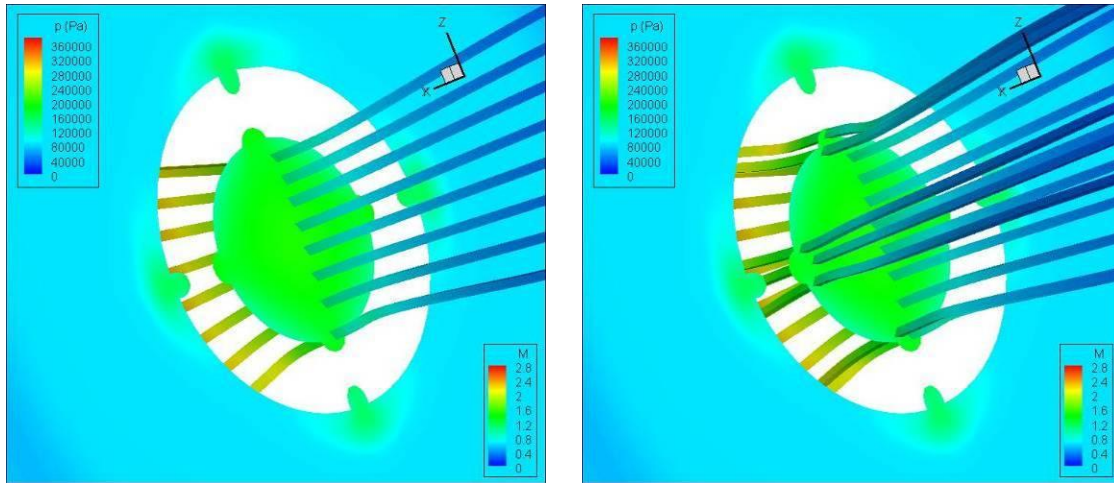


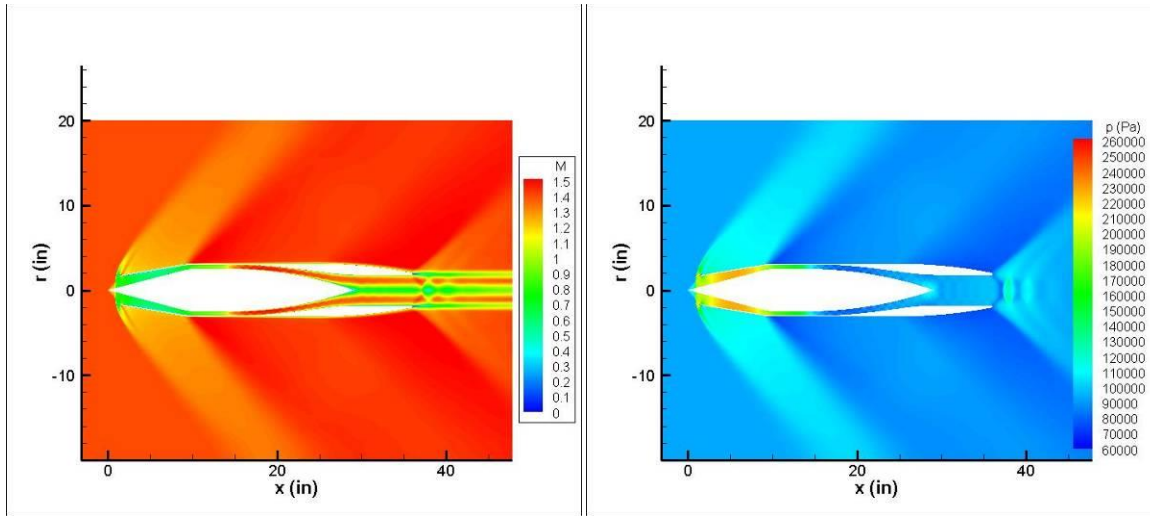
Figure 98 – Stream mark

While the troughs were placed in the design to provide secondary flows to enhance mixing with fuel, that effect was not found. In addition, the bleed holes did not provide much enough air spill to eliminate the normal shock out in front of the inlet. Without some hint of design flexibility, this design concept was dropped from this effort. A re-evaluation of the traditional axi-symmetric design was conducted.

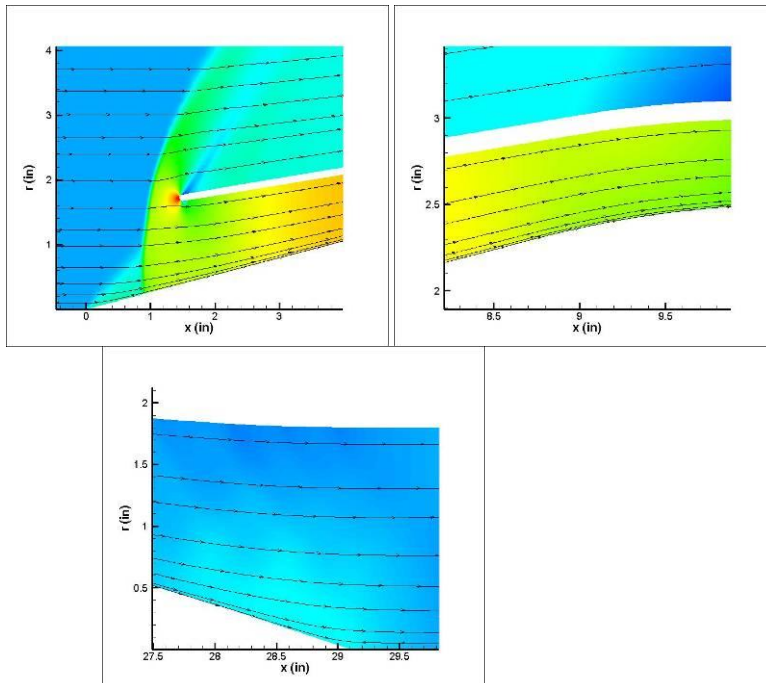
Final Ramjet Design and CFD

With information gained in previous designs, a new axi-symmetric ramjet designed based on what was need for flying a ramjet as just a drag device. Once the internal ramjet engine flow-path was established using SRGUL, two-dimensional CFD was used to examine the flow in more detail before proceeding to a three-dimensional analysis. All results presented here are for calorically perfect air flow only (no fuel).

Figure 99 shows CFD results for the $M = 1.4$, 3000ft altitude case. The desired Mach number was dropped to 1.4 due to improved weight estimates of the overall vehicle during boost. This case required a computational mesh with 57 blocks and approximately 200,000 cells. A normal shock is set up in the isolator (at approximately $x = 14$ in) as shown in the pressure plot. Figure 100 shows streamlines at critical points of the flow-path.



(a) Mach Number (b) Pressure Plot
Figure 99 - Results from the Axi-symmetric CFD Simulation



(a) At the Inlet (b) Entrance to Isolator (c) End of Center Body
Figure 100 - Streamlines at Different Points in the Ramjet

For the $M = 1.4$, 3000ft case, the aerodynamic drag is 177.5 lbs with 30% attributed to viscous drag. The mass capture was calculated to be 6.5 lbm/s. At $M = 1.67$, the drag went up to 231.7 lbs. The total pressure recovery along a streamline down the middle of the engine is on the order of 0.95.



3D CFD Results of Ramjet Design

A three-dimensional analysis was conducted utilizing a 180° model to determine center of pressure with an angle of attack. The solid model without webs is shown in Figure 101.

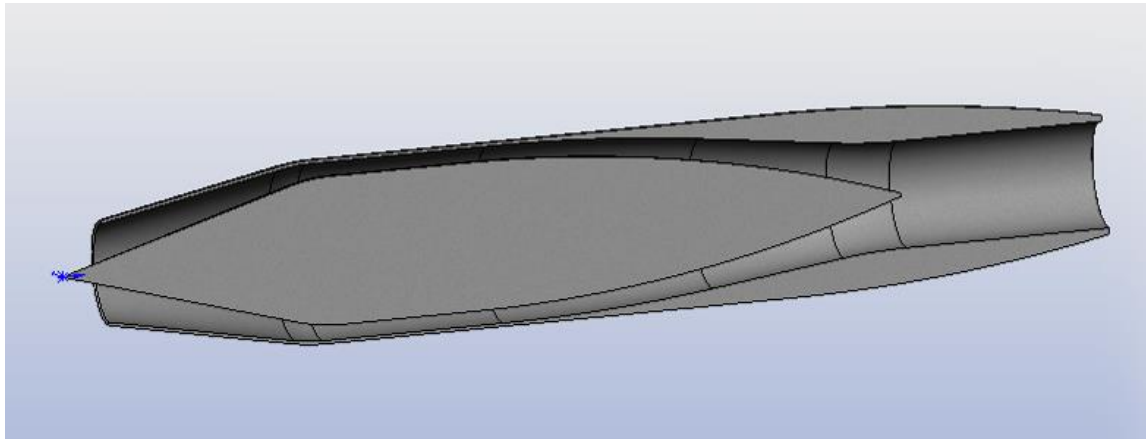


Figure 101 - Solid Model without Webs for the 3D CFD Analysis

The results of the CFD for this model indicated that, as expected, a normal shock wave exists at the entrance to the inlet for this relatively low Mach number. Higher Mach number test cases were run, where the normal shock wave was swallowed between Mach 2.5 and Mach 3.0. Figure 61 shows a Mach number and total pressure profiles of the inlet at Mach 2.0 and 3 kft altitude conditions. This normal shock seemed reasonable based on a 1.2 area contraction ratio of the internal portion of the inlet. Because the flight Mach number would be fairly low during our initial tests, an investigation was initiated to devise a way to spill air at low flight speeds while capturing more air at higher flight speeds.

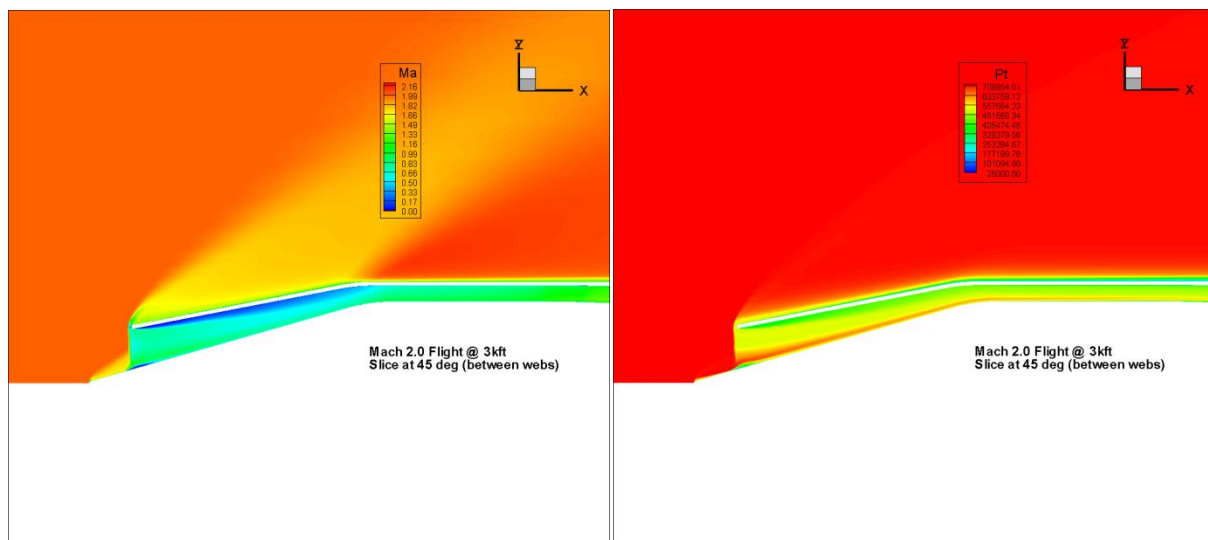




Figure 61 - Mach & Total Pressure Profiles of Traditional Inlet

Applied Thermal Sciences drew from inward turning inlets, and axi-symmetric center-body designs to conceive a new configuration for the ramjet, which is shown in Figure 62. The inlet provide for air spillage with the swept cowl lip, where a spill crotch was provide for each internal module of the ramjet flow-path. There are four internal modules that are separated by webs/struts to hold the cowl to the center-body. The swept lip of the cowl leading edge changes the shock emanating from the surface. The resulting effect is a weaker shock, or eliminating it at the lower flight Mach numbers. Figure 63 shows the difference for the King's Crown design at Mach 2.0. Note that the flow at Mach 2.0 through the inlet stays supersonic.

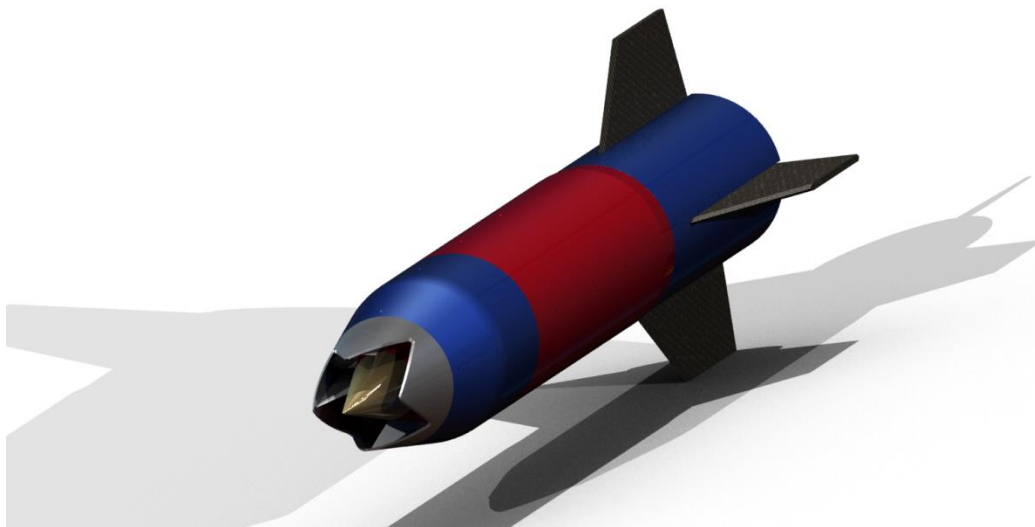


Figure 62 - Axi-symmetric Ramjet with King's Crown Inlet

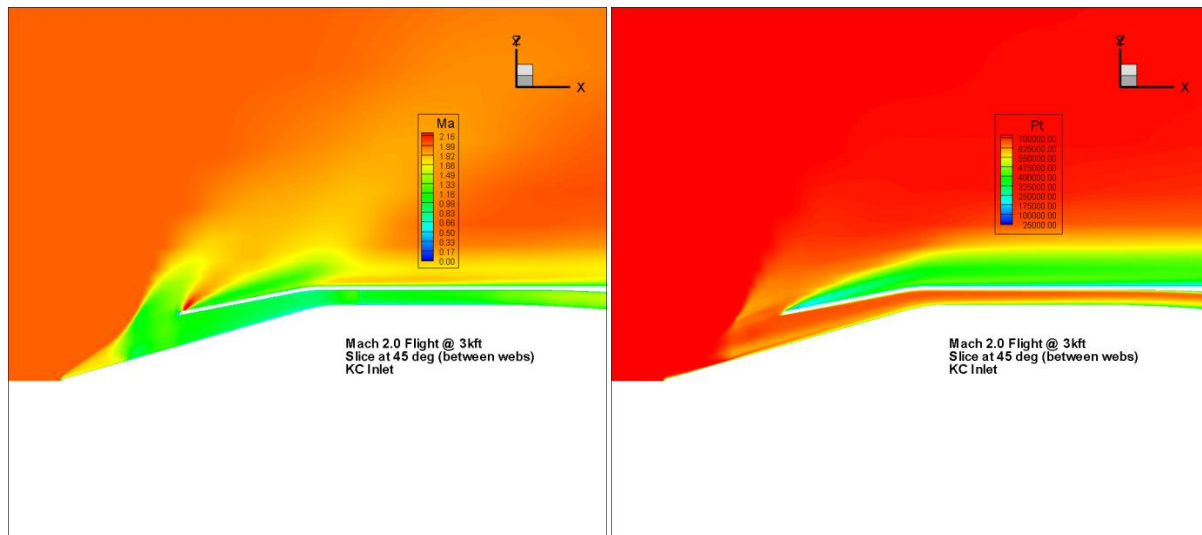


Figure 63 - Mach and Total Pressure Profiles for King's Crown Inlet

Because of its characteristics found in preliminary analysis, the King's Crown inlet design was used in the final flight ramjet design.

Task 2.3 – Structural Design

Axi-symmetric Ramjet Design

The initial ramjet design had an OD of 6.00 in, a center body maximum OD of 3.900 in and an overall length is 24.1 in. This design is shown Figure 1023 with external lines and the center-body in a transparent shade to show the electronics inside. In order to fit the electronics on the ramjet, the center body was hollowed out. Results of this effort on the axi-symmetric design showed that it was feasible to install electronics on his ramjet design.

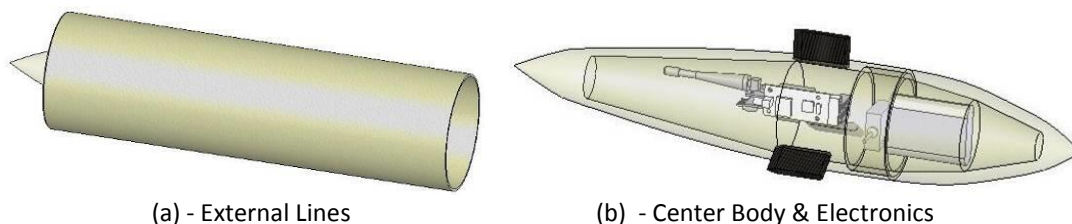


Figure 1023 - Axi-symmetric Ramjet with Payload

Further Revised Ramjet Design



The following is the mechanical design of the non-burning Ramjet test article design with a traditional inlet. The ramjet is 6.210 in OD and 36 in long with the center body being a 5.00" OD and is 29 in long. The ramjet is fabricated from fiberglass epoxy material. The design is shown in Figure 103 with the outer cowl shown as transparent. The cowl and center body are separated by 4 webs that run most of the length of the center body. The ramjet components for fabrication include a FWD section and an AFT section, with the FWD section housing the electronics. The FWD section of the ramjet is shown in Figure 104 and the AFT section of the ramjet is shown in Figure 105.

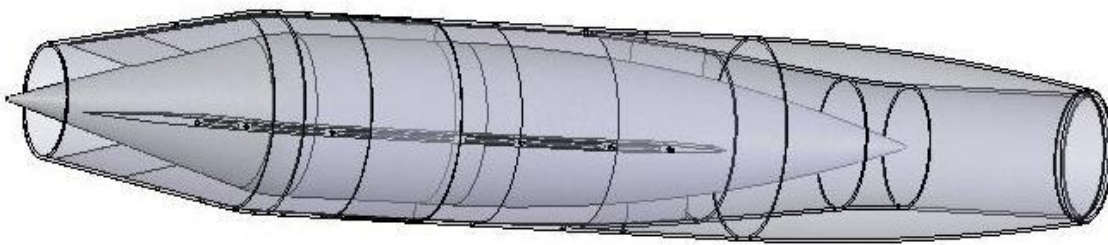
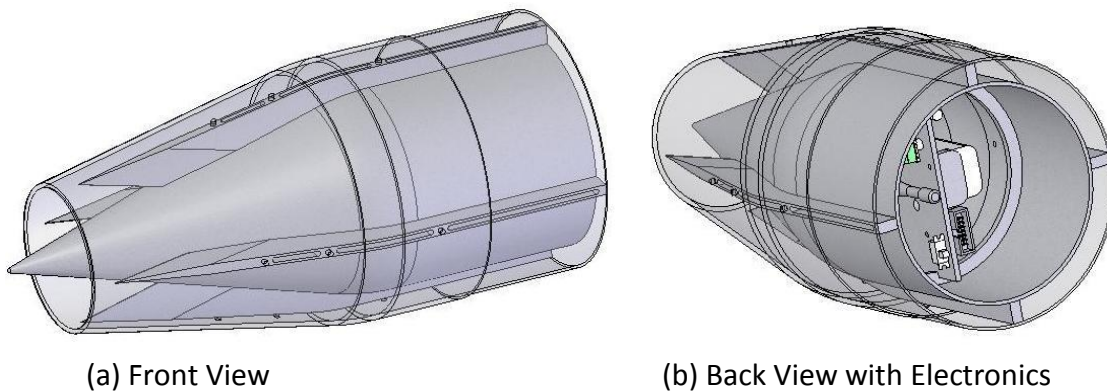


Figure 103 – Current Ramjet Design



(a) Front View

(b) Back View with Electronics

Figure 104 – FWD Section of Ramjet

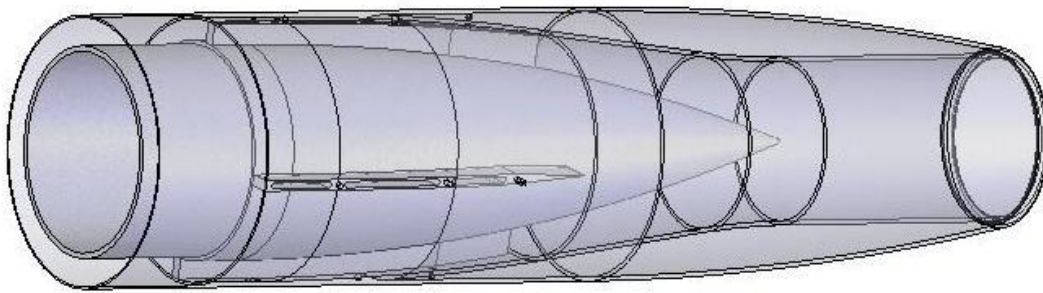


Figure 105 – AFT Section of Ramjet

Supersonic Vehicle with Ramjet Description

The flight vehicle consists of three main sections: FWD Ramjet section, MID payload bay, and AFT booster section. A picture of one of the vehicles is shown in Figure 106. The overall vehicle lengths are 349.3 cm (137.5 in) and the airframe outside diameter of 15.77 cm (6.21 in).



Figure 106 – Picture of Ramjet Flight Vehicles

FWD Ramjet Section

The FWD Ramjet section houses the flight computer. This flight computer records 4 pressures, accelerations, altitude and GPS data. The nosecone and FWD airframe section was made of fiberglass/epoxy. The FWD nosecone uses a 12 degree cone, a 15.67cm (6.170 in) base diameter and an overall ramjet length, with shroud, of 122.5 cm (44.3 in). The Ramjet includes a streamer and a main parachute onboard.

To aid with separation of the ramjet from the booster section, an Animal Motor Works J450 solid propellant motor and a small black powder charge controlled by a G-Wiz Accu-Fire was embedded into the center-body of the ramjet.. The Accu-Fire is utilized to detect motor burn out and ignites the motor in the ramjet. Separation occurs at approximately 5.5 sec after lift-off



at maximum velocity of 1500 ft/sec. The second stage motor is designed to burn for approximately 2.3 sec. During this second stage burn the shroud will open and allow air to flow thru the ramjet.

The shroud shown in Figure 109 is design for installation on the FWD section to prevent flow through the ramjet during boost. It is constructed of Derlin plastic and secured with 2 #4-40 nylon screws and an RTV seal. This shroud is used to minimize drag during launch and prevent air flow into the ramjet section. The shroud will be deployed during the 2nd stage motor burn. A timer in the ramjet that detects the 1st stage motor burn-out will send a signal to ignite the charge in the shroud after approximately 1.0 sec.



Figure 107 – Assembled Ramjet

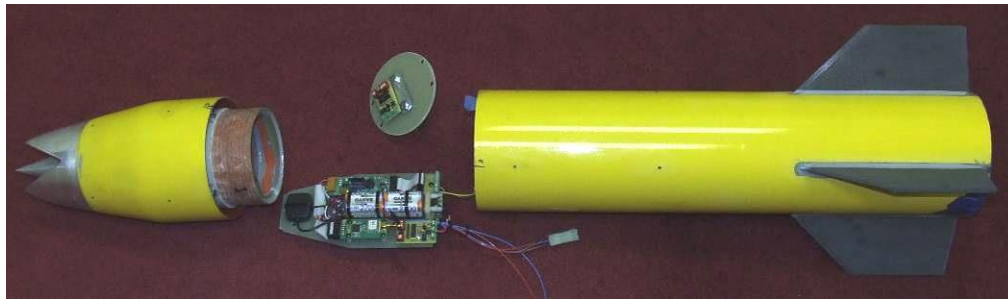


Figure 108 – Ramjet with all components shown



Figure 109 – Ramjet Shroud

Ramjet Coupler & MID Payload Bay & Booster Section

The MID payload bay section houses the electronics that will deploy the boost section parachutes and the separation of the ramjet. The MID section is constructed of light weight high strength carbon fiber/epoxy and is shown in Figure 110. The Ramjet coupler is constructed of fiberglass epoxy and 4 carbon fiber epoxy alignment rods mate to the AFT section of the ramjet with a slip fit between the Ramjet Coupler and the MID Payload Bay. The Ramjet Coupler houses a drogue parachute deployed at apogee. The Ramjet Coupler is shown in Figure 111.



Figure 110 –MID Payload Bay Section



Figure 111 – Ramjet Coupler Section

The AFT motor section was built to install the motor in an 11.43 cm (4.500 in) ID tube at the launch site. The motor is installed before launch and secured with 3 bolts to the AFT motor section. The main parachute is located in the AFT motor section secured to the MID payload



bay, the motor and the AFT motor section shown in Figure 112. The drogue parachute is deployed at apogee by the electronics in the MID payload bay. The attachment between the MID payload bay and the AFT motor section is a slip fit, secured with 8 #4-40 nylon screws to the booster section until the main parachute is deployed.



Figure 112 –Booster Section

Launch and Recovery Zone

The launch site is located in Cherryfield, ME approximately 1 hour and 30 minutes East, South-East of Bangor, ME. The launch area is on the Jasper Wyman & Son blueberry fields as shown in Figure 113. FAA and Maine DOT permits are required for flight testing. The launch procedures follow the Tripoli High Power Rocketry Safety Code as guidelines for FAA approval.



Figure 113 – Aerial Map of Launch and Recovery Area (Cherryfield, ME)

Task 3.1 – Boost Vehicle

Task 3.3 – Boost Vehicle with Separation of Ramjet Test Article

The flight vehicle consists of three main sections: FWD Ramjet section, MID payload bay, and AFT booster section. A picture of one of the vehicles is shown in Figure 114. The overall vehicle lengths are 349.3 cm (137.5 in) and the airframe outside diameter of 15.77 cm (6.21 in).



Figure 114 – Picture of Flight Vehicle



November 2009 Flight - FWD Ramjet Section

The FWD Ramjet section houses the flight computer. This flight computer records 4 pressures, accelerations, altitude and GPS data. The nosecone (i.e. shroud) and FWD airframe section is made of fiberglass/epoxy. The FWD nosecone is a 12 degree half-angle cone a 15.67cm (6.170 in) base diameter and an overall ramjet length with shroud of 122.5 cm (44.3 in). The recovery parachutes is located in the AFT section of the ramjet as shown in Figure 115 and Figure 116. The Ramjet has a streamer and a main parachute onboard.

The Ramjet is designed to separate from the booster section assisted by an Animal Motor Works J450 solid propellant motor, with a small black powder charge controlled by a G-Wiz Accu-Fire. The separation was set to occur at approximately 5.5 sec after lift-off at maximum velocity of 1500 ft/sec. The second stage motor has a burn time of approximately 2.3 sec. During this second stage burn the shroud will deploy and allow air to flow thru the ramjet.

The shroud shown in Figure 117 is installed on the FWD section of the ramjet. It is constructed of Derlin plastic and secured with 2 #4-40 nylon screws and an RTV seal. The shroud is employed to minimize drag during launch and prevent air flow into the ramjet section. A timer in the ramjet that detects the 1st stage motor burn-out will send a signal to ignite the charge in the shroud after approximately 1.0 sec.



Figure 115 – Assembled Ramjet

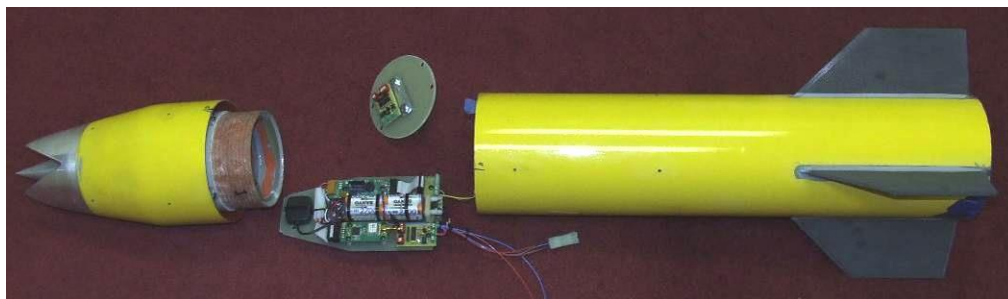


Figure 116 – Ramjet with all components shown



Figure 117 – Ramjet Shroud

November 2009 Flight - Ramjet Coupler & MID Payload Bay & Booster Section

The MID payload bay section houses the electronics that will deploy the boost section parachutes and the separation of the ramjet. The MID section is constructed of light weight high strength carbon fiber/epoxy and is shown in Figure 118. The Ramjet coupler is constructed of fiberglass epoxy and 4 carbon fiber epoxy alignment rods mate to the AFT section of the ramjet with a slip fit between the Ramjet Coupler and the MID Payload Bay. The Ramjet Coupler will house a drogue parachute deployed at apogee. The Ramjet Coupler is shown in Figure 119.



Figure 118 – MID Payload Bay Section



Figure 119 – Ramjet Coupler Section

The AFT motor section was built to install the motor in an 11.43 cm (4.500 in) ID tube at the launch site. The motor will be installed before launch and secured with 3 bolts to the AFT motor section. The main parachute is located in the AFT motor section secured to the MID



payload bay, the motor and the AFT motor section shown in Figure 120. The drogue parachute will be deployed at apogee by the electronics in the MID payload bay. The attachment between the MID payload bay and the AFT motor section is a slip fit and 8 #4-40 nylon screws will secure the booster section to the MID sections until the main parachute is deployed.



Figure 120 – Booster Section

November 2009 Flight - Solid Propellant Motors

First stage motor is ATS N3407 ammonium-nitrate (AN) based solid propellant. The propellant is made using 60% Ammonium Nitrate, 20% Magnesium powder, 16.2% R20LM binder and 3.8% Mondur MR curing agent, all by weight. The grain geometry is 8.306 cm (3.270 in) OD by 3.81 cm (1.500 in) ID by 15.875 cm (6.250 in) long with a total of 9 grains uses in one motor. The total weight of propellant is approximately 8.278 kg (18.25 lb). The nozzle has a throat diameter of 1.944cm (0.785 in) and an area ratio of 10.14:1. The motor produces a maximum thrust of 4715.1 N (1,060 lb), with a burn time of 5.6 sec and a total impulse of 17,264 N-s. Typical thrust curve shown in Figure 121. The motor casing weight is 6.98 kg (15.39 lb), with a total weight with propellant of 15.25 kg (33.64 lb). A picture of a rocket motor is shown in Figure 122.

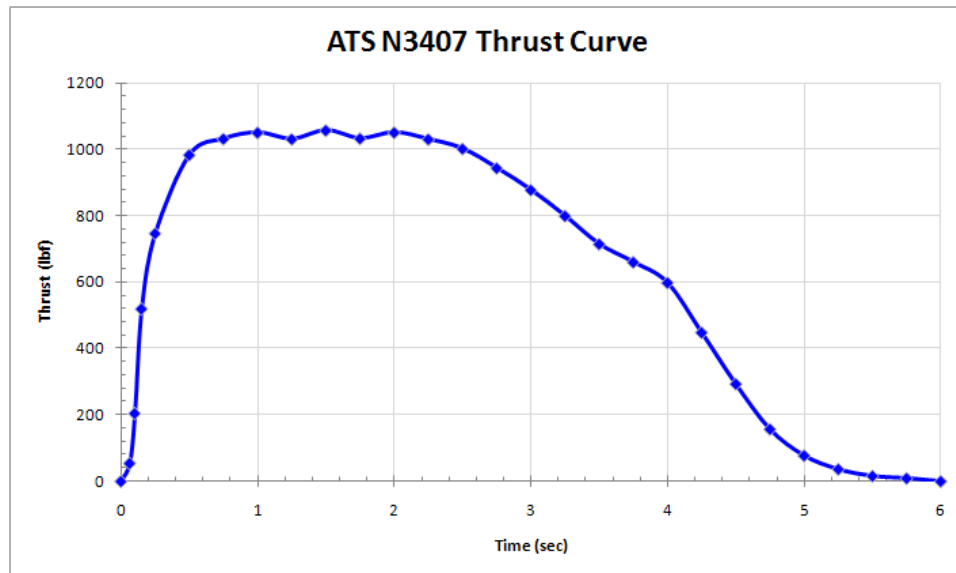


Figure 121 – First Stage Motor Thrust Curve



Figure 122 – Carbon Fiber/Epoxy Motor Casing

Second stage or Ramjet separation motor will be an Animal Motor Works (AMW) J450ST commercial AP propellant. The motor burn time is 2.3 sec with a maximum thrust of 563.2 N (126.6 lbf) and an average thrust of 459 N (103 lbf). Total impulse of this motor is 1070 N-sec. The propellant weight is 533 gm (1.17 lb). The thrust curve for the J450 motor is shown in Figure 123.

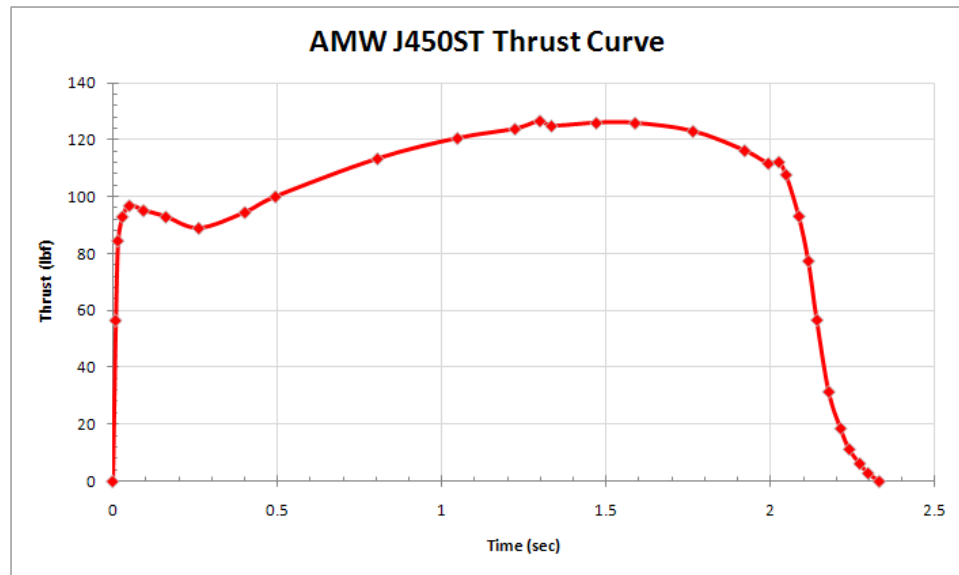


Figure 123 – Second Stage Ramjet Thrust Curve

November 2009 Flight - Electronics

R-DAS from AED is the main flight data acquisition computer mounted in the Ramjet vehicle. The R-DAS consists of main board, a GPS expansion board with antenna and a telemetry board. A PML Co-Pilot will be used as a back-up electronic device on the Ramjet to ensure the recovery. In addition to the R-DAS and C-Pilot on the Ramjet, a timer board will be triggered by a break wire between the Ramjet and the Booster. The break wire will also be used to initiate the shroud deployment. These components along with a battery pack are mounted in the FWD section of the ramjet. The R-DAS will be sampling at a rate of 200 Hz and stored on-board. The system will be recording acceleration, GPS and five pressure readings. One is a barometric on-board sensor, and four Kulite Model #: XCEL-3-IA-080-100A pressure transducers are mounted along the flow path of the Ramjet. One of the pressure transducers is mounted on the R-DAS. One miniature Kulite pressure transducer is mounted at the tip of the nosecone, a second is mounted in approximately 1.5 in up the cone, the third is approximately 6.25 inches along the flow path, and the fourth transducer is 11.75 inches along the internal flow path mounted in the center body section. The pressure transducer locations are shown in Figure 124. Data will be sent to a ground station at a rate of 10 Hz and GPS data will be updated at 2Hz. Pictures of the R-DAS flight computers and the Co-Pilot system are shown in Figure 125.

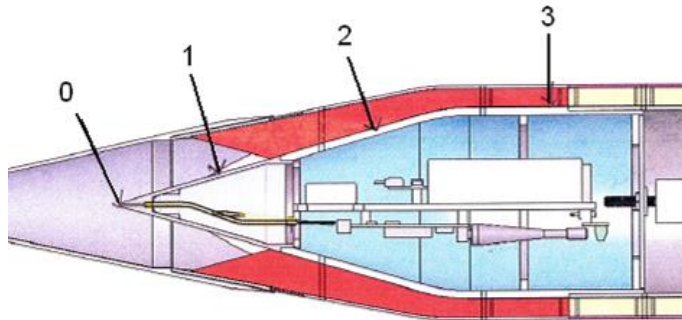


Figure 124 – Ramjet Pressure Transducer Locations

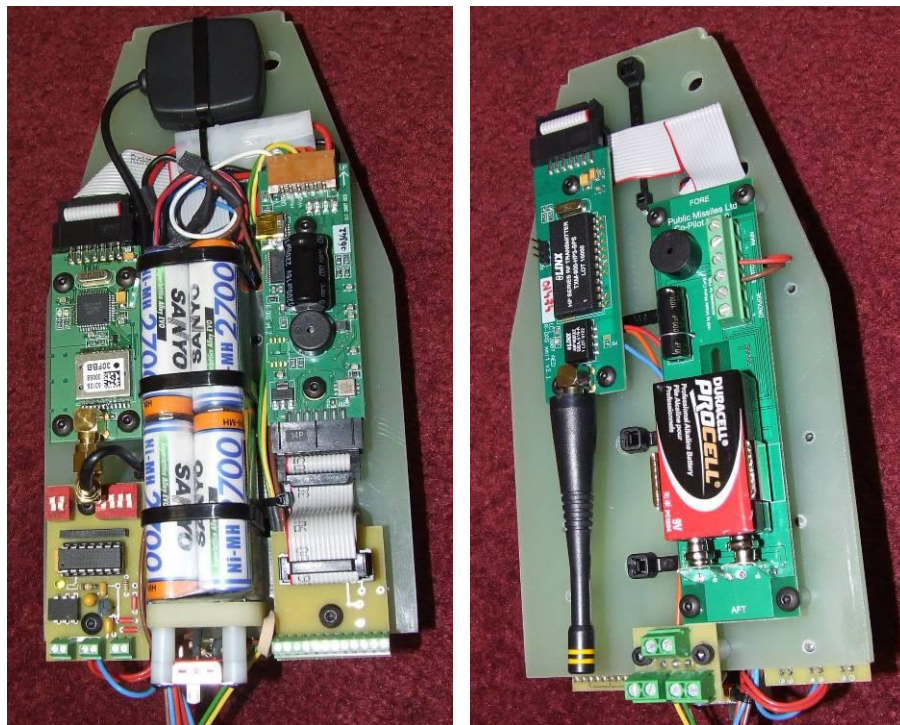


Figure 125 – R-DAS Flight Computer



Table 12 – Pressure Transducers

Number	Location	Serial Number	Vehicle
0	Nosecone Tip	Pressure Transducer (SN: 7663-6-141)	Vehicle #1
1	1.5" Back	Pressure Transducer (SN: 7663-6-156)	Vehicle #1
2	6.25" Back	Pressure Transducer (SN: 7663-6-167)	Vehicle #1
3	11.75" Back	Pressure Transducer (SN: 7663-6-139)	Vehicle #1
0	Nosecone Tip	Pressure Transducer (SN: 7663-6-169)	Vehicle #2
1	1.5" Back	Pressure Transducer (SN: 7663-6-148)	Vehicle #2
2	6.25" Back	Pressure Transducer (SN: 7663-6-164)	Vehicle #2
3	11.75" Back	Pressure Transducer (SN: 7663-6-150)	Vehicle #2

The MID section, two PML Co-Pilots will control the deployment of the drogue and main parachutes for recovery of the Booster Section. There are two Co-Pilots mounted in the MID payload bay. Both Co-Pilot are programmed with a Mach Delay (from detection of launch) of 15 sec and deploy the drogue parachute at apogee. One of the Co-Pilots will be programmed to deploy a main parachute at 304.8 m (1000 ft) above ground level and a back-up or second Co-Pilot will be programmed to deploy a main parachute at 243.8 m (800 ft) above ground level. The Co-Pilot system is shown in Figure 126. A G-Wiz Accu-Fire will also be mounted in the MID payload bay and it will control the separation event. This electronics package was designed to detect motor burn out. Once the motor burnout is detected a signal is sent to ignite a charge in the second stage motor. The Accu-Fire system is shown in Figure 126.



Figure 126 – Accu-Fire (Left) & Co-Pilots (Right) Electronics

November 2009 Flight – 1st Launch

The first vehicle was launch at 12:41 pm EST on November 18, 2008 shown in Figure 127. This vehicle with un-fueled ramjet payload lost telemetry 3 second after lift-off. The ramjet separation event was visually confirmed by several people at the launch. The booster drogue and main parachute deployment was also visually confirmed and a compass barring of the



landing area is known. The ramjet drogue and main parachute deployment was also visually confirmed, the exact landing area being determined.



Figure 127 – November 2009 Launch

November 2009 Flight – 2nd Launch

The second vehicle was launched at 3:41 pm EST on November 18, 2009 and recovered 0.45 miles from the launch pad. This vehicle maintained telemetry transmission the entire flight. A high definition video of the launch is available upon request. The GPS flight data has been plotted and is shown in Figure 128 with Table 13 listing the major events during the flight. Figure 129 is a plot of the onboard ramjet acceleration and altitude measurements. Figure 130 is a plot of the ramjet velocity and altitude measurements. Figure 131 plots the pressure transducers located along the ramjet internal flow path with the ramjets calculated velocity. Figure 132 shows the separation event from frames the ground video of the launch.

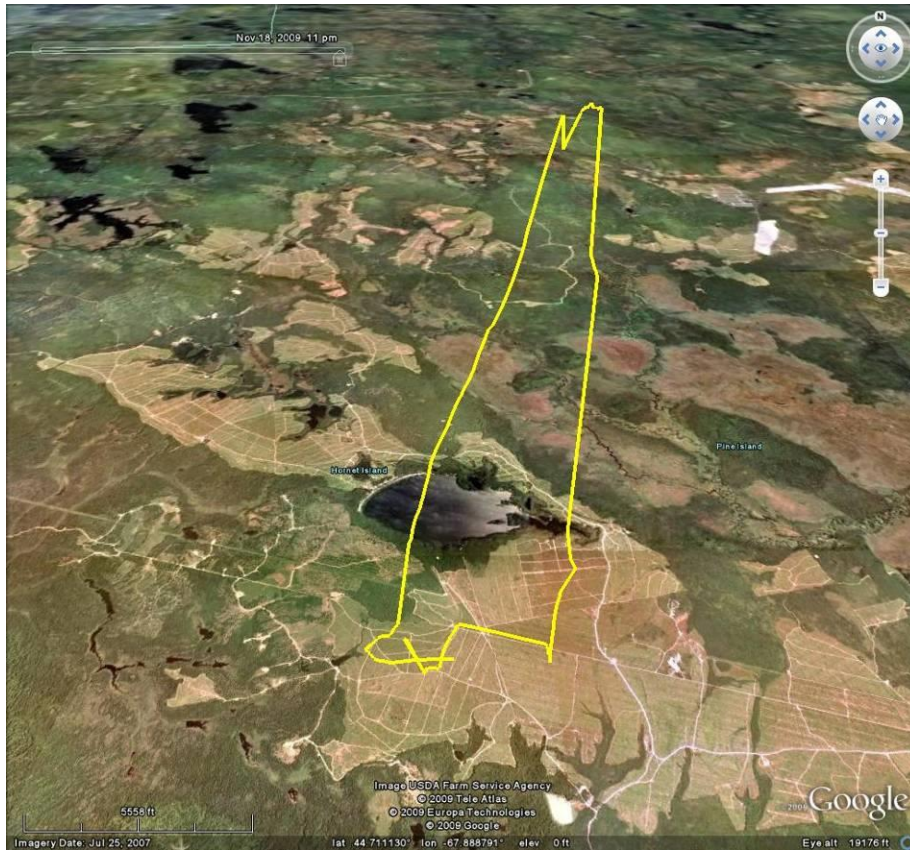


Figure 128 - 3D Plot of the 2nd Vehicle's Flight

Table 13 - Summary of 2nd Flight Vehicle Launched

Event	Time	Velocity (Calculated)	Altitude (Measured)	Altitude (Calculated)
Launch:	0.000 sec	0 ft/s	0 ft	-
Enter Ma1:	3.345 sec	1106 ft/s (Ma 1.0)	3259 ft	1821 ft
2 nd Stage Motor Starts:	4.250 sec	1236 ft/s (Ma 1.122)	5144 ft	2892 ft
Shroud Deployed:	5.400 sec	1244 ft/s (Ma 1.124)	3410 ft	4332 ft
2 nd Stage Motor Burnout:	6.940 sec	1346 ft/s (Ma 1.217)	2488 ft	6309 ft
Maximum Velocity (Ramjet):	6.990 sec	1347 ft/s (Ma 1.217)	2635 ft	6376 ft
Exit Ma1:	8.415 sec	1106 ft/s (Ma 1.0)	6311 ft	8116 ft

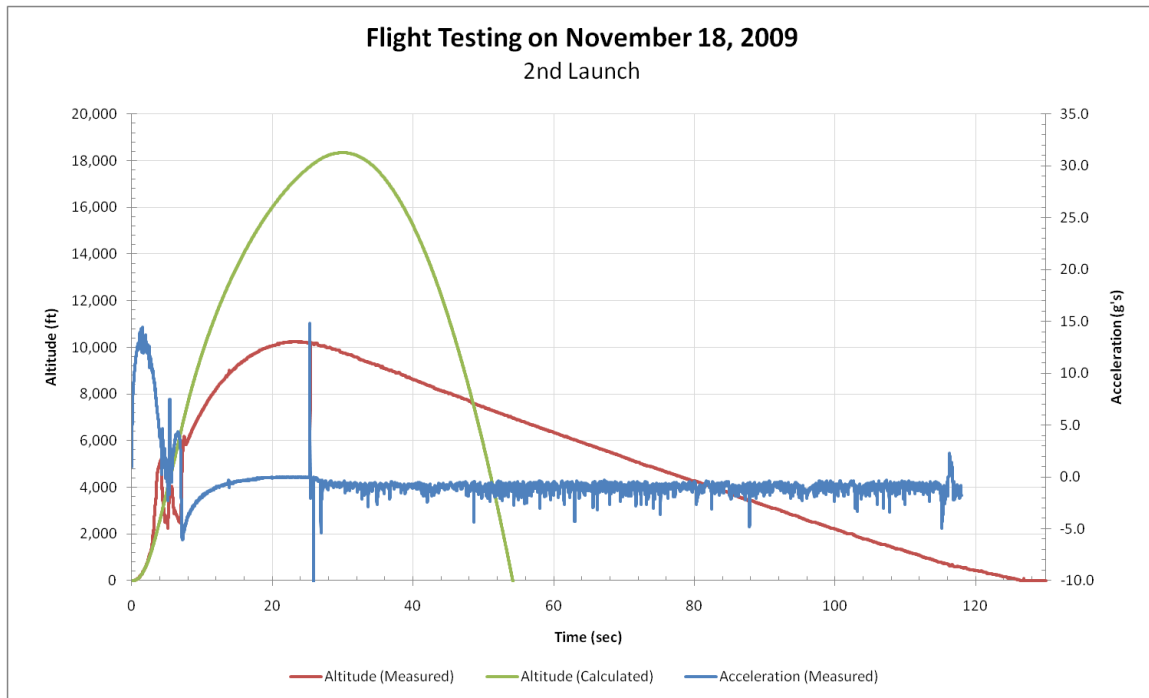


Figure 129 - 2nd Vehicle Altitude and Acceleration Data

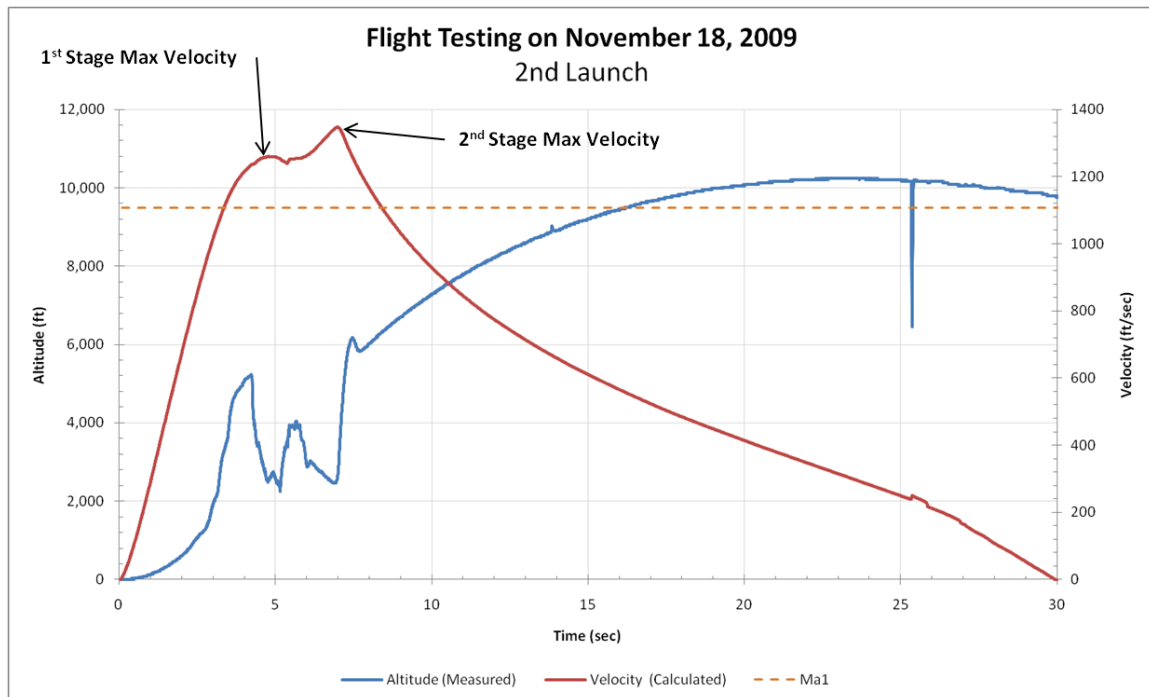


Figure 130 - 2nd Vehicle Altitude and Velocity Data

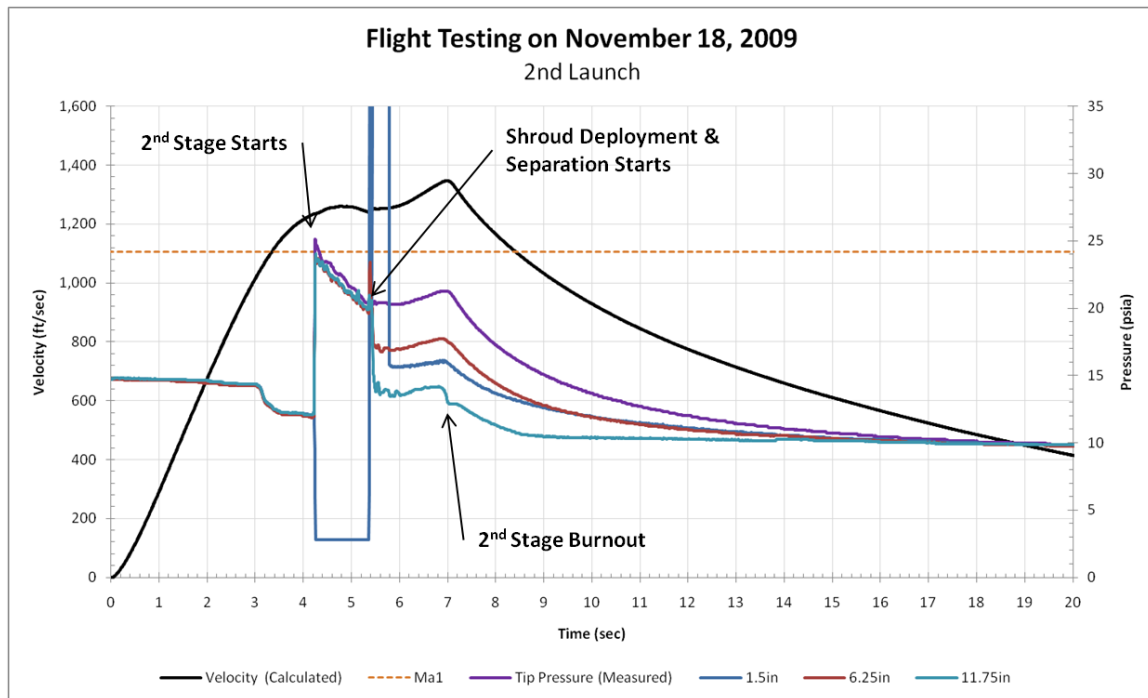


Figure 131 – 2nd Vehicle Velocity and Nosecone Tip Pressure Data

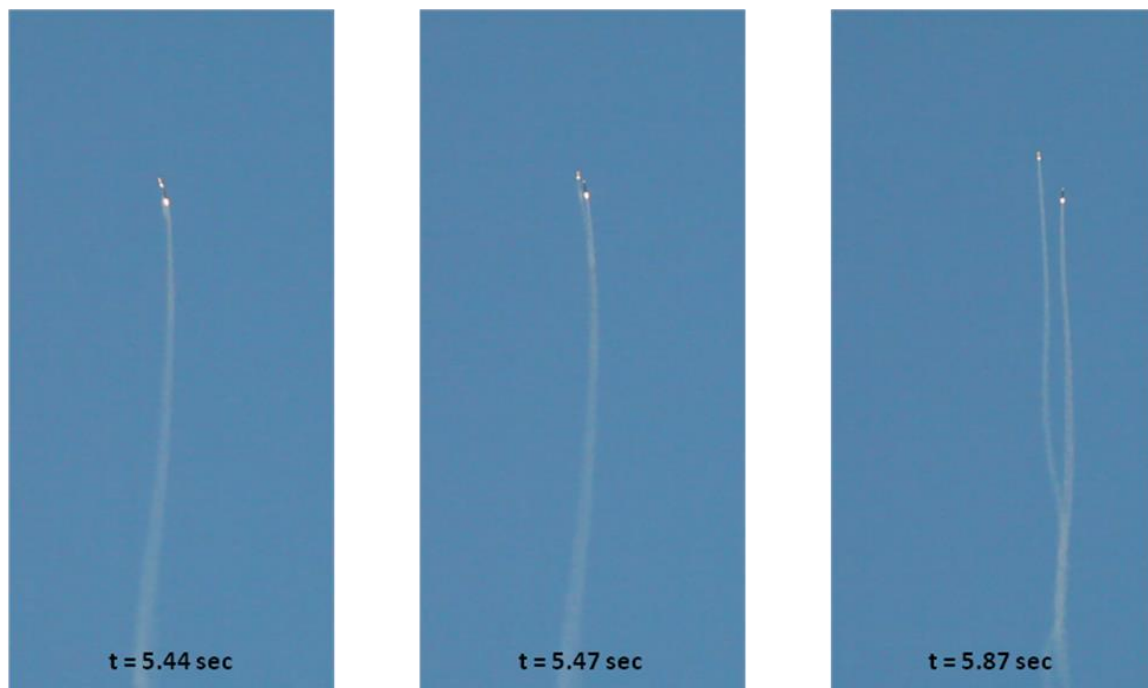


Figure 132 – Frames from Video of Separation Event